The Role of the GTPase-Activating Protein TBC1D4 (AS160) in Mouse Kidney

---

Dissertation

zur

Erlangung der naturwissenschaftlichen Doktorwürde

(Dr. sc. nat.)

vorgelegt der

Mathematisch-naturwissenschaftlichen Fakultät

der

Universität Zürich

von

Marianna Di Chiara

aus

Italien

Promotionskomitee:

Prof. Dr. Carsten Wagner (Vorsitz)

Prof. Dr. Johannes Loffing (Leitung der Dissertation)

Prof. Dr. Olivier Devuyst

Prof. Dr. Hadi Al-Hasani

Zürich, 2014

Summary

The reabsorption and secretion of electrolytes and fluids by the kidney critically depends on the activity of renal ion and water transport proteins and channels in the apical and basolateral plasma membrane of the renal epithelial cells. In the last two decades, many of the renal ion and water transporting proteins have been identified, but the molecular mechanisms underlying the regulation of their activity remains elusive. Interestingly, the activity of many of the renal ion and water transporting proteins is controlled by the regulation of the trafficking of these proteins to or from the plasma membrane. Previous in vitro studies on various cell culture models suggested that the Rab GTPase-activating protein (Rab GAP) TBC1D4 participates in the control of the intracellular trafficking of the epithelial sodium channel (ENaC), the water channel aquaporin 2 (AQP2), and the Na^+-K^+-ATPase localized in the apical and basolateral plasma membrane of certain renal epithelia, respectively. TBC1D4 is thought to retain ENaC, AQP2, and Na^+-K^+-ATPase-bearing vesicles in the cytoplasm and thereby to reduce the cell surface abundance of these proteins similar to the well known and previously reported effects of TBC1D4 on the glucose transporter GLUT4 in fat and skeletal muscle cells. The goal of this thesis was to define the in vivo role of TBC1D4 in the kidney and to test the hypothesis that TBC1D4 controls the intracellular trafficking of renal ion and water transporting proteins. To reach this end, wildtype and TBC1D4 knockout (KO) mice were studied by functional, morphological, biochemical, and molecular-biological techniques.

TBC1D4 is highly abundant in the renal tubular system

First, I contributed to studies that localized TBC1D4 along the renal tubular system (Lier et al., 2012). Using co-immunostainings for a variety of nephron-specific marker molecules, immunohistochemistry revealed high levels of TBC1D4 abundance in parietal epithelial cells (PEC) of Bowman's capsule, in descending and ascending thin limbs, the thick ascending limb (TAL), the distal convoluted tubule (DCT), the connecting tubule (CNT) and the collecting duct (CD). This distribution pattern matches well with the expression of TBC1D4 mRNA levels as determined later by qRT-PCR on mouse microdissected nephron segments.

TBC1D4 deficiency does not affect renal sodium and water handling

First, TBC1D4 KO mice were grossly phenotyped. Mice were normal in terms of organ morphology, physical appearance and survival. Urinary ion excretion, osmo-

larity and plasma ion concentrations, as well as blood pressure levels were similar for wildtype (WT) and TBC1D4 KO mice. Likewise urinary and plasma aldosterone levels were not different between genotypes. Even when challenged by 2 weeks feeding of a low Na^+ and high K^+ diet or by 24 hours of water restriction, TBC1D4 KO mice did not show any phenotype different from the one of WT mice. Consistently, immunoblotting did not reveal any difference in the abundance of renal ion and water transporting proteins including ENaC, AQP2, and Na^+-K^+-ATPase between genotypes under each condition.

TBC1D4 deficiency improves glucose tolerance

On standard diet and after overnight fasting, TBC1D4 KO mice had lower plasma glucose and insulin levels than WT mice. The glucose tolerance was slightly improved, whereas the insulin sensitivity was impaired in TBC1D4 KO mice compared with WT mice. Furthermore, TBC1D4 KO mice gained less bodyweight under a high fat diet than their WT littermates.

TBC1D4 co-localizes with and appears to regulate GLUT4 in the kidney

As we did not find any evidence that TBC1D4 controls ENaC, AQP2 and Na^+-K^+-ATPase in the kidney, we next addressed the question whether TBC1D4 may also regulate GLUT4 in the kidney. First, we showed by qRT-PCR on microdissected nephron portions and by immunohistochemistry that the distribution pattern of TBC1D4 and GLUT4 mRNA and protein matches very well along the TAL, DCT, CNT, and CD of WT mice, while TBC1D4 expression in the PEC matched with the glucose transporter (GLUT1). Interestingly, in TBC1D4 KO mice, renal GLUT4 and GLUT1 levels were significantly reduced as assessed by immunohistochemistry and immunoblotting. In primary TAL cells isolated from the kidneys of WT and TBC1D4 KO mice, basal glucose uptake was increased and could not be anymore stimulated by insulin in TAL cells of TBC1D4 KO mice, consistent with the metabolic data.

Microarray analysis did not provide evidence for compensatory up-/down-regulation of proteins involved in regulation of membrane trafficking

To test for potentially up- and/or down-regulated trafficking genes that may compensate for the loss of TBC1D4 in renal epithelia, we isolated by COPAS (complex object parametric analysis and sorting technique) green fluorescent DCTs from WT and TBC1D4 KO mice. Microarray analyses revealed no differential regulation of Rab GAPs and Rab guanine exchange factors (Rab GEFs), other family members

of the TBC1 family, or other genes involved in membrane trafficking and in salt and water homeostasis. However, stearoyl-CoA desaturase-1 (Scd1), which is crucial in in fatty acid metabolism, was significantly down-regulated in DCT cells of TBC1D4 KO mice and warrants future studies. In the context of this thesis, I also established a human embryonic kidney (HEK293) cell line stably transfected with the DCT-specific NaCl cotransporter (NCC) in order to have a cell-based assay in which to study the possible role of TBC1D4 for NCC. However, although functional assays demonstrated the utility of the cells to study the phosphorylation of NCC, the project was abandoned as NCC was not targeted to the cell surface in these cells and as the in vivo studies did not reveal any evidence that TBC1D4 may regulate renal Na^+ transporting proteins.

Summary and Conclusion

In sum, this thesis provides evidence that in contrast to previous findings in vitro, TBC1D4 does not control ENaC, AQP2 and the Na^+-K^+-ATPase in the kidney in vivo. However, TBC1D4 plays a role in whole body glucose homeostasis and appears not only to control, as previously shown by others, GLUT4 in fat and skeletal muscle cells, but also in the kidney. In the kidney TBC1D4-regulated and GLUT4-mediated glucose uptake might supply distal tubule with substrates for anaerobic glycolysis, which may contribute to the higher ischemic tolerance of distal tubules compared with proximal tubules. Moreover, TBC1D4-dependent regulation of GLUT4 might be important in the post-prandial state, where glucose availability and insulin levels in the blood rise and renal tubular working load increases.

Zusammenfassung

Die Resorption sowie Sekretion von Elektrolyten und Flüssigkeit durch die Nieren hängt entscheidend von der Aktivität renaler Ionen- und Wassertransportproteine an der apikalen und basolateralen Membran in renalen Epithelzellen ab. In den letzten zwei Jahrzehnten konnten mehrere renale Ionen- und Wassertransportproteine identifiziert werden, jedoch sind die molekularen Mechanismen zur Regulierung der Aktivität dieser renalen Transportproteine noch weitgehend unbekannt. Interessanterweise unterliegt die Kontrolle der Aktivität vieler dieser Ionen- und Wassertransportproteine der Regulierung des Transports zu oder weg von der Plasmamembran. Frühere in vitro Studien in verschiedenen Zellkulturmodellen legten nahe, dass das Rab GTPase-aktivierende Protein (Rab GAP) TBC1D4 an der Kontrolle des intrazellulären Transports des epithelialen Natriumkanals (ENaC), des Wasserkanals Aquaporin 2 (AQP2), jeweils in der apikalen Membran, und der Na^+-K^+-ATPase in der basolateralen Membran in bestimmten Nierenepithelzellen beteiligt ist. TBC1D4 wird vermutet ENaC-, AQP2- und Na^+-K^+-ATPase-enthaltende Vesikel im Zytoplasma zurückzuhalten und dadurch die Proteinmenge an der Zelloberflächen zu reduzieren, ähnlich wie beim bereits beschriebenen Effekt von TBC1D4 auf den Glukosetransporter GLUT4 in Fett- und Muskelzellen. Das Ziel dieser Doktorarbeit war es, die in vivo Rolle von TBC1D4 in den Nieren zu erforschen und die Hypothese zu bestätigen, dass TBC1D4 den intrazellulären Transports renaler Ionen- und Wassertransportproteine kontrolliert. Um dieses Ziel zu erreichen, wurden funktionale, morphologische, biochemische und molekular-biologische Studien an Wildtyp (WT)- und TBC1D4-Knockout (KO)-Mäusen durchgeführt.

TBC1D4 kommt vermehrt im renalen Tubulussystem vor

Zu Beginn dieser Arbeit habe ich an der Studie zur Lokalisierung von TBC1D4 im renalen Tubulussystem beigetragen (Lier, Gresko, Di Chiara, Loffing-Cueni, & Loffing, 2012). Durch Ko-Immunofärbung für verschiedene nephron-spezifische Markermoleküle zeigten immunhistochemische Analysen eine hohe TBC1D4-Expression in den parietalen Epithelzellen der Bowman-Kapsel, dem absteigenden und aufsteigenden dünnen und dem dicken aufsteigenden Ast der Henleschen Schleife (TAL), der Pars convoluta des distalen Tubulus (DCT), dem Verbindungstubulus (CNT) und im Sammelrohr (CD) auf. Das Verteilungsmuster stimmte mit dem TBC1D4 mRNA Expressionsniveau, das später durch qRT-PCR in mikrodissektierten Maus-Nephronsegmente bestimmt wurde, überein.

Der Verlust von TBC1D4 hat keinen Effekt auf den Salz- und Wasserhaushalt

Zu Beginn wurden TBC1D4 KO-Mäuse bezüglich augenscheinlicher Abnormalitäten untersucht. TBC1D4 KO-Mäuse waren hinsichtlich Organmorphologie, physischer Erscheinung und Lebensdauer unauffällig. Die Ionenausscheidung im Urin sowie die Osmolarität, die Plasmaionenkonzentration und der Blutdruck waren ähnlich zwischen WT- und TBC1D4 KO-Mäusen. Zusätzlich waren die Aldosteronspiegel im Urin und Plasma zwischen den Genotypen unverändert. Selbst durch Fütterung einer stimulierenden niedrig Na^+-hoch K^+-Diät oder durch einen 24-stündigen Wasserentzugs zeigten die TBC1D4 KO-Mäuse keinen veränderten Phänotyp im Vergleich zu den WT-Mäusen. Damit übereinstimmend waren im Immunoblot keine Unterschiede in der Proteinmenge renaler Ionen- und Wassertransportproteine, einschliesslich ENaC, AQP und Na^+-K^+-ATPase, zwischen den Genotypen und unter verschiedenen Konditionen zu erkennen.

TBC1D4 ko-lokalisiert mit GLUT4 und scheint GLUT4 in der Niere zu regulieren

Da wir keine Hinweise darauf, dass TBC1D4 ENaC, AQP2 und die Na^+-K^+-ATPase in der Niere kontrolliert, gefunden haben, stellten wir uns die Frage, ob TBC1D4 auch GLUT4 in der Niere reguliert. Wir konnten durch qRT-PCR an mikrodissektierten Nephronsegmenten und durch immunohistochemische Analysen eine hohe Übereinstimmung der Gen- und Proteinexpression von TBC1D4 und GLUT4 im TAL, DCT, CNT und CD zeigen, während die Expression von TBC1D4 in den parietalen Epithelzellen mit der des GLUT1-Glukosetransporters übereinstimmte. Interessanterweise zeigten immunohistochemische Analysen und Immunoblotting in TBC1D4 Mäusen reduzierte GLUT4- und GLUT1-Proteinmengen. In primären TAL-Zellen, isoliert aus Nieren von WT- und TBC1D4 KO-Mäusen, war die basale Glukoseaufnahme erhöht und konnte in TAL Zellen von TBC1D4 KO-Mäusen nicht weiter durch Insulin stimuliert werden, was mit den metabolischen Daten übereinstimmt.

Micoarray-Analysen ergaben keinen Hinweis auf eine kompensatorische Herauf- oder Herunterregulierung möglicher Proteine beteiligt an der Membrantransport-Regulierung

Um mögliche herauf- oder herunterregulierte Transport-Gene zu testen, die den Verlust von TBC1D4 in renalen Epithelien kompensieren könnten, isolierten wir mit Hilfe der „fluoreszenz-aktivierten Sortierung mehrzelliger Objekte“-Technik (COPAS), grün-fluoreszierende DCTs von WT- und TBC1D4 KO-Mäusen. Microarray-Analysen ergaben keine veränderte Regulierung der Rab GAPs und Rab Guanin-

Austauschfaktoren (Rab GEFs), Familienmitglieder der TBC1 Familie, sowie anderer Gene beteiligt im Membrantransport und an der Salz- und Wasserhomöostase. Jedoch war die Expression von Stearoyl-CoA Desaturase-1 (Scd1), ein Gen von entscheidender Bedeutung im Fettsäurestoffwechsel, signifikant in DCT Zellen von TBC1D4 KO-Mäusen herunterreguliert. Dieser Befund garantiert weitere Studien. Im Zusammenhang mit dieser Dissertation habe ich eine Zellline (HEK293 Zellen) mit einer stabil-transfektierten Expression des DCT-spezifischen NaCl-Kotransporters (NCC) entwickelt, welche zur Aufkärung einer möglichen Rolle von TBC1D4 auf den NCC dienen sollte. Obwohl funktionale Assays die Nützlichkeit dieser Zellen zur Erforschung der Phosphorylierung von NCC bestätigten, wurde das Projekt eingestellt, da NCC nicht an der Zelloberfläche detektiert werden konnte und in vivo Studien keinen Anhaltspunkt dafür gaben, dass TBC1D4 bei der Regulierung renaler, Na^+-transportierender Proteine eine Rolle spielt. Zusammenfassend belegt diese Dissertation, dass TBC1D4 nicht wie vermutet ENaC, AQP2 und die Na^+-K^+-ATPase in der Niere in vivo reguliert. TBC1D4 spielt jedoch eine Rolle in der systemischen Glukosehomöostase und scheint nicht nur, wie zuvor durch andere Gruppen beschrieben GLUT4 im Fett- und Skelettmuskelzellen zu regulieren, sondern auch in der Niere. In der Niere, könnte die TBC1D4-regulierte und durch GLUT4-vermittelte Glukoseaufnahme die distalen Tubuli mit Substraten für die anaerobe Glykolyse versorgen. Diese erhöhte Zufuhr von Glukose könnte zu einer verbesserten ischämischen Toleranz der distalen Tubuli gegenüber der proximalen Tubuli beitragen. Des Weiteren könnte die TBC1D4-abhängige Regulation von GLUT4 nach Aufnahme einer Mahlzeit (postprandial) von Bedeutung sein, da in dieser Phase die Glukoseverfügbarkeit und die Insulinspiegel im Blut steigen und sich die Arbeitsbelastung des renalen Tubulus erhöht.

Acknowledgement

I would like to deeply thank Prof. Johannes Loffing for giving me the opportunity to perform my PhD studies on this very interesting and challenging project in his laboratory. I am very grateful for his scientific support, helpful guidance, and encouragement throughout my thesis. Without him, this dissertation would not have been possible.
Special credits go to my thesis committee members, Prof. Carsten Wagner, Prof. Olivier Devuyst, and Prof. Hadi Al-Hasani. Thank you for your scientific inputs. Furthermore, I thank Carsten for helping with the administrative duties, Olivier for collaborating with the ex vivo experiments and Hadi, for coming twice all the way from Duesseldorf.
I would like to warmly thank Dr. Dominique Loffing-Cueni for the generation and breeding of the mice, the help with experiments, for technical as well as for moral support. I would like to thank Dr. Bob Glaudemans for his collaboration with the glucose uptake experiments. I would like to acknowledge current and former colleagues for their support and for creating a pleasant working atmosphere: Solveig, Claudia, Monique, Nourdine, Dario, Wan-Hui, Katja, Marian, Abhijeet, Stéphanie, Agnieszka, Mads, Nikolay, Jan, David, Ines, Yuya and Chiara.
Many thanks go to my colleagues Christine and Sarah for their support and help. A musical thanks goes to Stéphanie for the LaTeX-meetings but also for her friendship and to all my musician colleagues for the weekly wonderful music. To all my friends for all the laughs and the exciting scientific and non-scientific discussions: Barbara, Christin, Sophie, Rebecca, David, Elmar, Martin, Tobias, Janika and especially Friedemann. Ringrazio la mia famiglia, mio fratello Daniel, miei zii e mie zie, nonna e nonno.
I want to thank Sebastian for his daily energy and support, from whom I would not be without.
Questa tesi è dedicata a voi, Mamma e Papà, per il vostro immenso sostegno ed amore. Grazie a voi sono arrivata dove sono adesso!

Table of Contents

List of Figures

List of Tables

Abbreviations

A.U.	arbitrary unit
ad lib.	ad libitum
ADH	antidiuretic hormone
AICAR	5-aminoimidazole-4-carboxamide-1-β-D-ribofuranoside
Ala (A)	alanine
Akt	RAC-β serine/threonine-protein kinase
AMPK	adenosine monosphosphate-stimulated protein kinase
ANP	atrial natriuretic peptide
AP2	adaptor protein
AQP2	aquaporin 2
AS160	Akt substrate of 160 kDa
ASDN	aldosterone-sensitive distal nephron
ATL	ascending thin limb of Henle's loop
AUC	area under the curve
AVP	arginine vasopressin
CAP1	channel activating protein 1
CaR	calcium ion-sensing receptor
CBD	calmodulin-binding domain
CBP-D28k	Calbindin-D28k
CD	collecting duct
CDI	central diabetes insipidus
ClCKb	chloride channel Kb
CNT	collecting tubule
COPAS	complex object parametric analysis and sorting technique
CTAL	cortical TAL
DNA	desoxyribonucleic acid
DCT	distal convoluted tubule
dDAVP	1-desamino-8-D-arginie vasopressin

DTL	descending thin limb of Henle's loop
ECaC1	apical Calcium-channel
EDL	extensor digitorum longus
EGF	epidermal growth factor
EGFP	enhanced green fluorescent protein
ENaC	epithelial Na-channel
ET-1	endothelin-1
FHHt	familial hyperkalemic hypertension
GAP	GTPase activating protein
GAPDH	glyceraldehyde 3-phosphate dehydrogenase
GBM	glomerular basement membrane
GDF	GDI displacement factor
GDP	guanosine diphosphate
GDF	GDI displacement factor
GDI	GDP dissociation inhibitor
GEF	Guanine exchange factor
GFR	glomerular filtration rate
GGT	geranylgeranyl transferase
GOI	gene of interest
GSV	GLUT4 storage vesicles
GTP	guanosine triphosphate
HBSS	Hanks' balanced salt solution
HEK293	human embryonic kidney 293
HCDH	3-hydroxyacyl-Coenzyme A dehydrogenase
HD	enoyl-Coenzyme A hydratase/3-hydroxylacyl Coenzyme A dehydrogenase
HFD	high fat diet
HKG	house keeping gene
HSHFD	high salt high fat diet
I1	protein phosphatase 1 inhibitor 1
ICC	intercalated cells
ICCh	immunocytochemistry
ICH	immunohistochemistry
ICW	in cell western
IGF-1	insulin-like growth factor-1

IMCD	inner medulla collecting duct
KO	knockout
LNa/HKD	Low Na/high K diet
Lys (K)	lysine
MCAD	acyl-Coenzyme A dehydrogenase medium chain
mCCD	mouse cortical collecting duct
MDCK	Madine-Darby kidney cells
MTAL	medullary TAL
mTORC2	mechanistic target of rapamycin complex 2
NaPiIIa	Na-coupled phosphate co-tranporter
NCC	Na-Cl-cotransporter
NCX1	Na-Ca-exchanger
NDI	nephrogenic diabetes insipidus
NHE3	Na-H-exchanger 3
NKCC2	Na-K-2Cl-cotransporter
OSR1	oxidative stress response kinase-1
PCT	proximal convoluted tubule
PDGF	platelet-derived growth factor
PEC	parietal epithelial cell
PFA	paraformaldehyde
PGC-1	peroxisome proliferative activated receptor gamma, coactivator 1
PHA	pseudohyoaldosteronism
PKA/PKB	protein kinase A/B
PKD1	protein kinase D1
PI3K	phphatidyl-inositol 3-kinase
PMA	phorbol 12-myristate 13-acetate
PP4	protein phosphatase 4
Pro (P)	proline
PST	proximal straight tubule
PT	proximal tubule
PTB	phosphotyrosine interaction domain
PTB-1B	protein tyrosine phosphatase 1 β
PTH	parathyroid hormone
PV	parvalbumin
qRT-PCR	quantitative real-time polymerase chain reaction

RAAS	renin-angiotensin-aldosterone system
REP	Rab escort protein
ROMK	potassium inwardly rectifying channel
RSK1	p90 ribosomal S6 kinase-1
Scd1	stearoyl-CoA desaturase 1
SD	standard diet
Ser (S)	serine
SGK1	serum- and glucocorticoid-inducible kinase 1
SGLT1/2	Na-glucose co-transporter1/2
SNARE	soluble N-ethylmaleimide sensitive factor accachement protein receptor
SPAK	STE20/SPS1-related proline/alanine-rich kinase
T2DM	type 2 diabetes mellitus
TA	tibialis anterior
TAL	thick ascending limb
TBC	Tre2-Bub2-Cdc16
TGN	trans-Golgi network
Thr (T)	threonine
TL	thin limb of Henle's loop
Trp (W)	tryptophan
TRPM6	transient receptor caption potential channel
Tyr (Y)	tyrosine
VAMP	vesicle-membrane associated protein
WNK	with no lysine protein kinase
WT	willd-type

1 Introduction

1.1 The mammalian kidney

The mammalian kidneys are paired, bean-shaped organs lying on each side of the vertebral column behind the abdominal cavity. A thin renal capsule covers the kidney and provides stability and protection. The so-called hilus is the only opening of the capsule and the entry site for the renal artery and nerves. The hilus is also the exit site for the renal vein, ureter and lymphatics. Although the kidneys only represent 0.5% of the total body weight, they receive 20 % of the cardiac output [Boron and Boulpaep, 2009]. This seemingly disproportional distribution of blood is in fact crucial to maintain salt and water homeostasis, as will be covered in the following sections. The kidneys consist of two regions, a granular outer region (the cortex) and inner region (the medulla), the latter comprising an outer and an inner portion (Figure 1). The kidneys serve several whole body-homeostatic functions, such as the regulation of electrolytes and water, blood pressure and the maintenance of acid-base balance.

Furthermore, the kidneys filtrate and excrete toxic metabolites and waste products (e.g. urea, ammonium, K^+, organic acids and bases) from the blood, reabsorb important nutrients (glucose, amino acids) and produce hormones (renin, erythropoetin, calcitriol). The nephron is the functional unit of the kidney where fluid filtration, secretion and reabsorption takes place (Figure 1). The number of nephrons is linearly correlated with body weight. The kidney of a mouse contains around 15.000 nephrons, whereas that of a rat possess 30.000-40.000, a human 1 - 1.4 million and an elephant around 7.5 million [Alpern et al., 2013].

Each nephron consists of vascular loops in the Bowman's capsule, called the glomerulus, and a tubular system, which forms urine from the primary filtrate in the tubular lumen. Upon entering the vascular pole from afferent arterioles, blood is drained through the glomerular filtration barrier formed by fenestrated endothelial cells, the glomerular basement membrane (GBM) and slit diaphragms of interdigitating foot processes of podocytes [Boron and Boulpaep, 2009] (Figure 2). The resultant

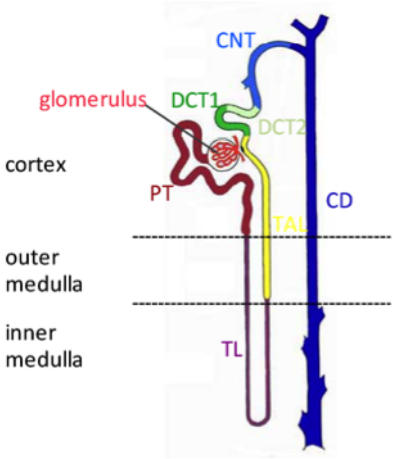

Figure 1: **The functional unit of the kidneys: the nephron** One nephron consists of a filtration unit, the glomerulus, and a tubular system divided into proximal tubule (PT), thin limbs of Henle's loop (TL), the thick ascending limb of Henle's loop (TAL), the early and late distal convoluted tubule (DCT1 and DCT2) and the connecting tubule (CNT). Around 5-8 nephrons end in one common collecting duct (CD). The transition from the cortex to the outer medulla is marked by the PT leading into the TL and the transition from outer to inner medulla is marked by the TL leading into the TAL. (Picture kindly provided by J. Loffing and B. Kaissling.)

ultrafiltrate [liquids, small solutes ($<$ 5 nm) and proteins $<$ 65 kDa] enters the Bowmans space and is further processed as it moves along the tubule. The tubular segment includes the proximal tubule (PT) divided into the proximal convoluted tubule (PCT), the proximal straight tubule (PST) or S1, S2, and S3 segment, the thin limbs of Henle's loop (TL) divided into descending and ascending thin limps (DTL and ATL), and the distal nephron. The distal nephron is especially important for the fine-tuning of ion excretion (e.g. Na^+, K^+, HCO_3^-), for the regulation of pH, and for the reabsorption of water. Within this distal part are five distinguishable segments, namely; the thick ascending limb of Henle's loop (TAL), the early and late distal convoluted tubule (DCT1 and DCT2, respectively), the connecting tubule (CNT), and the collecting duct (CD). Each segment fulfills specific task(s) and underlies definite regulatory mechanisms, which are discussed in detail in the next chapters.

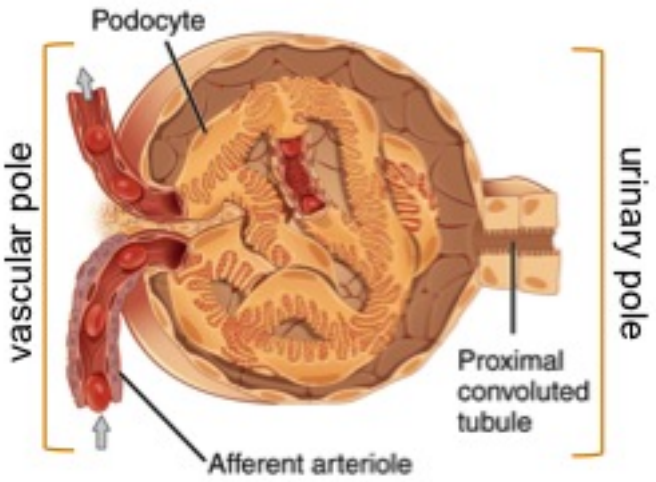

Figure 2: **The filtration unit of a nephron: the glomerulus** The formation of urine starts with blood entering from afferent arterioles at the vascular pole into the Bowman's capsule and being filtrated through fenestrations in the endothelial layer, the glomerular basement membrane (GBM) and slit diaphragms of podocytes. This pre-urine formed in the Bowman's space is further process as it leaves the glomerulus at the urinary pole. (Picture modified from Wikipedia_glomerulus)

1.2 Na^+ reabsorption along the nephron

One important function of the kidney is to maintain ion- and water homeostasis in the body. Na^+ reabsorption is of particular interest as it regulates extracellular fluid osmolality and volume. Above 99 % of Na^+ is reabsorbed via transepithelial transport along the nephron [Boron and Boulpaep, 2009]. The major driving-force for this transepithelial Na^+ transport and basically all transport processes in the kidney is generated through the Na^+-K^+-ATPase; a pump expressed at the basolateral membrane of each nephron segment. Through ATP consumption, the Na^+-K^+-ATPase takes up two K^+ and extrudes three Na^+ ions against its concentration gradient out of the cell creating a low $[Na^+]_i$ and a negative cell voltage [reviewed in Curthoys and Moe [2014]]. This gradient allows for Na^+-uptake by co- or counter-transport of various substrates (e.g. glucose, amino acids, phosphate, and sulfate) (Figure 3).

In the PT, most of the Na^+ (around 60 %) in the ultrafiltrate is taken up through the apical membrane by Na^+-coupled or -exchange secondary active transport processes, e.g. by the Na^+-glucose co-transporter 1 (SGLT1; Slc5a1) or 2 (SGLT2; Slc5a2), which co-transports one glucose molecule together with two or one Na^+, respectively. Phosphate is primarily taken up by the type IIa Na^+-coupled phos-

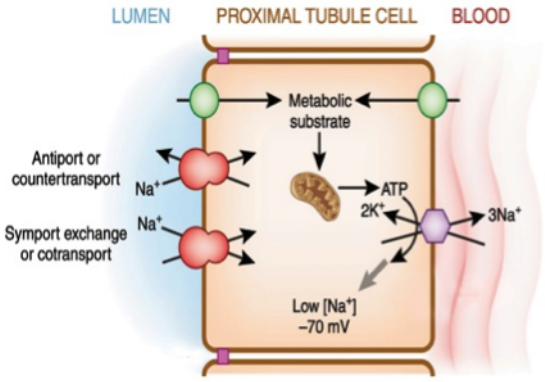

Figure 3: **Schematic overview of sodium-dependent transcellular transport processes in PT cells** A transport gradient for Na^+ from the luminal (urine) side to the blood side is generated via the ATP-consuming Na^+-K^+-ATPase leading to a low intracellular Na^+ concentration and a negative cell potential used for Na^+-mediated uptake (Y) and excretion (X) of various substrates (e.g. glucose, phosphate, sulfate). (Picture modified from Curthoys and Moe [2014].)

phate co-transporter (NaPi-IIa; Slc34a1) [Bacic et al., 2004; Hernando et al., 2000; Villa-Bellosta et al., 2009]. Next to the Na^+-coupled co-transport, Na^+ entry is also achieved by e.g. the electroneutral Na^+-hydrogen-exchanger 3 (NHE3; Slc9a3). A modest increase in Na^+-hydrogen-exchange has been described during increased glomerular filtration rate (GFR) accompanied by volume expansion [Zhou et al., 2006]. In addition, different neurohormonal and dietary influences can modify Na^+ reabsorption in the PT. The two catecholamines, namely norepinephrine and epinephrine, low angiotensin II levels and a low Na^+ intake all have stimulatory effects on Na^+ uptake [Hall et al., 1998; McDonough, 2010; Riquier-Brison et al., 2010], whereas dopamine, high angiotensin II levels and a high Na^+ diet have inhibitory effects on Na^+ uptake [Hegde et al., 1989; McDonough, 2010; Wang et al., 1993]. In the TAL, about 30 % of the filtered Na^+ is reabsorbed by the Na^+-K^+-$2Cl^-$ co-transporter (NKCC2; Slc12a2). Crucial for the functioning of NKCC2 is the lumen-positive, transepithelial potential difference generated by the potassium inwardly rectifying channel (ROMK; Kcjn1). Gene mutations in NKCC2, ROMK, the chloride channel Kb (ClCKb; CLCNKB), barttin (barttin; BSND) and the calcium ion-sensing receptor (CaR; Casr) cause Bartter syndrome I-V, respectively. Patients with Bartter syndrome present symptoms of renal salt wasting, hypokalemic metabolic alkalosis, hypercalciuria, and lowered blood pressure (reviewed in Rossier et al. [2013]). NKCC2 activity can be antagonized with pharmacological agents

known collectively as loop diuretics (e.g. furosemide and bumetanide), which prevent NaCl reabsorption in this nephron section. The TAL is also an important segment for paracellular uptake of Na^+, Ca^{2+} and Mg^{2+}. The final adjustment of urinary [Na^+] occurs in the distal segments. In the DCT, 8 % of Na^+ is reabsorbed by the thiazide-sensitive NaCl co-transporter (NCC; Slc12a3), which is expressed at the apical membrane. The late DCT (DCT2) can be distinguished from the early DCT (DCT1) by the co-expression of the amiloride-sensitive epithelial Na^+ channel (ENaC; Scnn1) [Loffing et al., 2001]. Loss-of-function mutations in the human NCC gene cause Gitelman's syndrome (familial hypokalemia-hypomagnesemia) with symptomes such as hypokalemic metabolic alkalosis, hypomagnesima and hypercalcemia [Mastroianni et al., 1996; Monkawa et al., 2000]. In addition, the DCT is crucial for Mg^{2+} homeostasis mediating active magnesium uptake by the transient receptor cation potential channel (TRPM6; Trpm6), which colocalizes with the cytoplasmic Mg^{2+}- and Ca^{2+}-binding protein parvalbumin (PV; Pvalb) in the DCT1 [Voets et al., 2004] Furthermore, the DCT regulates around 15 % of the filtered load of Ca^{2+} by transcellular Ca^{2+} transport through the apical Ca^{2+} channel (ECaC1; Trpv5), the cytosolic calcium-binding protein calbindin D28K (CBP-D28k; Calb1) and the basolateral Na^+-Ca^{2+}-exchanger (NCX1; Scl8a1), from the late DCT continuing on to the CNT [Hoenderop et al., 2001; Loffing et al., 2001; Loffing and Kaissling, 2003; Reilly et al., 1993]. In the CNT and CD, ENaC takes up most of the remaining Na^+ (1-2%). The major hormone regulating ENaC function is aldosterone; thus the nephron segments expressing ENaC are also referred to as the aldosterone-sensitive distal nephron (ASDN), which includes the DCT2, CNT and CD. Alongside ENaC expression, hallmarks of the ASDN are the expression of the mineralocorticoid receptor (MR; Nr3c2) and the 11β-hydroxysteroid dehydrogenase-2 enzyme (11β-HSD2; hsd11b2), which counteracts inappropriate MR activation via glucocorticoids, whose plasma levels exceed 100-1000 times the levels of plasma mineralocorticoids [Bostanjoglo et al., 1998; Loffing and Kaissling, 2003]. Detailed processes in the regulation of distal Na^+ transporting proteins (NKCC2, NCC, ENaC and the Na^+-K^+-ATPase) are described in the upcoming sections.

1.3 Regulation of NKCC2, NCC, ENaC and the Na^+-K^+-ATPase

Na^+ reabsorption in the TAL is increased by an augmentation of intracellular cAMP levels through various hormones, particularly vasopressin, but also parathyroid hormone (PTH), glucagon and calcitonin [Bailly, 1998]. The responsiveness to vaso-

pressin in the TAL underlines the synergism of H_2O conservation with i) its effects upon the TAL, the main diluting segment modulating medullary osmolality, and ii) its major target, the CD, where the adjustment of final urine volume occurs [Brenner and Rector, 2004]. Through binding of the peptide hormone to its receptor, the vasopressin receptor V2, the G-stimulatory protein (Gs) activates the adenyl cyclase (AC), which leads to an increase in the intracellular second messenger (cAMP) concentration. In turn, enhanced concentrations of cAMP lead to i) augmented exocytosis and phosphorylation of NKCC2 at the apical membrane, via protein kinase A (PKA) at position serine 126 (Ser126) [Knepper et al., 1999; Rieg et al., 2013] and/or ii) increased transcription of NKCC2 (as suggested by the cAMP response element in the 5'-promoter region of this gene) [Knepper et al., 1999; Mount, 2006].

In the last few years, studies on the regulatory mechanisms of NCC function and salt reabsorption in the DCT have focused on the WNK-SPAK/ORS1 pathway [reviewed in [Gamba, 2012]] (Figure 4). WNK [with no lysine (K) protein kinase] proteins are serine/threonine kinases lacking a highly conserved lysine in their catalytic domain [Wilson et al., 2001; Xu et al., 2005]. The WNK family contains four members, named WNK1-4 [McCormick and Ellison, 2011].

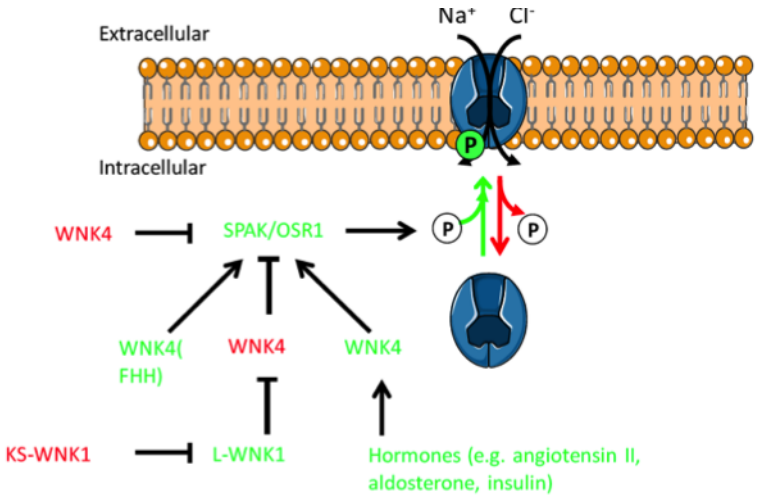

Figure 4: **Regulatory mechanisms of NCC phosphorylation via the WNK-SPAK/ORS1 pathway** NCC phosphorylation and thus activity is regulated via Ser/Thr kinases such as WNK1 (stimulatory; in green) and WNK4 (inhibitory; in red) and the STE20/SPS1-related proline/alanine-rich kinase (SPAK) and the oxidative stress response kinase-1 (OSR1) (both stimulatory) [Kahle et al., 2010]. Hormones and mutations in the WNK4 gene causing familial hyperkalemic hypertension (FHHt) can convert WNK4 to an activator of NCC. WNK4 is further regulated via two splice variants of WNK1, the long isoform (L-WNK1) suppressing WNK4 activity thus activating NCC and the kidney specific isoform (KS-WNK1) suppressing L-WNK1. (Kindly provided by J. Loffing)

So far, WNK1, WNK3 and WNK4 have been identified as being involved in renal NCC-regulation [reviewed in Gamba [2012]]. WNK proteins can also regulate the activity of other WNK kinases. For example, the ubiquitously expressed full-length WNK1 with kinase activity (L-WNK1) suppresses WNK4, what leads to up-regulation of NCC activity [Yang et al., 2005]. The kidney-specific short isoform (KS-WNK1), whose expression is restricted to the distal nephron, inhibits L-WNK1 [Subramanya et al., 2006]. KS-WNK1 is hypothesized to be a negative regulator of L-WNK1 catalytic domain, as it itself bears no kinase activity [Kroiher et al., 2001] (Figure 4). Gene mutations in WNK1 (Wnk1) and WNK4 (Wnk4) are causative for pseudohypoaldosteronism type II (PHAII), also known as familial hyperkalemic hypertension (FHHt) or Gordon's syndrome with symptoms including hypertension, hyperkalemia, hyperchloremic metabolic acidosis and hypercalciuria [Wilson et al., 2001; Yang et al., 2007]. The phenotype of this disease, which resembles an NCC-gain-of-function mutation, mirrors the phenotype of Gitelman's syndrome and can be normalized via thiazide-treatment [Mayan et al., 2002]. Thiazides, or more precisely hydrochlorothiazides, are a class of diuretic drugs known to specifically inhibit NCC. Moreover, hormones such as aldosterone, angiotensin II and insulin can alter NCC activity via their effects upon WNK4-signalling [Lai et al., 2012; San-Cristobal et al., 2009; Sohara et al., 2011; Susa et al., 2012]. The interaction of WNK-activation and NCC-phosphorylation is not direct, but is rather mediated via the protein kinase of the STE20 family termed STE20/SPS1-related proline/alanine-rich kinase (SPAK) and the oxidative stress response kinase-1 (OSR1) (Figure 5) [Vitari et al., 2005]. WNK1 and WNK4 activate SPAK/ORS1 by phosphorylation of a conserved threonine residue in the T-loop of the kinase domain (Thr233 for SPAK and Thr185 for ORS1) [Vitari et al., 2005] (Figure 5).

Activated SPAK/ORS1 have been shown to phosphorylate NKCC1, NKCC2 and NCC on serine/threonine residues in the cytosolic N-terminus (Figure 5) [Mercier-Zuber and O'Shaughnessy, 2011]. An important phosphorylation site for SPAK/-ORS1 is Thr60 in the human NCC (Thr58 in murine NCC). In patients with Gitelman syndrome, defective phosphorylation at Thr60 abolishes NCC activity and also reduces adjacent phosporylation at Thr46 and Thr55 [Pacheco-Alvarez et al., 2006; Richardson et al., 2008]. On the other hand, in $WNK48^{D561A/+}$ knock-in mice Thr53, Thr58 and serine 71 (Ser71) (human Thr55, Thr60 and Ser73) are constitutively phosphorylated resulting in PHAII [Yang et al., 2007]. Moreover, SPAK-mediated regulation of NKCC2 and NCC has been suggested to be inversely regulated: while deletion of SPAK increases NKCC2, it diminishes NCC activity. Moreover, the kidney-specific SPAK isoform (KS-SPAK), preferentially expressed in the TAL, is suggested to be a putative inhibitor of NKCC2, whereas full-length

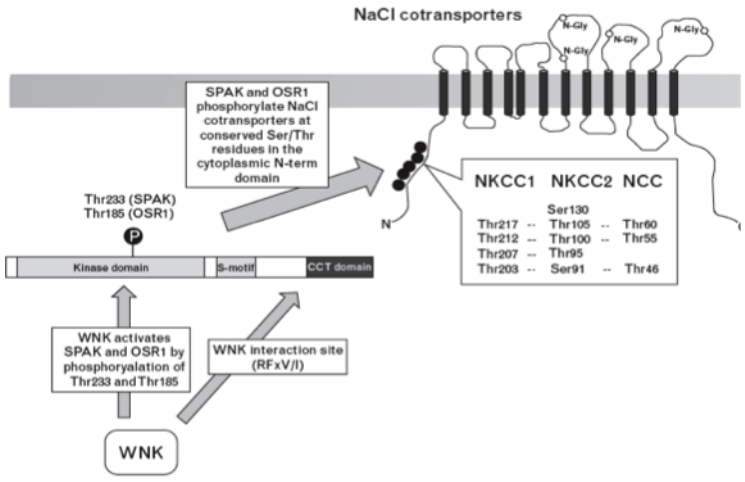

Figure 5: **Phosphorylation of SPAK/ORS1 by WNK and NKCC1, NKCC2 and NCC by SPAK/ORS1** WNKs regulate SPAK/ORS1 via phosphorylation at Thr233 (SPAK) and Thr185 (ORS1) in their kinase domain. On the other hand, SPAK and ORS1 phosphorylate NKCC1, NKCC2 and NCC at conserved Ser/Thr residues in the N-terminus (adapted from Vitari et al. [2005])

SPAK, preferentially expressed in the DCT, primarily activates NCC [McCormick et al., 2011]. Recently, another inactive SPAK isoform (SPAK2) has been discovered in the kidney; this kinase has also been shown to inhibit NKCC2 function, but to a lesser extent than KS-SPAK [Park et al., 2013]. Further regulatory proteins in the DCT affecting renal salt homeostasis and blood pressure control are the co-factor y-adducin, which modulates NCC activity in its dephosphorylated state in a dose-dependent manner [Dimke et al., 2011]; the protein phosphatase 4 (PP4), which inhibits NCC activity through the interference with the Thr58 phosphorylation site (pT58) [Glover et al., 2010]; and the hormone vasopressin [Mutig et al., 2010] [Pedersen et al., 2010; Saritas et al., 2013]. However, it is still unclear whether the vasopressin-mediated regulation of NCC is a direct or indirect effect. In fact, previous ex vivo data on isolated mouse DCTs did not show any increase in intracellular cAMP levels in response to the synthetic analogue of vasopressin, dDAVP (1-desamino-8-D-arginine vasopressin) [Imbert et al., 1975]. Recently, the protein phosphatase 1 inhibitor 1 (I1) and the protein kinase D1 (PKD1) have been shown to modulate the phosphorylation status of NCC [Picard et al., 2014; Trompf, 2013]. In addition, the aldosterone-induced protein serum- and glucocorticoid-inducible kinase 1 (SGK1) and ubiquitylation might play a role in the control of the thiazide-sensitive co-transporter [Vallon et al., 2009] (see section below). In the ASDN, ENaC

is crucial for extracellular fluid maintenance, Na^+ and K^+ homeostasis and blood pressure control. Hormones, posttranslational modifications (e.g. phosphorylation, ubiquitylation), trafficking, and proteolytic cleavage can all influence the activity of the channel. The mineralocorticosteroid aldosterone, the main hormone activating ENaC, passes the cell membrane unrestricted and causes different intracellular events. I) Aldosterone is thought to bind to the MR. The MR is then translocated to the nucleus, where it acts as transcription factor initiating the transcription through cis-elements in the 5' flanking region of the Scnn1a gene-promoter [Mick et al., 2001]. ENaC consists of three subunits, namely α, β, and γ with each subunit possessing two transmembrane domains (M1 and M2) connected by a long extracellular loop. Transcriptional activation of α-ENaC with subsequent assembling of the cytoplasmic β- and γ-subunits is thought to be one of the determining steps for the processing and trafficking of functional Na^+ channels to the cell surface. II) Aldosterone is thought to induce SGK1 expression. SGK1 decreases the ability of Nedd4-2, an E3 ubiquitin-protein ligase, to degrade ENaC via ubiquitylation. As shown from experiments in human embryonic kidney 293 cells (HEK293), SGK1-phosphorylation at position Thr246 in the conserved tryptophan domain (WW domain) of the human Nedd4-2 leads to sequestration of Nedd4-2 to the scaffolding proteins 14-3-3 [Wiemuth et al., 2010]. Under non-stimulated conditions, Nedd4-2 interacts via its WW domain with a proline- and tyrosine-rich PPXY (PY) motif in the C-terminus of ENaC resulting in increased ubiquitylation, decreased membrane abundance and proteasomal degradation [Staub et al., 1996]. In addition to the Nedd4-2-ENaC regulation, the ligase has also been shown to downregulate apical NCC expression [Arroyo et al., 2011]. Here again, the interaction between Nedd4-2 and NCC is abrogated through SGK1, although in contrast to ENaC, Nedd4-2-mediated NCC-inhibition does not occur via a PY motif. Furthermore, Vallon and coworkers demonstrated that SGK1 affects NCC expression and phosphorylation by using an SGK1-knockout (KO) mouse line [Vallon et al., 2009]. Interestingly, SGK1 has also been shown to be involved in the WNK4-signaling pathway [Rozansky et al., 2009]. In the Xenopus leavis oocyte expression system, the kinase phosphorylates WNK4 at pS1169 and pS1196 and thus attenuates the inhibitory effect of WNK4 on NCC activity. Other volume regulating hormones are known to increase (e.g. vasopressin, insulin) or to decrease [(e.g. atrial natriuretic peptide (ANP), endothelin-1 (ET-1)] [Pandit et al., 2012; Wang et al., 2006] ENaC-dependent Na^+ reabsorption. Ergonul and collaborators showed a proteolytic cleavage in the α- and γ-ENaC subunits in the kidneys of rats restricted from Na^+ or treated with aldosterone. This cleavage resulted via ENaC-activation proteases, such as furin, elastase, and prostasin [also called channel activating protease 1 (CAP1)] through the excision of an inhibitory peptide within the extracellular loop. α-ENaC increased in a 85 kDa and a cleaved 30 kDa protein,

whereas γ-ENaC showed an increase of an excised 70 kDa protein and a decrease in the 90 kDa γ-subunit [Ergonul et al., 2006]. The relevance for this plethora of ENaC regulatory mechanisms becomes apparent in pathophysiologcial states. Loss-of-function mutations in either MR or ENaC cause salt wasting, dehydration, growth retardation, hyperkalemia and metabolic acidosis. This clinical picture is also referred as pseudohypoaldosteronism type I (PHAI). Most prominently, mutations in the PY domain in one of the three ENaC subunits prevents Nedd4-2 ubiquitylation resulting in a gain-of-function mutation referred as Liddle's syndrome. Some characteristic symptoms are salt-sensitive hypertension, hypokalemia, metabolic alkalosis, low plasma renin levels, and suppressed aldosterone secretion. Spironolactone and eplerenone, two pharmaceutical MR antagonists, can inhibit MR-dependent ENaC activity [Brown et al., 2003], whereas diuretics such as amiloride, benzamil and phenamil act directly on ENaC [Benos, 1982; Canessa et al., 1994; Kleyman and Cragoe, 1988].

Summa and coworkers have shown that aldosterone can also regulate the Na^+-K^+-ATPase [Summa et al., 2001]. The Na^+-K^+-ATPase consists of a heterotrimeric complex formed by a "catalytic" α-subunit, a β-subunit (important for the maturation and insertion of the Na^+-K^+-ATPase) and an additional γ-subunit, which is only expressed in certain tissues and not required for normal protein function [Geering, 1990; Gottardi and Caplan, 1993]. The Na^+-K^+-ATPase has been shown in intracellular pools [Barlet-Bas et al., 1990; Horisberger and Rossier, 1992], which can be rapidly recruited to the plasma membrane by hormonal and intracellular stimuli (e.g. aldosterone and cAMP). This rapid effect is known as short-term control [Gonin et al., 2001; Kiroytcheva et al., 1999; Summa et al., 2001]. On the other hand, long-term regulation relies on de novo synthesis and transcriptional regulation of the Na^+-K^+-ATPase [Barlet-Bas et al., 1990]. Furthermore, several other hormones have been shown to regulate the translocation and cell surface abundance of the Na^+-K^+-ATPase, such as dopamine [Chibalin et al., 1999], promoting its endocytosis, or vasopressin [Féraille et al., 2003], mediating a rapid translocation of intracellular pools similar to aldosterone. In addition, insulin has also been demonstrated to control the Na^+-K^+-ATPase [Comellas et al., 2010], what will be described in the upcoming sections.

1.4 Water reabsorption along the nephron

Maintaining the body's H_2O homeostasis, blood pressure, volume, and osmolarity are some of the most crucial physiological tasks of the kidneys. The glomeruli fil-

trate around 180 l of fluid per day, yet only 1-1.5 l are excreted as urine. Therefore, the excretion of urine accounts for less than 1 % of total filtrate. Distribution-wise, 67 % of the filtered water is reabsorbed in the PT, 15 % in the DTL and the final urinary volume concentration is determined via regulated water reabsorption in the CNT and CD, explained in detail in the next sections. Although water can diffuse through lipid bilayers, insertion of water channels, so-called aquaporins (AQPs), can greatly increase the permeability. 13 mammalian AQPs are known so far (AQP0-12), all small proteins of around 30 kDa and of which eight are expressed in the kidney [Nielsen et al., 2002]. The most important AQPs involved in renal water reabsorption are AQP1-4 (Figure 6). AQP1 is expressed at both the apical and basolateral side of PT and DLT cells and reabsorbs water in a transcellular and active, near iso-osmolar, manner. In AQP1-deficient mice, Ma and coworkers have shown a marked decrease in urinary osmolarity, which might be due to a defect in the formation of a hypertonic medullary interstitium [Ma et al., 1998]. In humans, a loss-of-function mutation in AQP1 leads to a urinary concentrating inability during water restriction (WR) [King et al., 2001]. Starting from the CNT, expression of AQP3 and AQP4 is found at the basolateral membrane, whereas AQP2 is primarily found in the apical membrane, although a weak expression has been observed in the basolateral membrane [Christensen et al., 2003]. AQP2 expression and localization is tightly regulated via different mechanisms (e.g. hormones, phosphorylation, ubiquitylation, trafficking). The main AQP2-controlling hormone is vasopressin, also known as arginine vasopressin (AVP) or antidiuretic hormone (ADH). Under conditions such as hypernatremia or hypovolemia, vasopressin is secreted from the posterior pituitary into the blood stream and transported to the kidneys where it binds to the basolateral V2 receptor, starting an intracellular signaling cascade leading to increased intracellular cAMP levels (see also 1.3, regulation of NKCC2). Further on, phosphorylation of AQP2 at pS256 via PKA has been demonstrated to be involved in the trafficking of AQP2 from intracellular vesicles to the apical membrane [Kamsteeg et al., 2000; Katsura et al., 1997]. Endocytosis with intracellular storage and/or lysosomal degradation of AQP2 is mediated via ubiquitylation at lysine 270 (Lys270) [Kamsteeg et al., 1999, 2006].

Moreover, several other factors are important for AQP2 regulation, e.g. angiotensin II [Stegbauer et al., 2011], extracellular tonicity [Hasler et al., 2005], long-term aldosterone treatment [Hasler et al., 2003] and insulin[Bustamante et al., 2005]. Furthermore, different mouse models show evidence for the essential function of AQP2: CD-specific AQP2 deletion causes polyuria with a decrease in urine osmolarity [Rojek et al., 2006]. Similarly, this could be observed in a CD-inducible AQP2 gene deletion mouse model and in CNT-specific AQP2 knockout mice [Korteno-

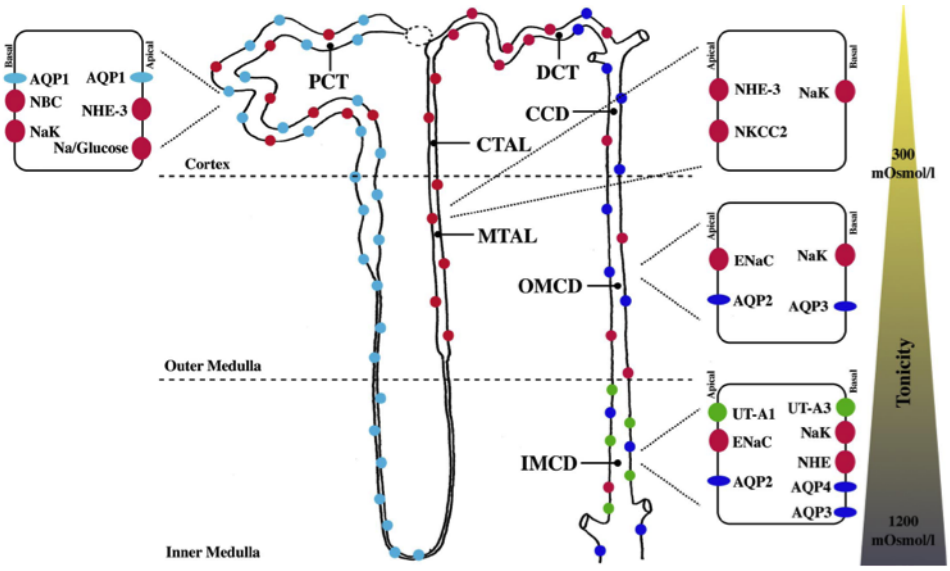

Figure 6: **Distribution of AQPs along the human nephron** AQP1 (light blue) is expressed at the apical and basolateral side of the PT and DLT, AQP2 at the apical side and AQP3 at the basolateral side from the CNT on to the CD. AQP4 can be found at the basolateral side of the inner medulla CD (IMCD) (AQP2-4: dark blue). OMCD = outer medulla CD. [Hasler et al., 2009]

even et al., 2013; Yang et al., 2006]. Nevertheless, CNT-AQP2 knockout mice are able to decrease urine volume when circulating plasma vasopressin levels are high [Kortenoeven et al., 2013]. Whereas mice bearing a total AQP2 gene deletion die within days after birth [Rojek et al., 2006], a loss-of-function mutation of AQP2 in humans is not known to be lethal (reviewed in [Robben et al., 2006]). However, these patients do represent a disability in concentrating urine. This syndrome is known as nephrogenic diabetes insipidus (NDI) (reviewed in Robben et al. [2006]). Not only loss-of-function mutation in AQP2, but also in the V2 receptors or in one of the proteins involved in the signaling cascade can cause NDI. In the case of central diabetes insipidus (CDI), where vasopressin production and/or secretion in the brain is impaired, patients show polyuria and polydipsia [Saito et al., 1997, 1999]. Administration of dDAVP rescues the phenotype in these patients, whereas in NDI patients, administration of dDAVP has no effect and hence cannot prevent polyuria and polydipsia. Overall, APQs in the kidney, especially AQP1 in the proximal and AQP2 in the distal nephron, fulfill important roles in renal water handling.

1.5 Rab-GTPases

As described above, a key aspect in the regulation of many renal transporters and channels (e.g. NKCC2, NCC, ENaC, AQP2 and the Na^+-K^+-ATPase) is their temporal and spatial localization. Especially in polarized cells, as it is primarily the case in the kidney, a determined positioning between intracellular membrane compartments is indispensable. Mediating the budding of vesicles from donor membranes and the transport, fusion and docking of these cargo-vesicles to specific acceptor membranes is carried out by so-called Rab GTPases (simplified Rab proteins), which are part of the small GTPases Ras superfamily. Rab GTPases form the largest group of the > 100 members of the Ras superfamily with 66 Rab GTPases known in humans and around 11 known in yeast, named Yptp/Sec4p [Pereira-Leal and Seabra, 2000; Schwartz et al., 2007]. Rab GTPases function as molecular switches, changing between two conformational states: the GDP-bound, "off" and the GTP-bound, "on" state. The conversion between the GDP- and GTP-bound form occurs in specific regions of the Rab protein, termed switch I, switch II and interswitch. These regions are known to interact with Rab effector proteins. GTP-binding is facilitated through guanine exchange factors (GEFs) as GDP is bound very tightly and cytosolic GTP levels are relatively high (1 mM). Although Rab GTPases are able to hydrolyze GTP to GDP at a low intrinsic rate, hydrolysis is enhanced via GTPase activating proteins (GAPs), which terminate the active, GTP-bound state of Rab GTPases (see 1.6). Beyond this simplicity, there are further proteins involved in the circuitry, e.g. the Rab escort protein (REP), geranylgeranyl transferase (GGT), the Rab GDP dissociation inhibitor (GDI) and the GDI displacement factor (GDF) (Figure 7). However, the functional description of these proteins goes beyond the scope of this thesis.

In his review "Rab GTPases as coordinators of vesicle transport", Stenmark describes the faith of Rab proteins from vesicle sorting over to vesicle uncoating, motility, tethering and fusion/docking [Stenmark, 2009]. During vesicle motility, Rab GTPases, as exemplified for Rab27, together with motor proteins (e.g. myosin Va) propel cargo-vesicles along microtubules and actin filaments [Wu et al., 2002]. In neuronal exocytosis, membrane fusion with v (vesicle)-SNAREs (soluble N-ethylmaleimide sensitive factor attachment protein receptor) such as the VAMP2 (vesicle-membrane associated protein) on cargo-vesicles and the t (target)-SNAREs [e.g. syntaxin, synaptosomal protein 25 (SNAP25)] on plasma membranes is mediated via Rab27A and Rab3A and their effector protein, rabphilin [Tsuboi and Fukuda, 2005]. In summary, Rab proteins are master regulators of secretory and endocytotic pathways. The finding of distinct Rab GTPases being expressed solely in certain

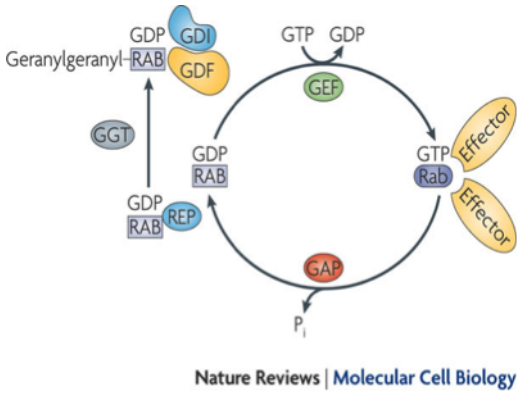

Figure 7: **Rab GTPase-regulated vesicular trafficking (I/II)** Rab GTPases activating proteins (GAPs) hydrolyze GTP to GDP, inactivating RabGTPases whereas guanine exchange factors (GEFs) catalyze GDP to GTP, activating Rab proteins. Other factors for the regulation and stabilization of RabGTPases to GDP are the Rab escort protein (REP), geranylgeranyl transferase (GGT), the Rab GDP dissociation inhibitor (GDI) and the GDI displacement factor (GDF). In the active state, RabGTPases bind to their effector proteins [Stenmark, 2009].

membranes makes them suitable molecular markers for different membrane compartments. As exemplified, Rab13 represents tight junctions, whereas Rab10 has been found in GLUT4 storage vesicles (GSV). Rab14 is used as a marker for GLUT4 containing-endosomes, and Rab4A, 4B and 8A are used to stain early endosomes [Chen and Lippincott-Schwartz, 2013a,b]. Furthermore, some Rab proteins are cell-type or cell specific, e.g. Rab17 is only expressed in epithelial cells and Rab3 is specifically found in neurons [Stenmark, 2009].

1.6 Rab GEFs and GAPs

The key switch for Rab GTPases activation is the exchange of GDP to GTP, realized by the GEFs (see 1.6.1, Figure 8). The counter-acting part, leading to the inactivation of Rab proteins and thus to a hold in trafficking are the Rab GAPs (see 1.6.2, Figure 8).

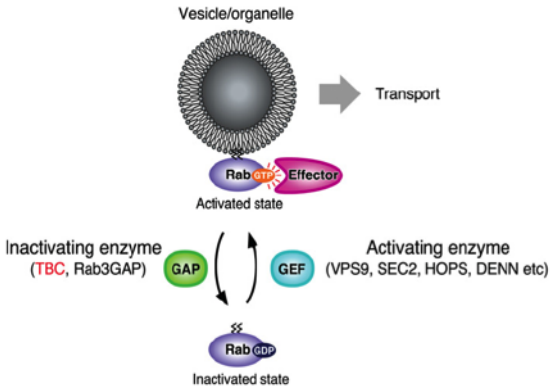

Figure 8: **Rab GTPase-regulated vesicular trafficking (II/II)** Activating enzymes, so-called guanine exchange factors (GEFs), lead to the binding of Rab proteins to GTP and their specific effector proteins in order to direct the transport of vesicles and organelles. Rab GTPases activating proteins (GAPs) of the TBC- and Rab3GAP-family hydrolyze GTP to GDP, inactivating Rab proteins [Fukuda, 2011].

1.6.1 Rab GEFs

Many efforts have been undertaken to analyze the interaction between Rab GTPases and GEFs. Yoshimura and coworkers described 17 GEFs of the DENN (DENN/MADD domain containing)/connecdenn family and their specificity towards Rab GTPases in humans [Yoshimura et al., 2010]. The GEF DENND1A activates Rab35 and binds to clathrin and clathrin adaptor protein 2 (AP2) of early endosomes. DENND2 helps recycling mannose-6-phosphate receptor from late endosomes back to the trans-Gogli network (TGN) together with Rab9 [Lombardi et al., 1993; Riederer et al., 1994]. Moreover, Rab8 and Rab10 have been found to be key players in apical and basolateral trafficking, respectively, with Rab8 functioning primarily in the transport of actin-rich membrane protrusions [Peränen et al., 1996] and in the primary cilium [Yoshimura et al., 2007]. Mutations in the fly homolog of DENND4, CRAG, showed defects in polarized sorting similar to inactivation of Rab8 and Rab10 in Madin-Darby canine kidney cells (MDCK) [Denef et al., 2008; Schuck et al., 2007]. Recently, Sano and collaborators showed that DENND4c, known as a Rab10-GEF, is part of the GLUT4 trafficking-cascade upon insulin-stimulation in adipocytes [Sano et al., 2011]. GEFs are very important for intracellular trafficking and regulation of Rab proteins, and research on DENN proteins just is in the fledgling states.

1.6.2 Rab GAPs

A key and one of the best-characterized members of the family of Rab GAPs contains the Tre2-Bub2-Cdc16 (TBC)-domain, which facilitates Rab protein inactivation. The TBC-domain was first described as a conserved domain among the tre-2 oncogene and yeast cell cycle regulators Bub2 and Cdc16 and consists of around 200 amino acids. So far, more than 40 proteins possessing the TBC-domain, also termed GAP domain, are known in humans and mice. Furthermore, GAPs are characterized through two amino acids in their TBC domain, forming the catalytic site responsible for GTP hydrolysis: arginine (R) and glutamine (Q) or the RQ finger [Albert et al., 1999]. Only 29 GAPs have been shown to possess the RQ finger, whereas other TBC-domain containing GAPs have a replacement of either R or Q with another amino acid or neither R nor Q. It is suggested that these GAPs might be inactive, but this has still to be clarified.

1.7 TBC1D4

1.7.1 Expression and structure

One Rab GAP that received increasing attention in the last couple of years because of its implication in the regulation of glucose homeostasis is TBC1D4. TBC1D4 is highly conserved among mammalian species. The GAP enzyme is expressed on chromosome 13 and 14 in humans and mice, respectively. The murine protein consists of around 1300 amino acids with a molecular weight of approximately 160 kDa (Figure 9). In the literature, TBC1D4 is also referred to as Akt substrate of 160 kDa (AS160). Indeed, TBC1D4 was found after a screen for novel substrates of the seronine/threonine kinase Akt (or protein kinase B: PKB) [Kane et al., 2002]. TBC1D4 is further build up by two phosphotyrosine interaction domains (PTB) near the N-terminus and, close to the TBC or GAP-domain at the C-terminus, by a calmodulin-binding domain (CBD). In addition, seven Akt-phosphorylation sites are known, which are important for the regulation of TBC1D4 (see later section). TBC1D4 expression can be found at low levels in liver, testis, pancreas, and at high levels in kidney, brain, lung, muscle and fat tissue [Chen et al., 2011; Lansey et al., 2012].

Spliced and shorter isoforms are known, but their role is yet less clear. A close homologue of TBC1D4 is the family member TBC1D1 (TBC1 domain family, member 1) (Figure 10). This GAP-enzyme is similarly structured with minor differences in

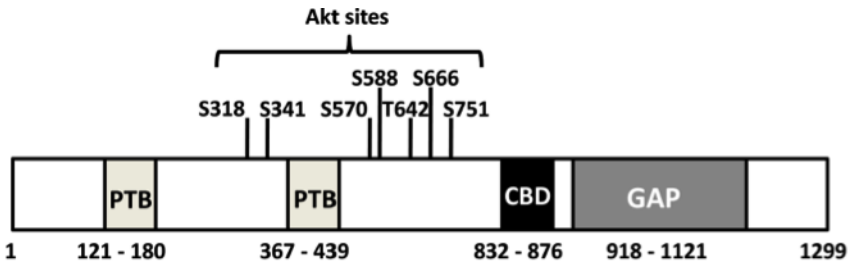

Figure 9: **Protein structure of human TBC1D4 with important domains and Akt phosphorylation sites** Human TBC1D4 consists of 1299 aa, within two phosphotyrosine interaction domains (PTB) at the N-terminus, and at the C-terminus a calmodulin-binding domain (CBD) and the GTPase activating protein GAP/TBC domain. The second PTB domain is flanked by seven Akt phosphorylation residues [Cartee and Funai, 2009].

length and phosphorylation sites. Besides Akt phosphorylation, TBC1D1 is as well phoshorylated by the AMP-kinase (AMPK), an important kinase in the metabolism of skeletal muscles (Winder, 2001). Next to TBC1D4, TBC1D1 is thought to be the major GAP in muscle tissue [Cartee and Funai, 2009; Dokas et al., 2013].

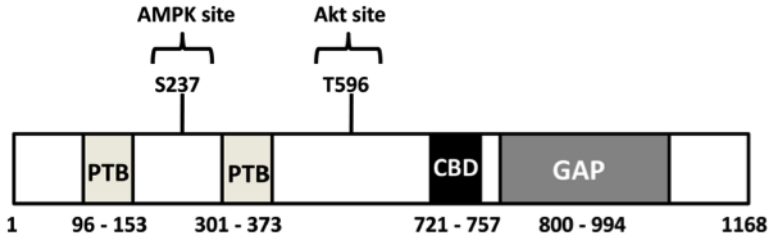

Figure 10: **Protein structure of human TBC1D1** Human TBC1D1 consists of 1168 aa, with a high similarity in structure to its close homologue TBC1D4. TBC1D1 contains an AMPK phosphorylation site at Ser237 and an Akt phosphorylation site at Thr596 (modified from Cartee and Funai [2009]).

1.7.2 Function

In addition, many studies have now shown that TBC1D4 and TBC1D1 are primarily involved in the intracellular trafficking of the insulin-regulated GLUT4-transport in fat and muscle cells [Cartee and Wojtaszewski, 2007; Kane et al., 2002]. The GAP attaches to small Rab GTPases, which keeps them inactive during basal states. In vitro assays demonstrated TBC1D4 GAP activity versus Rab2A, Rab4, Rab8A, Rab10,

and Rab11 [Larance et al., 2005; Mendes et al., 2010; Mîinea et al., 2005; Randhawa et al., 2008; Sano et al., 2007, 2008]. Rab GTPases promote translocation of GLUT4-containing/storage vesicles (GSVs). This occurs through PKBβ/Akt2 phosphorylation of TBC1D4 in response to insulin, after which TBC1D4 is sequestered by 14-3-3 proteins, leading to the conversion of Rab proteins into their active (GTP-bound) state. At this stage, GSVs are transported and GLUT4 transporters are inserted into the cell surface promoting glucose uptake.

1.7.3 Regulation

TBC1D4 is regulated through phosphorylation at seven known serine/threonine phosphorylation sites (Ser318, Ser341, Ser570, Ser588, Thr642, Ser666 and Ser751, equivalent in mice: Ser325, Ser348, Ser577, Ser595, Thr649, Ser673 and Ser758 [Chen et al., 2011; Geraghty et al., 2007; Sano et al., 2003]). In vitro as well as in vivo studies have demonstrated that next to the insulin stimulus other factors such as IGF-1 (insulin-like growth factor-1), EGF (epidermal growth factor), PDGF (platelet-derived growth factor), the phorbol 12-myristate 13-acetate (PMA) (a strong activator of the protein kinase C), leptin (an appetite-inhibiting hormone) and AICAR (5-aminoimidazole-4-caarboxamide-1-β-D-ribofuranoside) can inactivate TBC1D4 through a distinctive phosphorylation pattern [Geraghty et al., 2007; Sáinz et al., 2012; Thong et al., 2007]. The effect is mediated via different kinases; for example RSK1 (p90 ribosomal S6 kinase-1), which is activated via PMA; AMKP, which is activated via AICAR; and SGK1, which shares a high substrate specificity with Akt and itself is activated via aldosterone. Moreover, insulin and IGF-1 lead to TBC1D4-phosphorylation of Ser341 and Thr642, promoting the binding to 14-3-3 proteins [Geraghty et al., 2007]. On the other hand, AMPK phosphorylates TBC1D1 at Ser237 and Thr596 (paralog to TBC1D4 Thr642) to induce 14-3-3 binding [Chen et al., 2008]. Ramm and coworkers suggested that binding to 14-3-3 of Rab GAPs is important for insulin-stimulated GLUT4 translocation [Ramm et al., 2006]. Furthermore, the specificity of some protein isoforms is determining the interaction of TBC1D4 with other proteins, e.g. Akt2 is thought to be the major isoform required for insulin action within the Akt isoforms (Akt1-3) [Cho et al., 2001; Kempe et al., 2010; Ng et al., 2008; Schultze et al., 2012]. Likewise, binding of TBC1D4 to the 14-3-3 protein is stronger towards the β, ϵ, and σ isoforms, and rather weak towards the γ and θ isoforms [Liang et al., 2010].

1.8 TBC1D4 in vitro and in vivo

The role of TBC1D4 is well characterized from in vitro and in vivo studies in so-called classical insulin-responsive tissues, namely fat and skeletal muscle tissue. The two tissue types together take up 80-90 % of the ingested glucose, with skeletal muscle tissue having the greater glucose disposal capacities.

1.8.1 TBC1D4 in vitro

In 3T3-L1 adipocytes, knockdown of TBC1D4 results in increased cell surface expression of GLUT4 at the basal state [Eguez et al., 2005; Larance et al., 2005]. Moreover, when mutating four main phosphorylation sites (Ser318, Ser588, Thr642 and Ser751) to non-phosphorylatable alanine (TBC1D4-4P mutant), insulin-stimulated GLUT4 translocation as well as membrane docking and insertion are impaired in 3T3-L1 adipocytes [Bai et al., 2007; Jiang et al., 2008; Sano et al., 2003] and L6 myocytes [Thong et al., 2007]. In addition, overexpression of the 4P-mutant affects GLUT4 exocytosis, but not its endocytosis in 3T3-L1 adipocytes [Zeigerer et al., 2004]. Beyond the analysis of TBC1D4 in classical insulin-responsive tissues, several groups described its GAP function in non-classical insulin responsive tissues, for example the pancreas [Bouzakri et al., 2008], lung [Comellas et al., 2010], brain [Grillo et al., 2009], and kidney [Alves et al., 2010; de Baaij et al., 2013; Jung and Kwon, 2010; Kim et al., 2011; Liang et al., 2010]. Bouzakri and coworkers showed that TBC1D4 deletion causes an increased basal insulin excretion whereas glucose-stimulated insulin secretion is impaired in sorted human pancreatic β-cells and murine MIN6B1 cells. Interestingly, loss of TBC1D4 leads to increased apoptosis and caspase-3 activation, pointing to a prosurvival role of pancreatic TBC1D4. In the lung, insulin stimulates Na^+-K^+-ATPase translocation through Akt phosphorylation of TBC1D4 and Rab10 activity [Comellas et al., 2010]. Interestingly, Akt-dependent GLUT4 translocation was shown in rat hippocampus after intra-cranial insulin injection, although without a direct proof of TBC1D4 involvement [Grillo et al., 2009]. In the kidney, TBC1D4 has been described to be involved in the trafficking regulation of AQP2, ENaC, and Na^+-K^+-ATPase (discussed in greater detail in the following sections) [Alves et al., 2010; Kim et al., 2011; Liang et al., 2010].

1.8.2 TBC1D4 in vivo

Recently, different genetically modified mice models with altered TBC1D4 expression and phosphorylation patterns have been created, primarily demonstrating the GAP-impact on whole-body glucose homeostasis [Chen et al., 2011; Ducommun et al., 2012; Lansey et al., 2012; Wang et al., 2013]. The group of Lansey et al. generated a TBC1D4-deficient mouse line ($D4^{-/-}$) by the excision of exon 1, including the transcription start and part of the downstream intron. Further, another group analyzed the phenotype of TBC1D4-deficient mice with an excision of the tenth exon harboring the T649A mutation site [Chen et al., 2011; Ducommun et al., 2012; Wang et al., 2013]. Furthermore, a TBC1D4 T649A knockin mouse line (D4 T649 KI) has been generated in order to investigate the effect of the crucial Thr649 binding site to 14-3-3 proteins, when mutated to a non-phosphorylatable alanine [Chen et al., 2011]. In contrast to the other mouse lines, the GAP domain in the TBC1D4 T649A knockin mice is still functional. Further models such as a $TBC1D4^{-/-}$ mouse model (similar to our model, see 3.2.13), a knockout model of the close homologue TBC1D1 ($D1^{-/-}$) an a double knockout of TBC1D4 and TBC1D1 (TBC1D4/TBC1D1 knockout: $D4/D1^{-/-}$) have been designed by Chadt and coworkers [Chadt et al., 2015, 2008]]. In Table 1 the phenotype in regard to glucose homeostasis of these models is summarized. For body weight gain, fasted plasma glucose levels, insulin sensitivity and glucose uptake in adipocytes, the $TBC1D4^{-/-}$ model of Chadt et al. behave differently compared to the other two $TBC1D4^{-/-}$ models [Lansey et al., 2012; Wang et al., 2013]. In terms of BW gain, plasma glucose and insulin levels as well as glucose uptake in muscle, the TBC1D4 KI mouse line reveals a similar phenotype as the TBC1D4 KOs. Since the KI mouse model overexpresses the dominant negative regulator, whereas the KOs have lost this molecular break, these similarities are surprising. But in fact, the KI mice have increased GLUT4 abundances in adipocytes and soleus muscle as well as an increased ex vivo insulin-stimulated glucose uptake in adipocytes, which is opposite to what is observed in the $TBC1D4^{-/-}$ mice (Table 1).

As previously mentioned, TBC1D4 is a close homologue of TBC1D1 and both have been shown to regulate GLUT4 trafficking [Chadt et al., 2008; Dokas et al., 2013; Szekeres et al., 2012]. Interestingly however, TBC1D4 and TBC1D1 reveal fairly different expression patterns. Whereas TBC1D4 is mainly expressed in adipocytes and oxidative muscles (e.g. soleus, vastus lateralis muscles, etc.), TBC1D1 shows almost no abundance in adipocytes, but is instead mainly expressed in glycolytic muscles [e.g. extensor digitorum longus (EDL), tibialis anterior (TA) and quadriceps]. As expected, GLUT4 expression in TBC1D1 and TBC1D4 KOs is specifically

	BW		PGlc fasted		Plns fasted		GT		IS		GLUT4			GU Adip		GU Soleus	
	♀	♂	♀	♂	♀	♂	♀	♂	♀	♂	Adip ♂	Sol ♂	EDL ♂	- ins ♂	ins ♂	- ins ♂	ins ♂
$D4^{-/-}$ (ex1)[1]	↔	↔	↓	↓	↓	↔	↔	↓	↓	↓	↓	↓	↔	↑	↓	↔	↓
$D4^{-/-}$ (ex10)[2]	↔	↔	↓	-	↔	-	↔	-	↓	-	↓	↓	↔	↑	↓	↔	↓
$D4^{-/-}$ (ex1)[3]	↓	-	↔	-	-	-	↔	-	↔	-	↓	↓	↔	↔	↓	↔	↓
$D4/D1^{-/-}$ [3]	↓	-	↔	-	-	-	↓	-	↓	-	↓	↓	↓	↔	↓	↔	↓
D4T469A KI[4]	↔	↓	↔	-	↔	-	↓	↓	-	-	↑	↑	-	↔	↑	↔	↓
$D1^{-/-}$ [3]	↓	-	↔	-	-	-	↔	-	↔	-	↔	↔	↓	↔	↔	↔	↔

Table 1: **Comparison between different TBC1D4 mouse models** Compared body weight (BW), plasma glucose (PGlc) fasted, plasma insulin (PIns) fasted, glucose tolerance (GT), insulin sensitivity (IS), GLUT4 content in different tissues (adip. = adipocytes, sol. = soleus, EDL = extensor digitorum longus) and glucose uptake (GU) in diefferent TBC1D4 and TBC1D1 knockout models: [1][Lansey et al., 2012], [2][Wang et al., 2013], [3][Chadt et al., 2015], [4][Chen et al., 2011]. All data points refer to their corresponding control (wild-type) mice, ↔ = similar, ↑ = increased, ↓ = decreased, - = not determined, ins = insulin, $D4^{-/-}$ = TBC1D4 knockout, ex = exon, D4/D1 = TBC1D4/TBC1D1 double knockout, D4 T649 KI = TBC1D4 T649 knockin, $D1^{-/-}$ = TBC1D1 knockout

reduced in areas where these Rab GAPs are normally highly expressed (Table 1). Further, as shown in table 1, data suggest that TBC1D1 might be important for the regulation of body weight given how the naturally occurring loss-of-function mutation in TBC1D1 prevents from diet-induced obesity in the diabetes-resistant SJL mouse strain [Chadt et al., 2008]. Although the $TBC1D4^{-/-}$ models (1-3) all miss the GAP enzyme, the findings were not always identical (Table 1). Discrepancies may be explained for instance by strain differences, the different targeting strategies for the generation of knockout and knockin mice, sensitivity of the applied method, age, and sex of the animals. One commonly used method to assess the variability between different studies is to perform a meta-analysis, which combines and compares the individual studies [Denker and Pollock, 1992; Matsuda and DeFronzo, 1999]. Overall, the results are very complex and no clear statement on TBC1D4 in vivo function can be made so far. On the one hand, $TBC1D4^{-/-}$ mice appear to be glucose tolerant, but on the other hand they are insulin resistant. In humans, both GAPs, TBC1D4 and TBC1D1, are known to interfere with glucose metabolism and are associated with type 2 diabetes mellitus (T2DM) and obesity, respectively [Chadt et al., 2008; Karlsson et al., 2005, 2006]. Patients with a truncation of TBC1D4 (R363X) suffer from sever postprandial hyperinsulinemia [Dash et al., 2009] and mutation of TBC1D1 (R125W) increases the risk of developing obesity [Meyre et al., 2008; Stone et al., 2006]. However, further research is needed

to understand the underlying molecular mechanisms and the variability between the different models.

1.8.3 TBC1D4 expression in the kidneys

Although the kidneys are not typically considered as insulin-responsive tissues, more and more evidence for renal TBC1D4 expression have accumulated from in vitro and in vivo studies [Alves et al., 2010; de Baaij et al., 2013; Jung and Kwon, 2010; Kim et al., 2011; Liang et al., 2010; Mendes et al., 2010]. In our work [Lier et al. [2012]: see appendix Paper 1], we described the detailed expression of TBC1D4 along the mouse nephron using immunohistochemistry (IHC) and canonical nephron segment-specific markers (Figure 11). TBC1D4 was found in the cytosol of parietal epithelial cells (PECs) of the Bowman's capsule, in the thin and thick limbs, in the DCT, and in the CNT/CD. In the latter, both, principal and intercalated cells stained for TBC1D4. In PT cells, no TBC1D4 signal was observed.

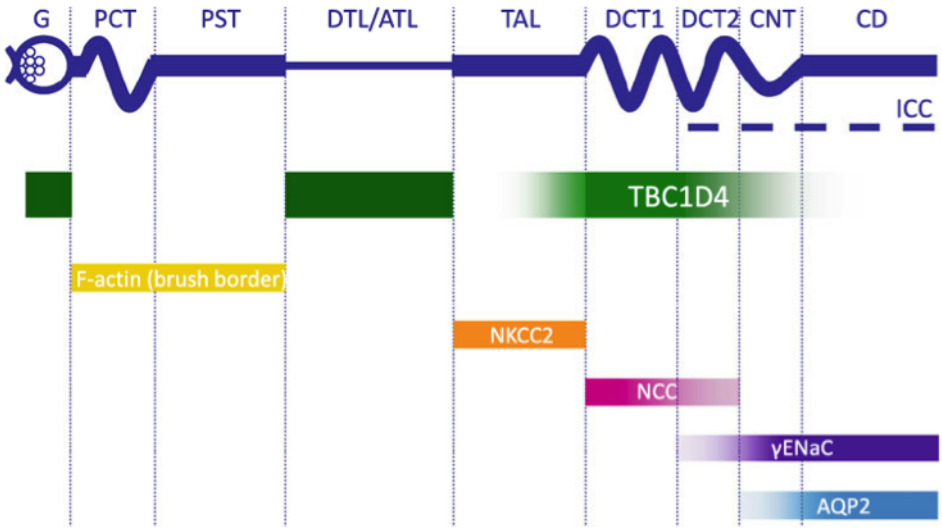

Figure 11: **Representation of TBC1D4 abundance along the nephron** TBC1D4 abundance along the nephron was analyzed by IHC using specific segmental markers and/or morphological characteristics. The Rab GAP was found in the glomerulus, in the thin limbs (DTL/ATL), recognizable by very distinctive morphological characteristics, in the TAL shown by co-localization with NKCC2, in the DCT1 and DCT2 with NCC, and CNT/CD with yENaC and AQP2. Only in the PT (PCT and PST), recognizable through f-actin staining in the brush border, no TBC1D4 expression was found (ICC = intercalating cells) [adapted from (Lier et al., 2012)].

The recent accumulation of in vitro findings of TBC1D4 being a possible regulator

in the intracellular trafficking of ENaC, AQP2 and the Na^+-K^+-ATPase, and thus crucial for renal ion and water homeostasis, is discussed in greater detail in 1.11.

1.9 The role of the kidneys in glucose homeostasis

The kidneys reabsorb all filtered glucose, around 180 g/day, within the first tubular segments after glomerular filtration. In healthy individuals the urine is essentially free from glucose. As mentioned in 1.2, the SGLTs, localized at the apical membrane, are responsible for renal glucose uptake in an insulin-independent manner (Figure 12).

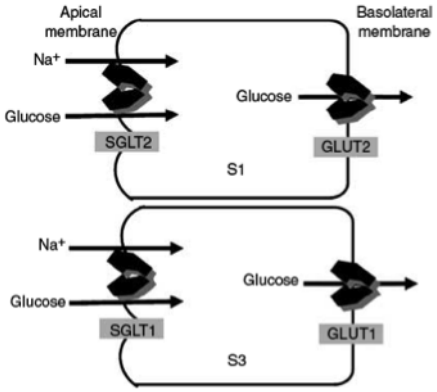

Figure 12: **Transepithelial glucose uptake in the PT** The Na^+-glucose co-transporter SGLT2, a low-affinity high-capacity transporter for glucose located at the apical side takes up glucose together with Na^+ in a 1:1 ratio in the S1 and S2 segments or PCT and the basolateral extrution of glucose is mediated via GLUT2. In the later part of the PT, the S3 segment or PST, the high-affinity low-capacity SGLT1 takes up one glucose molecule together with 2 Na^+ ions. GLUT1 at the basolateral side transports glucose out of the cell. [Lee and Han, 2007]

In S1 and S2 segments of the PCT, SGLT2 reabsorbs 90 % of the filtrated glucose together with Na^+ (ratio of 1:1) and with a low glucose affinity but high capacity. In the PST/S3 segment, the remaining 10 % of glucose are reabsorbed together with Na^+ (1 glucose:2 Na^+) by SGLT1, which in contrast to SGLT2 is a high-affinity low capacity transporter [Lee and Han, 2007]. With increasing intracellular glucose concentrations, glucose re-enters the systemic circulation via specific facilitative glucose transporters (GLUTs) expressed at the basolateral membrane. GLUT2 and GLUT1 facilitate glucose exit in the S1 and S3 segment, respectively. Beyond glucose filtration and reabsorption, the kidneys are able to perform gluconeogenesis. This renal task has been underestimated for many years as the net balance technique failed to

detect a difference between renal arterial and venous blood concentration [Björkman et al., 1980; Krebs and Yoshida, 1963]. This was due to the fact that the net balance technique does not take into account the contemporaneous and distinct release and uptake processes of glucose in the kidney. During an overnight fast, 20-25 % of the glucose release derives from the kidneys and 75-80 % from the liver. In humans, the kidney is, after the liver, the only organ with significant amounts of the glucose-6-phosphatase, a rate-limiting enzyme in gluconeogenesis. This enzyme is expressed in the renal cortex, more specifically in PT cells, which are able to produce energy by oxidative phosphorylation. Further, PT cells rely on oxygen as they cannot perform glycolysis, which renders them very sensitive to low oxygen levels. Thus, PT cells are one of the first cells to be damaged under hypoxic/ischemic states. In contrast, the renal distal tubule cells are able to perform anaerobic glycolysis. They possess glycolytic enzymes and thus can better handle a rather oxygen-poor/relatively hypoxic environment (as e.g. in the renal medulla). Also in the S3 segment, normally involved in transepithelial glucose transport, low levels of glycolytic enzymes have been detected, which may provide energy via the glycolytic pathway [Thorens, 1993]. Overall, the processes of oxidative phosphorylation and glycolysis in the kidneys account for around 10 % of glucose utilization of all ingested glucose, whereas 45 % is taken up in the liver for later glycogen formation, 30 % by the skeletal muscle, 15 % by the brain and a small percentage by the adipose tissue [Meyer et al., 2002b]. However, the molecular mechanisms underlying renal glucose utilization and consumption are not completely understood.

1.10 GLUT4 expression in the kidney

Several GLUTs (e.g. GLUT1, 2, 3, 4 and 12) have been suggested to be expressed in the kidneys at mRNA and protein levels [Brosius and Heilig, 2005; Linden et al., 2006]. However, the only well established GLUTs are, as mentioned above, GLUT1 and GLUT2 involved in the transepithelial glucose uptake in the PCT (S3 segment) and PST (S1/S2 segment), respectively. However, GLUT1 and GLUT2 in the PT represent an exception to the rule as in most cases GLUTs facilitate glucose transport from outside to inside the cell [Bell et al., 1990]. Next to GLUT1 and GLUT2 in the PT, the expression patterns and the role of other glucose transporters in the kidney are less clear. Beyond the PT, expression of GLUT1 has been found at moderate levels in cells of the thin and thick ascending limbs and at high levels in the connecting segment and the CD, with levels peaking in the intercalated cells of the CD [Thorens, 1993]. The distinct renal GLUT1 expression correlates with the glycolytic activity

in these cells [Ross et al., 1986; Uchida and Endou, 1988]. Furthermore, GLUT1 is present in the glomerulus; predominantely in mesangial cells, but also in podocytes, endothelial cells and in the PECs [Brosius et al., 1992; Heilig et al., 1997, 1995]. In podoyctes, GLUT1 has been found to be regulated by insulin [Coward et al., 2003, 2005]. Studies in other tissues have further demonstrated a regulation of GLUT1 via insulin and TBC1D4 similarly to GLUT4 [Calderhead et al., 1990; Clarke et al., 1994; Fischer et al., 1997; Mendes et al., 2010]. It has further been documented that GLUT4, the main insulin-responsive glucose transporter [Birnbaum, 1992] found in adipocytes and skeletal muscle cells [Cartee and Wojtaszewski, 2007; Sano et al., 2003], is expressed in the kidney. Similar to GLUT1, mesangial cells [Brosius and Heilig, 2005], podocytes [Coward et al., 2003], smooth muscle cells forming the endothelia [Brosius et al., 1992], the TAL [Chin et al., 1993] and distal tubules [Albiston et al., 2011] express GLUT4. Anderson and coworkers verified GLUT4 expression by immunogold staining in juxtaglomerular cells (renin secreting cells). Next to the expression, attempts were made to analyze the intracellular localization of GLUT1 and GLUT4. Anderson and coworkers hypothesized similar trafficking and secretory mechanisms for GLUT4 and renin [Anderson et al., 1998]. However, they discovered that renin accumulates in secretory granula, whereas GLUT4 localizes to vesicles in close vicinity to the TGN. Moreover, Rea and James showed basolateral membrane staining for GLUT1, and an enriched intracellular staining for GLUT4 in MDCK cells [Rea and James, 1997]. However, there are discrepant findings concerning GLUT1 and GLUT4 expression along the kidney, and no clear picture about the localization along the nephron, the intracellular expression and the function of other GLUT proteins in the kidney, apart from GLUT1 and GLUT2 in the PT, has so far been reliably drawn.

1.11 In vitro evidence for renal intracellular trafficking regulation by TBC1D4

Recently, several in vitro analyses have suggested a role for TBC1D4 in the trafficking regulation of renal water and ion channels and transporters including NCC, ENaC, AQP and the Na^+-K^+-ATPase. From experiments performed in Xenopus leavis oocytes, insulin treatment has been shown to augment NCC's activity together with its phosphorylation at Thr58. This effect is mediated by phosphatidylinositol 3-kinase (PI3K), mTORC2 and Akt1 [Chávez-Canales et al., 2013]. Moreover, Delpire and Gagnon identified a SPAK-binding motif (GRFEINLISP) on TBC1D4 [Delpire and Gagnon, 2007]. Hence, TBC1D4 might modulate NCC's action in regard to

trafficking, activity and/or phosphorylation. As a similar cascade is present in the TAL, this might be also true for NKCC2 regulation. From in vitro and mass spectrometry analysis, endogenous TBC1D4 was shown to interact with the N-terminus of the SNAP-tagged Na^+-K^+-ATPase α-subunit in MDCK cells [Alves et al., 2010]. Similar to GSVs, the Na^+-K^+-ATPase is stored in intracellular compartments and undergoes regulated intracellular epithelial membrane trafficking. Coexpression with TBC1D4 in COS cells shows intracellular retention of the Na^+-K^+-ATPase [Alves et al., 2010]. Furthermore, reduced activity levels of the adenosine monophosphate-stimulated protein kinase (AMPK), a kinase especially important for contraction-induced phosphorylation of TBC1D4, lead to an increase of Na^+-K^+-ATPase endocytosis in MDCK cells [Alves et al., 2010]. Recently, a connection between TBC1D4 and ENaC has been suggested [Liang et al., 2010]. Liang and colleagues showed that aldosterone promotes SGK1-mediated phosphorylation of TBC1D4, similarly to the insulin Akt-mediated phosphorylation of TBC1D4, which hence facilitates ENaC trafficking and insertion into the membrane in mouse cortical collecting duct (mCCD) cells. Another example of a putative role of TBC1D4 in vivo was demonstrated by the group of Kwon [Kim et al., 2011]. In mpkCCD cells and M1 cells, TBC1D4 siRNA knockdown resulted in increased AQP2 expression at the plasma membrane in the absence of dDAVP stimulation [Jung and Kwon, 2010; Kim et al., 2011]. The V2 receptor, which regulates AQP2 expression, is a G-protein coupled receptor acting via the cAMP and PKA signaling pathway. How TBC1D4 might be involved in the translocation cascade of AQP2 remains to be established. However, despite these numerous in vitro data suggesting a role for TBC1D4 in regulating renal ion and water transporting proteins, and the fact that TBC1D4 is expressed along the nephron, the in vivo role of TBC1D4 in the kidney is completely unknown.

2 Objectives of the thesis

The overall objective of this thesis was to analyze the physiological relevance of TBC1D4 in the kidney. Our immunohistochemical study revealed TBC1D4 abundance in distinct parts of the nephron [Lier et al., 2012]. Based on these findings and the in vitro data showing the involvement of TBC1D4 in the control of water and ion transporting proteins (ENaC, AQP2, Na^+-K^+-ATPase), the major objective was to define whether TBC1D4 regulates the intracellular vesicular trafficking and activity of these proteins and/or is responsible for renal glucose homeostasis in vivo. To this end, the following specific aims were addressed:

2.1 Investigation of the role of TBC1D4 in the kidney by using TBC1D4$^{-/-}$ mice

Based on in vitro data, we analyzed the role of TBC1D4 in the regulation of renal ion and water transporting proteins (e.g. ENaC, AQP2 and the Na^+-K^+-ATPase) by using a TBC1D4$^{-/-}$ mouse model. In addition, we investigated the renal gene and protein expression of GLUT4 along the nephron of wild-type (WT) mice as well as the role of TBC1D4 in the control of renal GLUT4 trafficking and activity by comparing the phenotype of WT and TBC1D4$^{-/-}$ mice.

2.2 Compensatory mechanisms in DCT cells of TBC1D4$^{-/-}$ mice assessed by microarray analyses

With our findings of TBC1D4 not being involved in the regulation of renal ion and water transporting proteins in vivo, we investigated a possible up- and/or down-regulation of gene products, which might compensate for the loss of TBC1D4 in renal tubules of TBC1D4$^{-/-}$ mice. To reach this objective, we used isolated-DCT cells by the complex object parametric analysis and sorting technique (COPAS) and

performed microarray analyses for the comparison of gene expression between DCT cells of WT and TBC1D4$^{-/-}$ mice.

3 Materials and Methods

3.1 Material

3.1.1 Compounds/Reagents

1,4-diazabicyclo(2,2,2)octane	Sigma-Aldrich, Germany
10x blocking buffer	Sigma-Aldrich, Germany
2-propanol Isopropanol	Sigma-Aldrich, Germany
3H-2-deoxyglucose	Perkin Elmer, USA
4-(2-hydroxyethyl)-1-piperazineethanesulfonic acid (HEPES)	AppliChem, Germany
4',6-diamidino-2-phenylindole (DAPI)	Sigma-Aldrich, Germany
5x FirePol Master Mix	Solis BioDyne, Estonia
5x ImProm-II^{TM} reation buffer	Promega, USA
Aceton	Sigma-Aldrich, Germany
Acrylamide	AppliChem, Germany
Agarose	Promega, USA
Albumin	VWR International
Aldosterone	Sigma-Aldrich, Germany
Ammonium persulfate (APS)	AppliChem, Germany
Ampicillin	Roche, Switzerland
Boric acid	Sigma-Aldrich, Germany
Bovine serum albumin (BSA)	Sigma-Aldrich, Germany
Calcium chloride ($CaCl_2$)	Riedel-de-Haen,Germany
Calyculin A	LifeTechnologies, USA
Collagenase	Worthington Biochemical Corp
Complete Protease Inhibitor Cocktail Tablets	Roche Diagnostics GmbH
CooAssay Protein Dosage Reagent	Uptima/Interchim, France
Coommassie brilliant blue G-250	Thermo Sientific, USA
Cytochalasin B	Sigma-Aldrich, Germany
D-Glucose	Sigma-Aldrich, Germany
Dexamethasone	Sigma-Aldrich, Germany
Dimethylsulfoxid (DMSO)	Fluka, Germany
Disodium hydrogen phosphate (Na2HPO4)	Fluka, Germany
Dithiothreitol (DTT)	AppliChem, Germany
DNase I	Sigma-Aldrich, Germany
dNTPs	Fermentas, Germany
Dulbecco's modified eagle medium (DMEM)	LifeTechnologies, USA

EcoRI	Fermentas, Germany
Emulsifier-SafeTM liquid scintillation cocktail	Perkin Elmer, USA
Ethylenediaminetetraacetic acid (EDTA)	Fluka, Germany
EZ-Link Sulfo-NHS-LC-Biotin	Thermo Sientific, USA
Fetal bovine serum (FBS)	Lonza, Switzerland
G-418 sulphate/Gentamycin	PAA laboratories, Inc., Austria
Gel Red Nucleic acid stain	Biotum, USA
GeneRulerTM 100 bp DNA Ladder	Thermo Sientific, USA
Glacial acetic acid	MERCK, Germany
Glycergel	DakoCytomation, Denmark
Glycerol	Sigma-Aldrich, Germany
Glycine	Biossolve, The Netherlands
Hank's balanced salt solution (HBSS)	Lonza, Switzerland
Hyaluronidase	Sigma-Aldrich, Germany
ImProm-II^{TM} reverse transcriptase	Promega, USA
Indinavir	Sigma-Aldrich, Germany
Insulin	Sigma-Aldrich, Germany
IsoFlo® (isoflurane)	Abbott AG, Switzerland
LB Broth Base	LifeTechnologies, USA
Magnesium chloride ($MgCl_2$)	Fluka, Germany
Magnesium sulfate ($MgSO_4$)	Sigma-Aldrich, Germany
Mannitol	Fluka, Germany
Metafectene Pro	Biontex, Switzerland
Methanol	Sigma-Aldrich, Germany
Nitrocellulose (Whatman Protran)	Millipore, USA
Non-essential amino acids	Gibco-BRL, The Netherlands
Normal goat serum (NGS)	LifeTechnologies, USA
Odyssey^{TM} Blocking Buffer	LI-COR Biosciences, Germany
Paraformaldehyde (PFA)	AppliChem, Germany
Penicillin/Streptomycin	LifeTechnologies, USA
Phosphatase inhibitor (PhosStop)	Roche, Switzerland
PhosStop	Roche, Switzerland
Potassium chloride (KCl)	Sigma-Aldrich, Germany
Potassium dihydrogen phosphate (KH_2PO_4)	Fluka, Germany
Potassium hydroxide (KOH)	Sigma-Aldrich, Germany
Quick change® XL1-blue supercompetent E. coli	Agilent Technologies, USA
Random primers	Promega, USA
RiboLock^{TM} RNase	Fermentas, Germany
RIPA Buffer, 1x	Thermo Sientific, USA
Select Agar	LifeTechnologies, USA
SingleQuots® BioWhittaker	Lonza, Switzerland
Sodium azide (NaN_3)	MERCK, Germany
Sodium chloride (NaCl)	Sigma-Aldrich, Germany
Sodium dodecyl sulfate (SDS)	Carl Roth GmbH, Germany
Sodium hydroxyde (NaOH)	Fluka, Germany
Sodium pyruvate	Gibco-BRL, The Netherlands
Sodium-cacodylatetrihydrate	Fluka, Germany

Streptavidin agarose resins (beats)	Thermo Sientific, USA
Sucrose	Fluka, Germany
Sulfo-NHS-LC Biotin	Thermo Scientific, USA
Super optimal browth base with catabolite repression (SOC)	New England Biolabs, USA
Tetramethylethylenediamine (TEMED)	AppliChem, Germany
Trishydroxymethylaminomethane (Tris)	Biossolve, The Netherlands
Triton-X	Sigma-Aldrich, Germany
Tween-20	Sigma-Aldrich, Germany
β-mercaptoethanol	Sigma-Aldrich, Germany

3.1.2 Instruments/Materials

2100 Bioanalyzer	Agilent Technologies, USA
850 professional IC ion chromatograph	Metrohm, Switzerland
ABL800 Flex (blood gas analyzer)	Radiometer, Denmark
Accu-Chek Aviva System	Roche, Switzerland
BP2000 Series II (Blood Pressure Analysis System)	Visitech Systems, USA
Cell culture CO2 incubator	Sanyo, USA
Centrifuge 5415 R	Eppendorf, Germany
Clinitubles (capillary tubes)	Radiometer, Denmark
CLS150X (steromicroscope)	Leica, Germany
COPAS	Union Biometrica, USA
Culture plates (6, 12 wells, etc.)	Nunc, Denmark
DM6000B microscope	Zeiss, Germany
Glass-slides	Duran Group, Germany
Housing cage (type II long IVC)	Techniplast, Italy
Leica DM IL	Leica Microsystems, Germany
LightCycler® 480 II instrument	Roche, Switzerland
LSM510Meta(confocal microscope)	Zeiss, Germany
Metabolic cage	Techniplast, Italy
Microm (cryostat)	Leica Microsystems, Switzerland
Micromanipulator	Narishige International, UK
Microtrainer LH (Lithium Heparin) tubes	BD Diagnostics, USA
NanoDrop ND-1000 spectrophotometer	Thermo Sientific, USA
Nylon sieves (250, 212, 100 and 40 μm)	BD, USA
Odyssey IR-scanner detection system	LI-COR Biosciences, Germany
Packard Tri-Carb 2900	Perkin Elmer, USA
Pico Prias™ vials	Perkin Elmer, USA
Polytron PT 2100 homogenizer	Kinematica, Switzerland
PTFE filter membranes (Transwell-COL)	Corning Costar, USA
Soniplus HD2070 (ultrasound sonicator)	Bandelin, Germany
Steritop 0.22 μm filter	Millipore, USA
TGradient thermocycler	Biometra, Germany
Thermomixer comfort	Eppendorf, Germany

3.1.3 Kits

Aldosterone EIA kit (mouse)	Cayman Chemicals, USA
High pure RNA isolation kit	Roche, Switzerland
Insulin ELISA kit (mouse)	ALPCO Diagnostics, USA
Light Cycler® 480 SYBR Green I Master kit	Roche, Switzerland
PowerPrep HP® Plasmid Minipred kit	Origene, USA
RNAqueous-Micro RNA isolation kit	LifeTechnologies, USA
SV total RNA isolation system kit	Promega, USA
Ultrasensitive insulin ELISA kit (mouse)	ALPCO Diagnostics, USA
ZR plasmid Minipred classic kit	Zymo Research, USA

3.1.4 Buffers

Ampicillin plates	20g/l LB broth base
	20g/l agarose
	100 μl/ml ampicillin
	ad to 1l, dH_2O
High salt buffer, 1x	0.1 % Triton X-100
	0.5 M NaCl
	5 mM EDTA
	50 mM Tris, pH 7.5
	ad to 100 ml, dH_2O
Laemmli buffer, 2 x	4 ml 10 % SDS (w/v)
	5 mg Coomassie brilliant blue G-250
	2 ml glycerol
	2.4 ml 0.5 M Tris, pH 6.8
	1.6 ml dH_2O
	100-200 mM DTT or
	500 mM β-mercaptoethanol
PBS, pH 7.3, 10x	2 g KCl
	2 g KH_2PO_4
	80 g NaCl
	11.5 g Na_2HPO_4
	adjust ph to 7.3
	ad to 1l, dH_2O
PBS + 0.1 % Tween	1 l PBS 10x
	10 ml Tween-20
	ad to 10l, dH_2O
4 % PFA, pH 7.4	4 % PFA
	ad to 1l, PBS 1 x
	heat solution to 75°C
	add 1 N NaOH (to dissolve PFA)
	adjust pH to 7.4
Running & transfer buffer (RTB), 10x	144 g glycine
	30.3 g Tris

	ad to 1l, dH_2O
Running buffer, 1x	100 ml RTB, 10 x
	890 ml dH_2O
	10 ml 10 % SDS (v/v)
Transfer buffer, 1x	100 ml RTB, 10 x
	700 ml dH_2O
	200 ml MeOH
TAE buffer, 10x	48.4 g Tris
	11.4 ml glacial acetic acid
	20 ml 0.5 M EDTA, pH 8.0
Tris-HCl, 0.5 M, pH 6.8	6 g Tris
	add dH2O (ca. 50 ml)
	adjust pH to 6.8
	ad to 100 ml, dH_2O
Tris-HCl, 1.5 M, pH 8.8	27 g Tris
	add dH2O (ca. 100 ml)
	adjust pH to 8.8
	ad to 150 ml, dH_2O
TBE buffer, 5x	54 g Tris
	27.5 g boric acid
	20 ml 0.5 M EDTA
	adjust pH to 8.0
	ad to 1 l, dH_2O

3.2 Methods

3.2.1 Mouse work

3.2.1.1 Ethical approval

All animal studies were conducted according to the Swiss animal welfare regulations and after ethical approval by the local veterinarian office (Kantonales Veterinäramt, Zürich) of Zurich, Switzerland. The authorized proposal for this thesis with the permission number 193/2010 is nominated "Regulation des Natrium- und Kaliumhaushaltes durch die Nieren: Zelluläre und molekulare Mechanismen".

3.2.1.2 Mouse housing

Mice were kept in ventilated cages (type II long IVC) in the animal facility of the Institute of Anatomy, University of Zurich. Mice were housed under standardized temperature- and humidity-conditions with a 12:12-h light-dark cycle (7 am-7 pm

light phase, 7pm-7am dark phase) and had free access to standard lab chow GLP 3430 (PROVIMI KLIBA, Kaiseraugst, Switzerland) and tap water, if not differently stated. Generally, female mice were used due to easier handling and housing and groups were age-matched.

3.2.1.3 Generation and genotyping of TBC1D4$^{-/-}$ mice

TBC1D4-deficiency was generated by targeted deletion of part of exon 1 of the TBC1D4 gene. Targeting strategy is shown in Figure 11 from Taconic's webpage http://www.taconic.com and has been described in Lier et al. [2012]. C57/Bl6 mice were obtained from Harlan (Horst, The Netherlands) and TBC1D4-deficient mice (B6129S5-TBC1D4tm1Lex) were purchased from the Texas Institute of Genomic Medicine (Houston, Texas, USA). For our studies, 129/SvEv-C57BL/6 TBC1D4-knockout (KO) mice were backcrossed into the C57BL6 background. Mice from the sixth backcrossed generation on were used.

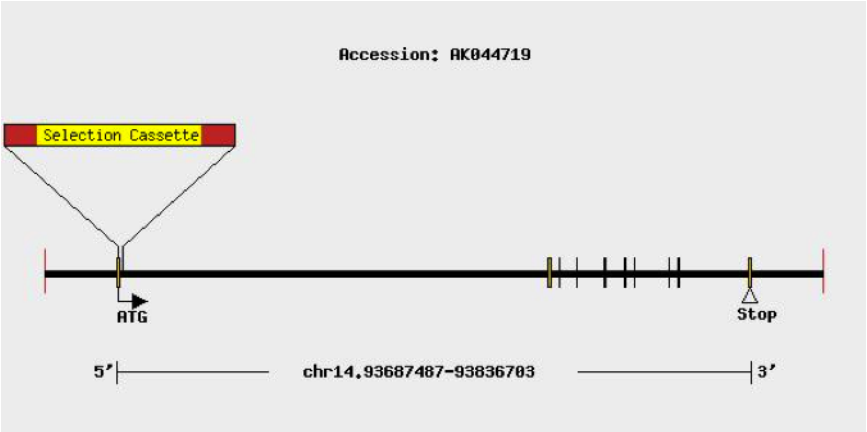

Figure 13: **Targeting strategy for TBC1D4 gene deletion from Taconic** http://www.taconic.com, partial deletion of exon 1 of the TBC1D4 gene

To identify the TBC1D4 locus, a PCR on genomic DNA from a toe or ear biopsy was performed using the 5x FIREPol® Master Mix containing 12.5 mM $MgCl_2$. A 2 % agarose gel separating the wild type band of 355 bp from the band of the TBC1D4 mutant allele of 257 bp was run in Tris-borate-EDTA (TBE, diluted 1x) buffer. Visualization of the bands was achieved by adding Gel Red Nucleic acid stain (Biotium, Hayward, USA). For estimation of the band size, the GeneRulerTM 100 bp DNA Ladder was used.

Step	Temp.	Time	
Denaturation	95 °C	5 min	
Denaturation	94 °C	30 sec	} 40 cycles
Annealing	60 °C	30 sec	
Elongation	72 °C	2 min	
Final Elongation	72 °C	10 min	
Cooling	4 °C	on hold	

Table 2: **PCR steps for TBC1D4 genotyping**

Primer	Sequence 5'-3'
Fwd primer	AGT AGA CTC AGA GTG GTC TTG G
Rev primer WT	GTC TTC CGA CTC CAT ATT TGC
Rev primer TBC1D4 KO	GCA GCG CAT CGC CTT CTA TC

Table 3: **Primers for TBC1D4 genotyping**

3.2.1.4 Generation and genotyping of PV-EGFP and PV-EGFP-TBC1D4$^{-/-}$ mice

The PV-EGFP mice were generated by Meyer and coworkers [Meyer et al., 2002a]. The enhanced green fluorescence protein, EGFP, is expressed under the parvalbumin (PV) promoter found in e.g. DCT1, neurons, heart and skeletal muscle cells [Cai et al., 2001; Picard et al., 2014; Wang et al., 2009]. Immunohistochemistry analysis proved EGFP expression in NCC-positive DCT1 cells, whereas β-ENaC positive cells in the DCT2 lacked the EGFP signal [Picard et al., 2014]. The PV-EGFP mice were used to perform COPAS (complex object parametric analysis and sorting). Heterozygous PV-EGFP transgenic mice were used for breeding, as one allel was sufficient for fluorescence detection (PV-EGFP^{+}). These transgenic mice were bred with TBC1D4$^{-/-}$ and WT (TBC1D4$^{+/+}$) mice to compare DCT genes of TBC1D4$^{+/+}$-PV-EGFP^{+} mice vs. TBC1D4$^{-/-}$-PV-EGFP^{+}mice. As PV is expressed in skeletal muscle, the transgenic EGFP^{+} allel was visually and postnatally identified by illuminating hairless skin with an UV lamp. Genotyping of the TBC1D4 gene was performed as described above.

3.2.1.5 Blood pressure measurements

Murine blood pressure was determined on conscious mice using the non-invasive computerized tail cuff method [Krege et al., 1995]. Measurements were performed between 9 am and 12 pm. Mice were adapted for 3 days prior to the experiments assessing 10 blood pressure measurements. During the experiment, 20 single blood pressure measurements were recorded and the systolic blood pressure (SBP) was

calculated by the average of a maximum of 20 corrected single measurements, but of at least 10 single measurements, using the provided data software.

3.2.1.6 Metabolic cage experiments

For the collection of physiological data (water and food intake, body weight, urine volumes, Na^+ and K^+ excretion, etc.), metabolic cage experiments were performed. Mice were kept in single mouse metabolic cages for 4 days with the first two days serving as adaptation. Metabolic cages allow the harvesting of urine and feces and to strictly control nutrient and fluid uptake. Data were collected every 24 hours.

3.2.1.7 Diets

For metabolic cage experiments, powdered food was used which was moistened with milliQ water to fit into the food porringer. The different diets used are listed in Table 4. The low Na^+/high K^+ diet (LNa/HKD), with 5 % K^+, was used with the aim to maximally activate the renin-angiotensin-aldosterone system (RAAS). In comparison, parameters of the standard lab chow/maintenance food are listed.

Name	Short	Comp.	Cat No	Na	K	Fat	Sugar	food:H_2O	annotation
standard diet	SD	ssniff	E15000-00	0.19	0.97	4.2	10.8	1:1.2	-
high fat diet	HFD	ssniff	E15186-30	0.19	0.97	30.2	13	3:1	-
high salt high fat diet	HSHFD	ssniff	E15186-30	0.19	0.97	30.2	23	3:1	ad Na to 5 %
low Na diet	LNaD	ssniff	E15430-20	< 0.03	0.97	5.2	11.3	1:1	-
low Na /high K diet	LNa/HKD	ssniff	E15430-20	< 0.03	0.97	5.2	11.3	1:1	ad K to 5 %
standard diet pelleted	-	KLIBA	3430	0.2	0.78	4.5	-	-	-

Table 4: **Diets and diet's composition**

3.2.1.8 Glucose tolerance (GTT) and insulin tolerance test (ITT)

In order to measure glucose and insulin tolerance, mice were starved overnight and for 3 hours, respectively. Before the experiment, mice were weighted and blood glucose was measured from a drop of the tail tip with the Accu-Chek Aviva System at time-point 0 min with a following intraperitoneal (i.p.) injection of 1.5 mg/g BW glucose or 0.75 mU/g BW insulin. Blood sugar levels were measured at timepoint 15, 30, 60, 120, 150 and 180 min for glucose tolerance and in 15 min-intervals for insulin tolerance over a total of 90 min.

3.2.1.9 Measurement of urinary parameters

Urinary aldosterone levels were measured using the aldosterone EIA kit. Values were normalized to urine volumes and expressed in ng/day. Urinary ion concentrations (Na^+, K^+ and Mg^{2+}) were determined using an automated 850 professional IC ion chromatograph and creatinine levels were measured by the Jaffe method [Seaton and Ali, 1984].

3.2.1.10 Measurement of blood parameters and mouse kidney harvesting

Mice were anesthetized with 3-4 % isoflurane under an air flow of 0.6 l/min. Blood glucose was measured as described in 3.2.1.8 and 300 μl of blood was redrawn from the right atrium. 100 μl of blood was immediately inserted into a blood gas analyzer through capillary tubes to measure e.g. ion (Na^+, K^+, Mg^{2+}), pH, pCO_2 and hematocrit levels. The remaining blood was centrifuged at 800 g for 3 min at 4°C in Microtrainer LH tubes in order to obtain pure blood plasma fractions. Mice were perfused through the heart with 1x PBS. Plasma insulin levels were determined using the mouse insulin ELISA kit and the ultrasensitive mouse insulin ELISA kit. Plasma aldosterone and corticosterone levels were measured at the Department of Pharmaceutical Sciences at the University of Basel, Switzerland by Prof. A. Odermatt (method described in more detail in Sorensen et al. [2013], supplementary data). Kidneys were harvested, immediately put into liquid nitrogen, and stored at -80°C until use.

3.2.1.11 Preparation of protein samples and western blot analysis

Whole kidney homogenization was performed as described [Busque and Wagner, 2009] using 400 μl of lysis buffer (200 mM Mannitol, 80 mM HEPES, 41 mM KOH, pH 7.5) supplemented with protease and phosphatase inhibitors. Samples were shredded for 30 sec at maximum speed using a Polytron PT 2100 homogenizer and centrifuged at 2'000 g for 10 min at 4°C. The supernatant was collected and an additional 400 μl was added to the pellet. Homogenization and centrifugation were repeated and supernatants were pooled. For fractionation into cytosolic and membrane enriched proteins, 400 μl of the supernatant were centrifuged at 100'000 g for 1 hour at 4°C. The supernatant (cytosolic fraction) was transferred to a new tube and the pellet (membrane fraction) was sonicated for 15 sec at 15 % power in 300 μl lysis buffer. Protein concentrations were assed with a Bradford assay. For western blot analysis, proteins lysates of 25-50 μg were solubilized in 2x Laemmli

buffer (supplemented with 500 mM β-mercaptoethanol). Lysates were separated by 8-12 % SDS-PAGE and transferred to nitrocellulose membranes. Membranes were blocked in Odyssey^{TM} blocking buffer on a rolling shaker on room temperature for 30 min and incubated with primary antibodies overnight at 4°C. All primary antibodies used are listed in table 5. For visualization, blots were incubated with a species-specific secondary infrared (IR)-labeled antibody from LI-COR diluted in 1x blocking buffer at room temperature for 2 hours and protected from light. The Odyssey IR-scanner detection system was used. Densitometric analyses were performed with the Odyssey v3.0 software.

		Dilution			
Antibody	**Host**	**WB**	**IHC**	**Source**	**Reference**
TBC1D4	Rabbit	4000	1000	Loffing	This study, Lier et al. 2012
TBC1D1	Rabbit	1000		Loffing	This study
GLUT4	Rabbit	10000	1000-5000	Millipore	This study
GLUT1	Rabbit	100	2000-10000	Sigma	This study
pAkt S473	Rabbit	1000		Cell Signaling	This study
Na^+-K^+-ATPase	Rabbit	10000		Feraille	This study
NKCC2	Rabbit	1000	10000	Loffing	Wagner et al. 2008
tNCC	Rabbit	10000		Loffing	Sorensen et al. 2013
pT53 NCC	Rabbit	5000		Loffing	Sorensen et al. 2013
pT58 NCC	Rabbit	5000		Loffing	Sorensen et al. 2013
pS71 NCC	Rabbit	5000		Loffing	Sorensen et al. 2013
α-ENaC*	Rabbit	1000		Loffing	Sorensen et al. 2013
β-ENaC*	Rabbit	7500		Loffing	Sorensen et al. 2013
γ-ENaC*	Rabbit	7500	20000	Loffing	Lier et al. 2012, Wagner et al. 2008
AQP2	Rabbit	5000	20000	Loffing	Lier et al. 2012, Wagner et al. 2008
CBP-D28k	Rabbit	5000	20000	Swant	Lier et al. 2012
β-actin	Mouse	10000		Sigma	
α-tubulin	Mouse	1000		Sigma	
IRDye®800CW	Rabbit	20000		LI-COR	
IRDye®680CW	Mouse	20000		LI-COR	

Table 5: **Antibody-concentration for Western Blot and IHC** proteins boiled for 5 min at 95°, italic = secondary antibody

3.2.1.12 RNA extraction from kidney and quantitative real-time PCR (qRT-PCR)

For total RNA extraction, whole kidneys were homogenized using the Polytron PT 2100 homogenizer in 1 ml of RNA lysis buffer of the SV total RNA isolation system kit. Further on, 175 μl of this mix were used for RNA extraction following the manufacturer's instructions. DNase digestion was directly carried out on columns. Quality, purity, and concentration of the total RNA extractions were measured using the NanoDrop ND-1000 spectrophotometer. 100-1000 ng of RNA were reverse transcribed in a 10 μl set-up with H_2O and random primers, heated up to 70°C for 5 min and chilled at 4°C for 5 min. Afterwards, 5x ImProm-II^{TM} reation buffer, 25 mM $MgCl_2$, ImProm-II^{TM} reverse transcriptase, dNTPs and RiboLock^{TM} RNase inhibitor were added with H_2O up to 20 μl for annealing at 25°C for 5 min, first-strand synthesis at 42°C for 60 min and inactivation of reverse transcriptase at

70°C for 15 min. Reverse transcription was performed with the TGradient thermocycler. Relative mRNA expression levels were determined through quantitative real-time PCR with the LightCycler® 480 II instrument and the Light Cycler® 480 SYBR Green I Master kit. 5-10 ng cDNA were used. Data were analyzed using the LightCycler® 480 Instrument Software v1.5. Genes of interest (GOI) were normalized to the house keeping gene (HKG) GAPDH, ratio = 2*Ct$^{(HKG-GOI)}$, all reactions were run in triplicates.

3.2.1.13 Immunohistochemistry (IHC)

Mouse kidneys were fixed through the abdominal aorta with a buffer of 3 % paraformaldehyde (PFA) dissolved in a 0.1 M cacodylate solution (detailed description [Lier et al., 2012; Loffing et al., 2001]). The fixative was rinsed out by perfusion with a 0.1 M cacodylate buffer for 5 min. The kidneys were removed and cut in 2-3 mm slices, mounted on cork, frozen in liquid proprane and stored at -80°C for later analysis. For immunohistochemistry (IHC), 4-5 μm cryosections of fixed kidneys were cut in a cryostat and mounted on chrom-alum gelatin coated glass-slides. Then, the sections were blocked for 10-30 min with 10 % normal goat serum (NGS) in PBS and incubated with the primary antibody in PBS/1 % BSA/0.04 % sodium azide (NaN_3) overnight in a humidified chamber at 4°C. Primary antibodies used are listed in table 5. Thereafter, the sections were washed three times in PBS for 10 min at room temperature and incubated with the species-specific fluorescent dye-labeled secondary antibody (Table 5) for 2 hours, protected from light, and at room temperature (see also 3.2.1.11). To counter-stain the nuclei, the blue fluorescent DNA marker, DAPI (4',6-diamidino-2-phenylindole; 1:1000) was added to the secondary antibody mix. Subsequently, the slides were washed again for three times in PBS and mounted with glycergel and added with the fading retardant 2.5 % DABCO. Immunofluorescent pictures were taken with the DM6000B microscope and the LSM510Meta was used for confocal microscopy. Pictures were processed using the Leica Application Suite Advanced Fluorescence Lite (LAS AF Lite) 2.6.0 software from Leica Microsystems, Switzerland.

3.2.1.14 Primary/ex vivo TAL cell culture

Primary TAL cells were prepared from microdissected tubules of 3-6 week-old male mice as described previously [Glaudemans et al., 2013]. Briefly, kidneys were removed and placed into ice-cold HBSS dissection solution (pH 7.4, 325 mOsm/kg H_2O). Each kidney was cut first along the midsagittal plane and then into 5-7

square pieces. These fragments were subjected to a 35-min collagenase treatment, which were subsequently sieved. The sieved tubular segments were collected in a 37°C albumin solution. The TAL tubules were selected on the basis of morphological characteristics using a light microscope (Leica DM IL), and collected by a glass pipet connected to a micromanipulator. Approximately 50 TAL segments were placed onto 0.33 cm^2 collagen-coated PTFE filter membranes (pore size 0.4 μm) in culture medium (CM) (DMEM:F12) supplemented with 15 mM HEPES, 0.55 mM Na^+-pyruvate, 0.01 % (v/v) non-essential amino acids, 2 % (v/v) FBS and a batch of SingleQuots®, pH 7.4 and incubated in a humidified chamber at 5 % CO_2 and 37°C. The CM was changed every 48 h. A monolayer of TAL cells developed from the tubular fragments after 12 to 15 days. Subsequently, the cells were cultured for 3 days in the absence of FBS to allow full differentiation.

3.2.1.15 Radioactive glucose uptake in primary TAL cells

GLUT4-specific glucose transport activity was studied in primary TAL cultures (n = 5-8) obtained from WT and TBC1D4$^{-/-}$ mice (n $\leq$ 3, each) in the presence or absence of insulin. Working protocols were adapted from glucose uptake experiments in fat and muscle cells [Lansey et al., 2012; Szekeres et al., 2012] as follows: cultures were incubated overnight in a serum- and insulin-free CM. The following day, each culture was washed 3 times using an uptake buffer (UB) (150 mM NaCl, 10 mM HEPES, $CaCl_2$, 5 mM KCl and 1 mM $MgCl_2$). Next, the TAL cultures were incubated for 30 minutes in UB supplemented with 100 μM D-glucose with or without 300 nM insulin. The transport function was determined by ^{3}H-2-deoxyglucose (^{3}H-DOG) uptake experiments (UB buffer supplemented with 0.5 μCi/ml ^{3}H-DOG and 100 μM glucose). After 15 minutes, the uptake was quenched with 50 μM cytochalasin B-supplemented UB buffer, following 4x 5 min UB washing steps. The cells were lysed in 1 % (v/v) SDS, added to 3 ml of Emulsifier-Safe™ liquid scintillation cocktail in polyethylene Pico Prias™ vials and intracellular radioactivity was quantified by liquid scintillation counting using the Packard Tri-Carb 2900. As a control, 10 μM indinavir [Murata et al., 2002] was used to determine the GLUT4-specific transport in cultures from WT and TBC1D4$^{-/-}$ mice. All values were expressed in pmol/h/cm^2.

3.2.1.16 Cell surface biotinylation

Differentiated TAL cells on filters were washed 5 min with ice-cold 1x PBS supplemented with 0.1 mM $CaCl_2$ and 1 mM $MgCl_2$. TAL cells were incubated for 40

min on a shaking rotor at 10 rpm/min at 4°C in 100 mg/ml Sulfo-NHS-LC-Biotin dissolved in 1x PBS (with 0.1 mM $CaCl_2$ and 1 mM $MgCl_2$) and washed two times for 5 min at 4°C in 1x PBS containing 0.1 mM $CaCl_2$, 1 mM $MgCl_2$ and 0.1 M glycine, to quench unbound biotin. The cells were lysed in 60 μl RIPA buffer (supplemented with phosphatase and protease inhibitors) for 90 min rotating at 10 rpm/min at 4°C and collected from filter by pipetting. Cells from 4 filters per condition were pooled. Afterwards, the samples were centrifuged at 10000 rpm for 10 min at 4°C. 160 μl of streptavidin agarose beats was added to an equal amount of supernatant and incubated overnight while rotating. The pellet and the remaining supernatant (total proteins = TL) were stored at -80°C. The next day, the beat-lysate samples were quickly centrifuged and the supernatant was collected (postbiotinylated proteins = PBP). The lysates (biotinylated proteins = BP) were washed 3x with 1x PBS and once with a 1x high salt buffer for 5 min at 4°C. An equal amount of 2x Laemmli buffer was added and samples were boiled for 10 min at 75°C. Protein fractions were used for Western blot analysis as described in 3.2.1.11.

3.2.2 Microarray

3.2.2.1 Isolation of single tubular fragments by complex object parametric analysis and sorting (COPAS)

For complex object parametric analysis and sorting (COPAS), 8-week old male TBC1D4$^{+/+}$-PV-EGPF^{+} and TBC1D4$^{-/-}$-PV-EGFP^{+} mice were used. Preparation of single tubular fragments and COPAS were performed by Claudia Sündermann. To isolate single tubular fragments, mice were anasthesized with isoflurane as described before and perfused through the heart with 10 ml of ice-cold PBS and subsequently, with 10 ml of digestion solution (1 mg/ml collagenase type-1, 1mg/ml hyaluronidase, 0.1mg/ml DNase I prepared in ice-cold KREBS buffer: 145 mM NaCl, 10 mM HEPES, 5 mM KCl, 1 mM NaH_2PO_4, 2.5 mM $CaCl_2$, 1.8 mM $MgSO_4$, 5 mM D-glucose, pH 7.3). Renal cortex from both kidneys was dissected under a stereomicroscope (CLS150X) and further minced and digested in 10 ml of fresh digestion solution for 17 min at 37°C. The tubular digest underwent several filtrations through nylon sieves of cell strainers of 250, 212, 100 and 40 μm pore size. The tubules retained by the 40 μm cell strainer were diluted with ice-cold KREBS to a total volume of 50 ml. All sortings were performed with the COPAS instrument. The full description and settings for fluorescent renal collection duct sorting can be found in Miller et al. [2006] and Picard et al. [2014]. In an eppendorf-tubes containing 1 ml of ice-cold KREBS buffer supplemented with 0.05 % BSA, 800 tubular

green fluorescent DCT1-segments were collected. For one animal, 10-15 eppendorf-tubes were yieled. Tubules were centrifuged at 800 g for 10 min, the supernatant was removed and the pellet resuspendend in RNA lysis buffer (see next section).

3.2.2.2 RNA extraction of COPAS sorted DCT-segments

RNA isolation was performed using the high pure RNA isolation kit, a kit adapted to extract RNA of small sample size with a high RNA purity yield ($A^{260/280}$ and $A^{260/230} \pm 2$). 30 μl of RNA lysis buffer was added to each tube, vortexed and pooled. In order to minimize loss of material, each tube was flushed with additional 20 μl, vortexed and added to the pool. The following steps were pursued according to the manufacturer's instructions with DNA digest on columns. Finally, RNA was yielded in 35 μl elution buffer. 10 μl of RNA extracts were used for qRT-PCR after reverse transcription (see previous sections) and 25 μl were handed to the Functional Genomics Center Zurich (FGCZ) for microarray analysis.

Primers gene	Primer sequence 5'-3' forward	Primer sequence 5'-3' reverse
COMMd6	GTCACGGGCCAGCTTATAGA	ACTTGGCCAGAGTGATCTGC
Dehydro	TTCGTGACCAGGCAATTCTT	CCCTTCTTGGATTTTGCCAG
Enoyl	GTCAATGCCATCAGTCCAAC	GGCTTCTGGTATCGCTGTAT
GAPDH	CATGGCCTTCCGTGTTCC	CCTGCTTCACCACCTTCT
Iqgap1	GGAGTTACTGCTGCTACGGT	TCCAGGACGGAGCCATAGTG
MACA	AGCCAATGATGTGTGCTTAC	GGCTTTACTAGCGGGTACTT
PGC1α	CGAGGACACGAGGAAAGGAA	CACTGGCCTGAATCTGTGGA
PGC1β	CACGGTTTTATCACCTTCCG	ATGGCTTCGTACTTGCTTTT
Ptprb	CACCCAGGGAGGTCCTATCA	GCGGCAATGCAGGTTTTGTA
Scd1 fwd	CAGGTTTCCAAGCGCAGTTC	ACTGGAGATCTCTTGGAGCA
Spry2 fwd	CCGATTGCTTGGAAGTTGGAC	GAACACATCTGAACTCCGTGA
TBC1D10a	TCGTCTTCGATGCCAGAAGG	GTCCAGCTCATCAAACTTCCC
TBC1D4	GCGCCAACGAATCTCTGGTGGAT	GCATGGGGCAGGTCTCGCAC

Table 6: **Primers used for qRT-PCR**

3.2.2.3 Transcriptomic comparison between TBC1D4$^{-/-}$ and WT DCTs using Affymetrix Microarray analysis

Affymetrix microarray analysis was used to investigate for differentially regulated mRNAs in the DCT, a segment with high TBC1D4 expression [Lier et al., 2012], between WT and TBC1D4-deficient mice. 4 mice per group (TBC1D4$^{+/+}$-PV-EGFP^{+} vs. TBC1D4$^{-/-}$-PV-EGFP^{+}) were used under standard conditions. All steps after RNA-lysates handover were performed by the FGCZ: quality analysis of each total RNA sample with the 2100 Bioanalyzer and NanoDrop ND-1000, generation

of labeled cDNA from 100 ng of total RNA, running the Affymetrix GeneAtlas microarray and the analysis of hybridization-images from cDNA on the gene chips. The microarray experiment compared 4 TBC1D4$^{-/-}$ samples versus 4 WT samples on Affymetrix 1.1 Mouse Gene Array. The resulting values of expression have been summarized on the gene level using RMA algorithm [Irizarry et al., 2003]. The analyses have been performed with Bioconductor libraries [Gentleman et al., 2004] encapsulated in the b-fabric system of the FGCZ. The pairwise comparison between TBC1D4$^{-/-}$ and WT was based on log2 expression ratios and p-values of the (unpaired, two-group, two-tailed) t-test. The significant genes were confirmed to have high absolute log2 fold change and low p-values. The detection filtering condition was also set to find the genes that have the expression above standardized background for this type of chip (Exp >10; log2 Exp > 3.322).

3.2.3 Cell culture

Human embryonic kidney 293 (HEK293) cells were cultivated in DMEM supplemented with 10 % heat-inactivated FBS and 1 % penicillin/streptomycin (100 U/ml). Starvation medium consisted of DMEM without supplements. Both media were filtered through a 0.22 μm filter before use. HEK293 cells were cultivated in T75 flasks in a cell incubator with an air atmosphere of 5 % CO_2 and 37°C. Medium was changed every two to three days and cells were splitted twice per week.

3.2.3.1 Transformation of bacteria

20 μl of Quick change®XL1-blue supercompetent E. coli cells together with 2 μl of pcDNA-3.1(+)-hNCC were heat shocked for 30 sec at 42°C and afterwards put on ice for 5 min. Thereafter, 400 μl of SOC medium was added to the bacteria mix and incubated for 1 h at 400 rpm at 37°C. Then, the mixture was centrifuged at 5000 rpm for 1 min and the pellet was resuspended in 1 ml SOC medium. 100 μl of supernatant was plated on ampicillin-agarose plates and incubated overnight at 37°C. The next day, 3 ml LB medium supplemented with ampicillin (50-100 μg/ml) was inoculated with a single bacterial colony picked from the plate. The infected LB medium was incubated overnight in a shaker at 300 rpm at 37°C, and DNA was extracted after 16-24 h using the ZR plasmid Minipred classic kit. For higher DNA yield, 100 ml LB medium with ampicillin was inocculated with 2 ml baterial solution and again, incubated for 16-24 h. DNA was extracted using the Power prep HP Plasmid Minipred kit.

3.2.3.2 Stable transfection of HEK293 cells

For transfection, $8*10^5$ cells were seeded into one well of a 6 well culture plate and grown until reaching 50-60 % confluency. Transfection was performed using Metafectene Pro and linearized (Eco RI) or circular pcDNA-3.1(+)-hNCC plasmid in a ratio of 6:1 (Metafectene:plasmid) by following manifacture's instruction. To achieve stable transfection, 1000 μl/ml G-418 sulphate was added after 48 h to select for only those cells who inserted the gentamycin-cassette from the pcDNA-3.1(+)-hNCC plasmid. The selection medium was changed every second day and cells were split at 80 % confluence. Non-transfected/control HEK293 cells were cultivated in parallel with approximately the same number of passages.

3.2.3.3 RNA and protein extraction

HEK293 cells grown on 6 well plates were scratched from plastic with 1 ml of PBS and collected in an eppendorf tube. Cells were quickly centrifuged and the pellet was used for either RNA or protein extraction. For RNA extraction, the pellet was resuspended in RNA lysis buffer from the RNAqueous-Micro RNA isolation kit with DNase I treatment and following the kit's protocol. The RNA concentration was measured using NanoDrop (see above). For protein extraction, the pellet was resuspended in RIPA buffer supplemented with 50 x protease inhibitor cocktail and 20x phosphatase inhibitor and incubated for 30 min on ice. Afterwards, the mix was centrifuged at 5000 rpm for 10 min at 4°C to pellet cell debris. Protein concentration of the supernatant was assessed by Bradford assay and 25-50 μg of total protein were used for western blot analysis as described before.

3.2.3.4 Immunofluorescence/Immunocytochemistry

HEK293 and HEK293-hNCC cells were grown on sterilized and collagen-coated 22-mm coverslips out in each well of a 6-well plate and up to a confluence of 60-80 %. The cells were washed two times with ice-cold PBS containing 1 mM $MgCl_2$ and 0.1 mM $CaCl_2$ and fixed in a methanol-acetone solution (1:1, v/v) for 5 min at 4°C. Further on, cells were fixed with 4 % PFA in 0.1 M phosphate buffer for 20 min at room temperature. Subsequently, cells were washed three times in ice-cold PBS and then put in blocking solution containing 0.04 % Triton X-100 to permeabilize the cells. Primary antibodies were added to the fixed cells in blocking solution (withouth Triton X-100) and incubated overnight at 4°C. Again, cells were washed three times in ice-cold PBS and secondary antibody as well as DAPI (1:1000) were

added. After 2-4 h of incubation at room temperature, cells were quickly washed with PBS. The following steps were performed as described under IHC (3.2.1.13).

3.2.3.5 In cell western (ICW)

5-10*10^3 HEK293-hNCC cells were seeded into each well of a 96 well plate. After reaching approximately 80 % confluency, treatment with 50 nM Calyculin A (CA) for 30 min was performed. Afterwards, cells were washed once with PBS and fixed with 4 % PFA in PBS for 20 min at 4°C. Cells were then washed three times in 0.1 % Triton X-100 in PBS on a shaker for 5 min and blocked using LI-COR blocking buffer for 30 min. Primary antibodies dissolved in LI-COR blocking buffer were incubated overnight at 4°C. The following washing and incubation steps were performed as described in 3.2.1.11. The secondary antibody concentration was adjusted to a much higher concentration of 1:100-1:200, and in the LI-COR scanner the focus was set accordingly to the height of the plate (+ 0.5 cm).

3.2.4 Statistical analysis

Statistical analyses were performed with the GraphPad Prism Software, Inc. (San Diego, California, USA). Data are represented as means ± SEM and were tested for significance using one- or two-way ANOVA analyses followed by unpaired student's t-test and Bonferroni multiple comparisons where appropriate. $P < 0.05$ was considered statistically significant.

4 Results

4.1 Project 1, part I: TBC1D4-deficiency and renal salt and water handling

4.1.1 No sign of hyper- or hypotension in TBC1D4$^{-/-}$ mice

From previous in vitro studies, we suggested TBC1D4$^{-/-}$ mice to show i) a PHAI-salt losing phenotype in case of TBC1D4 being a stabilizer of ENaC as described by data of our group and Liang and coworkers [Gresko, 2011; Liang et al., 2010]. Hence, TBC1D4 deficiency would lead to an impairment of ENaC membrane insertion, abundance and function with consequently decreased total body volume causing hypotension or ii) as demonstrated by Liang et al., lead to hypertension through increased ENaC activity by the removal of the negative trafficking regulator TBC1D4. Therefore, using the tail-cuff method, we measured the systolic blood pressure (SBP) of TBC1D4-deficient female and male mice and their corresponding wild-type (WT) littermates. Overall, the SBP did not change between WT and TBC1D4$^{-/-}$ mice independently of the gender (Figure 14 A and B). Solely, the SBP of male TBC1D4$^{+/-}$ vs. TBC1D4$^{-/-}$ mice was reduced under standard diet (SD) (Figure 14 B). To investigate whether TBC1D4$^{-/-}$ mice manifest a change in blood pressure under challenging dietary conditions, female TBC1D4$^{-/-}$ mice were kept for four months on a high fat diet (HFD, 30 % fat, Figure 14 C). After one additional month on a high salt high fat diet (HSHFD, 5 % Na^+, Figure 14 D), blood pressure measurement was repeated. Under neither condition, differences in mmHg between knockout and wild-type littermates could be observed.

4.1.2 TBC1D4$^{-/-}$ mice show no Liddle's syndrome- or PHAI-like phenotype

In order to gain more insights into the renal physiological role of TBC1D4, especially in regard to ion and water homeostasis, we performed metabolic studies, blood gas

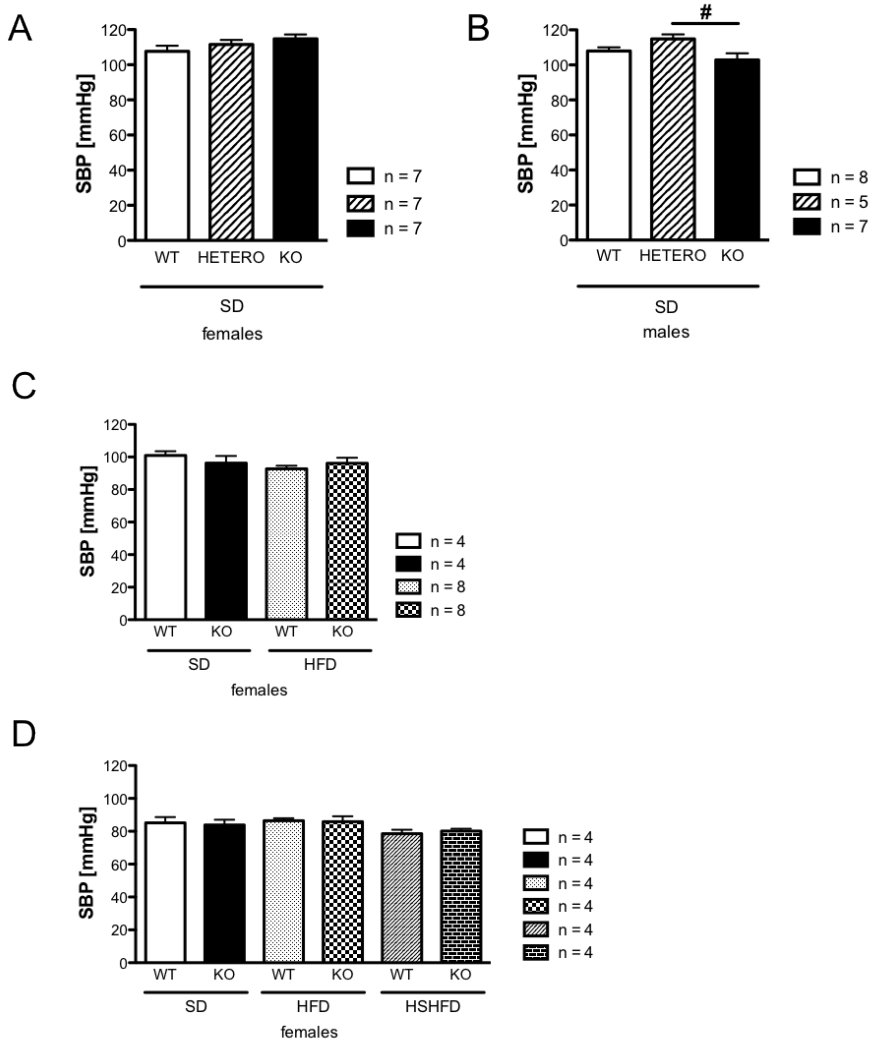

Figure 14: **TBC1D4$^{-/-}$ mice show no difference in SBP under different dietary conditions A** Systolic blood pressure (SPB) was measured using the tail-cuff method in wild-type (WT), TBC1D4$^{+/-}$ (HETERO) and TBC1D4$^{-/-}$ (KO) mice under standard diet (SD) (0.19 % Na^+, 4.2 % fat). No statistical difference was observed between WT and KO littermates. **B** Only in male HETERO vs. KO mice, SBP was reduced (114.8 $\pm$ 2.69 mmHg TBC1D4$^{+/-}$ vs. 102.83 $\pm$ 3.82 mmHg TBC1D4$^{-/-}$, $p < 0.05$). **C** SBP measured in female mice under SD and high fat diet (HFD) (0.19 % Na^+, 30 % fat) for four months. **D** SBP measured in female mice under SD, HFD and high salt-high fat-diet (HSHFD) (5 % Na^+, 30 % fat) in the same mice as in B after one month. No rise or drop in blood pressure was detectable in KO compared to WT littermates. Each bar depicts the average values of 3 days. Values are $\pm$ S.E.M. Statistical significance was calculated with the two-tailed and unpaired student's t-test (# vs. HETERO, $p < 0.05$).

	Standard diet (SD)				
	WT	n	**KO**	n	**p-value**
Bodyweight [g]	31.94 ± 2.18	8	30.88 ± 0.66	7	0.067
Food intake [mg/g BW//24 h]	109.929 ± 20.542	4	113.724 ± 26.837	4	0.913
Water intake [μl/g BW/24 h]	151.69 ± 39.2	4	138.079 ± 9.164	3	0.784
Urine excretion [μl/24 h]	23.266 ± 10.083	4	27.007 ± 13.976	3	0971
UOsmolarity [mOsm]	296.25 ± 56.092	4	412.0 ± 92.43	3	0.277
UNa^+ (norm. to Creat.)	8.988 ± 1.385	4	8.929 ± 1.137	4	0.975
UK^+ (norm. to Creat.)	32.999 ± 5.66	4	41.934 ± 5.970	4	0.312
URatio N^+/K^+	0.276 ± 0.026	4	0.221 ± 0.031	4	0.225
UAldosterone [ng/24 h]	13.36 ± 4.31	7	13.30 ± 4.46	6	0.957
pH	7.42 ± 0.03	4	7.41 ± 0.01	4	0.837
pCO_2[mmHg]	29.5 ± 2.54	5	26.43 ± 2.09	4	0.400
Haematocrit (%)	45.86 ± 1.24	5	44.03 ± 1.89	4	0.426
Na^+ [mM]	147.5 ± 0.65	4	146.25 ± 0.48	4	0.171
K^+ [mM]	4.30 ± 0.15	4	3.98 ± 0.29	4	0.359
Cl^- [mM]	112.75 ± 0.75	4	112.5 ± 0.50	4	0.791
Ca^{2+} [mM]	1.268 ± 0.02	4	1.295 ± 0.006	4	0.234
Corticosterone [nM]	658.71 ± 91.25	7	811.55 ± 76.52	6	0.235
Aldosterone [nM]	0.64 ± 0.13	7	0.86 ± 0.17	6	0.328

Table 7: **Metabolic and physiological parameters as well as blood gas and hormonal level of TBC1D4$^{-/-}$ (KO) and wild-type (WT) littermates on standard diet** Values are S.E.M., n = number, norm. to creat. = normalized to creatinine. Statistical significance was calculated using student's t test.

analyses and determined hormonal levels (e.g. aldosterone, corticosterone) in WT and TBC1D4$^{-/-}$ mice. Bodyweight, food and water intake were similar between WT and TBC1D4-deficient littermates on SD (Table 7). Although slightly higher levels were presented in TBC1D4$^{-/-}$ mice, urine volumes and osmolarity were not statistically different. We further wanted to investigate whether urinary ion excretion is changed, which is a common characteristic of Liddle's syndrome (e.g. higher K^+ excretion) or PHAI (e.g. increased Na^+ excretion). Neither fractional urinary Na^+ nor K^+ excretion was different between the genotypes. To exclude the possibility of counter-acting effects of altered aldosterone level, which might mask the effect of TBC1D4 for example on ENaC activity, we measured urinary and plasma aldosterone levels. However, despite our assumption of a regulatory compensation by altered aldosterone levels, TBC1D4$^{-/-}$ mice displayed similar aldosterone levels in both, urine and plasma, when compared to their WT littermates (Table 7). Moreover, blood gas analyses of important physiological parameters (pH, pCO_2, hematocrit) showed no alterations. Plasma electrolytes levels (Na^+, K^+, Cl^-, Ca^{2+}) were similar in both genotypes. Plasma corticosterone levels were slightly but not significantly elevated in TBC1D4$^{-/-}$ compared to WT mice (Table 7).

4.1.3 Similar protein levels of important water and salt transporters and channels in TBC1D4$^{-/-}$ mice on standard diet

Despite the strong in vitro effect of TBC1D4 deficiency in renal cells, TBC1D4$^{-/-}$ mice did not show any signs of hyper- or hypertension and of a dysregulation in plasma as well as urinary ion levels and volumes on SD when compared with their wild-type littermates. Compensation via altered aldosterone levels as shown by the analysis of urinary and plasma aldosterone did not occur. Potentially, other compensatory mechanisms might explain the rather normal phenotype of TBC1D4$^{-/-}$ mice. Therefore, we performed immunoblot analyses of various proteins involved in sodium and water transport along the nephron. In the TAL, which does not belong to the ASDN, protein abundance of the NKCC2 transporter was not altered in TBC1D4$^{-/-}$ mice. Furthermore, total NCC and its phosphorylation sites pT53, pT58 and pS89 in the DCT did not show significant changes between WT and TBC1D4$^{-/-}$ animals. Likewise, in the ASDN, all three subunits of ENaC (α, β, γ) as well as AQP2 were not different in protein abundance between the genotypes. In addition, protein levels of the Na^+-K^+-ATPase showed no alteration between TBC1D4$^{-/-}$ and WT littermates (Figure 15). Thus, in kidney lysates on SD of TBC1D4$^{-/-}$ compared to WT mice, no major difference in the abundance of pivotal proteins known to handle Na^+ and H_2O reabsorption was observed.

4.1.4 No change in physiological parameters in TBC1D4$^{-/-}$ mice when maximally stimulating the RAA-system with a low Na^+/high K^+ diet

Although under SD no abnormal renal phenotype was observed in TBC1D4-deficient mice, other mice with gene deletions (e.g. for the E3-ubiquitin ligase Nedd4-2, SGK1) have been demonstrated to reveal renal impairments only after metabolic challenges [Faresse et al., 2012; Ronzaud et al., 2013]. Therefore, mice were fed a diet containing low Na^+ (< 0.03 %) and high K^+ (5 %) levels (low Na^+/high K^+ diet; LNa/HKD) to maximally stimulate the RAA-system, a multi-organ hormonal system that is crucial for blood pressure regulation. Juxtaglomerular cells lining next to the afferent arterioles of the glomerulus secrete renin into the blood stream, when blood volume levels are low. In the blood, renin catalyzes the cleavage of liver angiotensinogen into angiotensin I, which is further cleaved by the angiotensin-converting enzyme to angiotensin II. Angiotensin II stimulates the aldosterone secre-

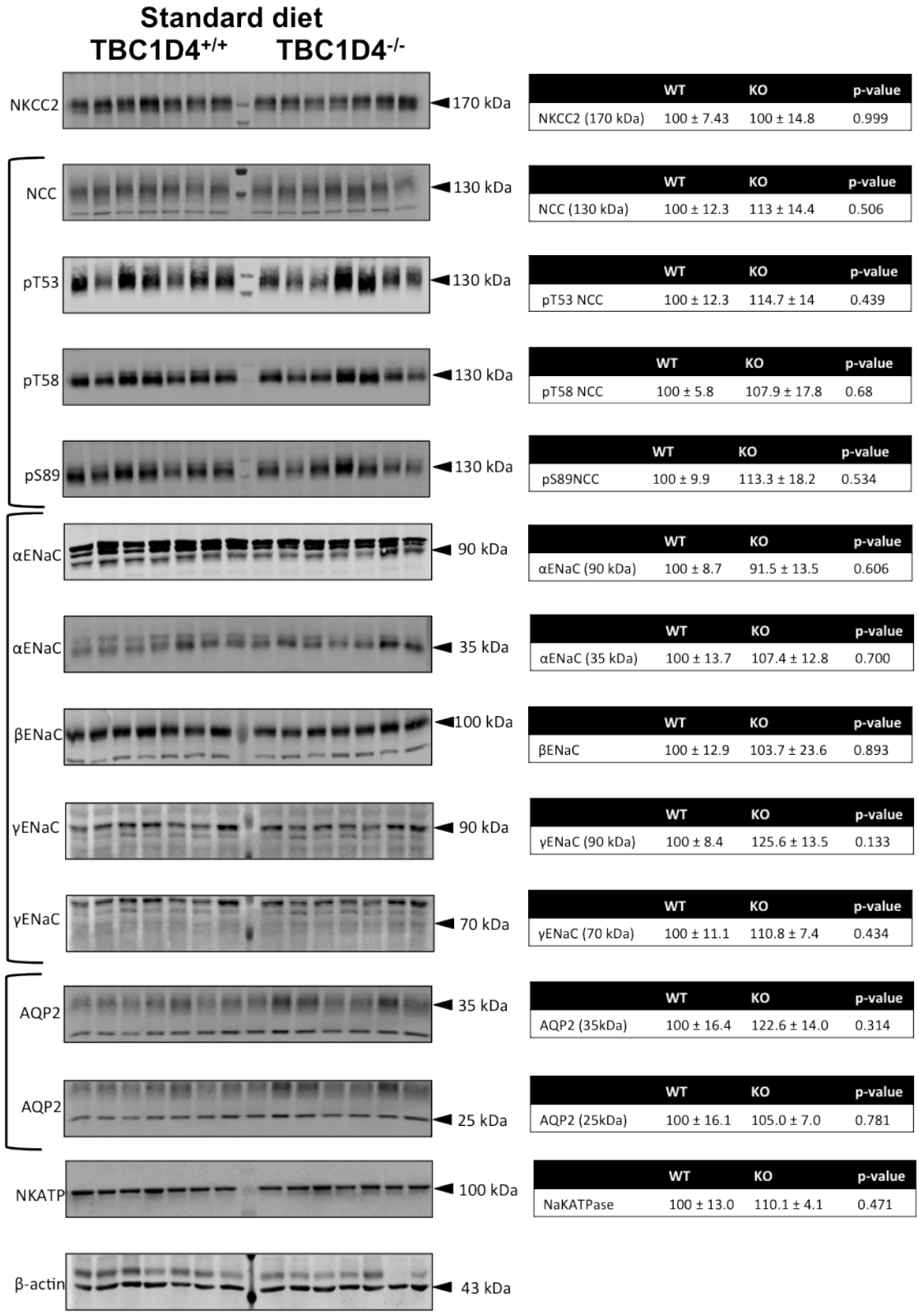

	WT	KO	p-value
NKCC2 (170 kDa)	100 ± 7.43	100 ± 14.8	0.999

	WT	KO	p-value
NCC (130 kDa)	100 ± 12.3	113 ± 14.4	0.506

	WT	KO	p-value
pT53 NCC	100 ± 12.3	114.7 ± 14	0.439

	WT	KO	p-value
pT58 NCC	100 ± 5.8	107.9 ± 17.8	0.68

	WT	KO	p-value
pS89NCC	100 ± 9.9	113.3 ± 18.2	0.534

	WT	KO	p-value
αENaC (90 kDa)	100 ± 8.7	91.5 ± 13.5	0.606

	WT	KO	p-value
αENaC (35 kDa)	100 ± 13.7	107.4 ± 12.8	0.700

	WT	KO	p-value
βENaC	100 ± 12.9	103.7 ± 23.6	0.893

	WT	KO	p-value
γENaC (90 kDa)	100 ± 8.4	125.6 ± 13.5	0.133

	WT	KO	p-value
γENaC (70 kDa)	100 ± 11.1	110.8 ± 7.4	0.434

	WT	KO	p-value
AQP2 (35kDa)	100 ± 16.4	122.6 ± 14.0	0.314

	WT	KO	p-value
AQP2 (25kDa)	100 ± 16.1	105.0 ± 7.0	0.781

	WT	KO	p-value
NaKATPase	100 ± 13.0	110.1 ± 4.1	0.471

Figure 15: **Western blot analysis of important salt and water transporting proteins of WT and TBC1D4$^{-/-}$ mice under SD** Left: Western blot analysis (WT and TBC1D4$^{-/-}$, n = 7), right: densitometric anaylses, values are ± SEM. Statistical significance was calculated using two-tailed and unpaired student's t test.

	Low Na^+/high K^+-diet (LNa/HKD)		
	WT	**KO**	**p-value**
Bodyweight [g]	22.0 ± 0.38	22.24 ± 0.73	0.778
Food intake [mg/g BW//24 h]	234.942 ± 24.842	217.766 ± 15.026	0.570
Water intake [μl/g BW/24 h]	348.662 ± 43.426	298.110 ± 18.705	0.316
Urine excretion [μl/24 h]	159.097 ± 36.666	118.455 ± 19.576	0.357
UOsmolarity [mOsm]	309.0 ± 49.13	327.4 ± 30.53	0.759
UNa^+ (norm. to Creat.)	5.284 ± 0.736	5.609 ± 0.433	0.903
UK^+ (norm. to Creat.)	894.308 ± 68.635	909.041 ± 94.252	0.903
Ratio N^+/K^+	0.006 ± 0.001	0.007 ± 0.001	0.622
UAldosterone [ng/24 h]	373.09 ± 51.29	353.88 ± 64.80	0.819
Corticosterone [nM]	304.41 ± 26.70	416.15 ± 59.98	0.127
Aldosterone [nM]	5.24 ± 1.05	5.15 ± 1.45	0.960

Table 8: **Metabolic and physiological parameters as well as blood gas and hormonal level of TBC1D4$^{-/-}$ (KO) and wild-type (WT) littermates on low Na^+/high K^+-diet** Values are S.E.M., WT and KO mice n = 5, norm. to creat. = normalized to creatinine. Statistical significance was calculated using student's t test.

tion from adrenal glands. Aldosterone mainly increases Na^+-retention by activation of ENaC, thus regulating circulating volumes and blood pressure. Also under these conditions, metabolic parameters such as bodyweight, water and food intake were not different between WT and TBC1D4$^{-/-}$ mice. Urine excretion and osmolarity as well as urinary Na^+ and K^+ levels were not significantly altered in TBC1D4$^{-/-}$ mice on LNa/HKD compared to wild-type mice. Renin mRNA levels of whole kidney lysates were measured, but neither renin mRNA (Figure 16) nor plasma and urinary aldosterone levels differed between the genotypes. Remarkably, plasma and urinary aldosterone levels were highly elevated in TBC1D4-deficient and WT mice, confirming the dietary effect of maximally stimulating the RAA-system (plasma SD vs. LNa/HKD aldosterone; WT $p < 0.005$ and TBC1D4$^{-/-}$ mice $p < 0.05$, urine SD vs. LNa/HKD aldosterone; WT $p < 0.005$ and TBC1D4$^{-/-}$ mice $p < 0.005$) (values shown in table 7 SD and table 8 LNa/HKD). Plasma corticosterone levels were slightly but not significantly increase in TBC1D4$^{-/-}$ animals compared to WT animals.

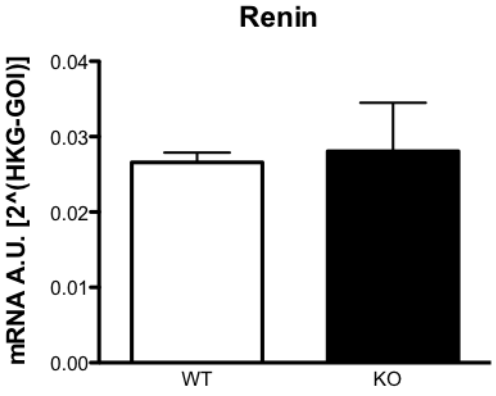

Figure 16: **Renin mRNA levels** Similar renin mRNA levels in whole kidney lysates of TBC1D4-deficient (KO) mice compared to WT mice. Values are ± S.E.M and normalized to GAPDH expression, n ≥ 3. Statistical significance was calculated using student's t test.

4.1.5 Similar proteins levels of important water and salt transporters and channels in TBC1D4$^{-/-}$ mice on low Na$^+$/high K$^+$ diet

Analogously to the studies on SD, we investigated the protein abundance of NKCC2, NCC, ENaC, AQP2 and the Na$^+$-K$^+$-ATPase in TBC1D4$^{-/-}$ mice under the challenging LNa/HKD. Again, neither the transporter abundance of NKCC2 and NCC nor the phosphorylation of NCC (pT53, pT58 and pS89) was different between KO and WT animals. The abundance of ENaC with its three subunits α, β, γ and the proteolytically cleaved bands of the α- (35 kDa) and γ-subunit (70 kDa) were unchanged in TBC1D4-deficient mice compared to WT mice. Furthermore, TBC1D4$^{-/-}$ mice showed similar protein abundance to WT mice for the 25 and 35 kDa band of AQP2, and the Na$^+$-K$^+$-ATPase (Figure 17). Overall, the challenging conditions did not reveal any differential regulation on renal water and salt transporters and channels between WT and TBC1D4$^{-/-}$ mice.

4.1.6 No apparent disturbances in the vasopressin-signaling pathway of TBC1D4$^{-/-}$ littermates

To investigate whether TBC1D4$^{-/-}$ mice might have a different urine concentrating ability caused by impairments in AQP2-transport as suggested by TBC1D4 deple-

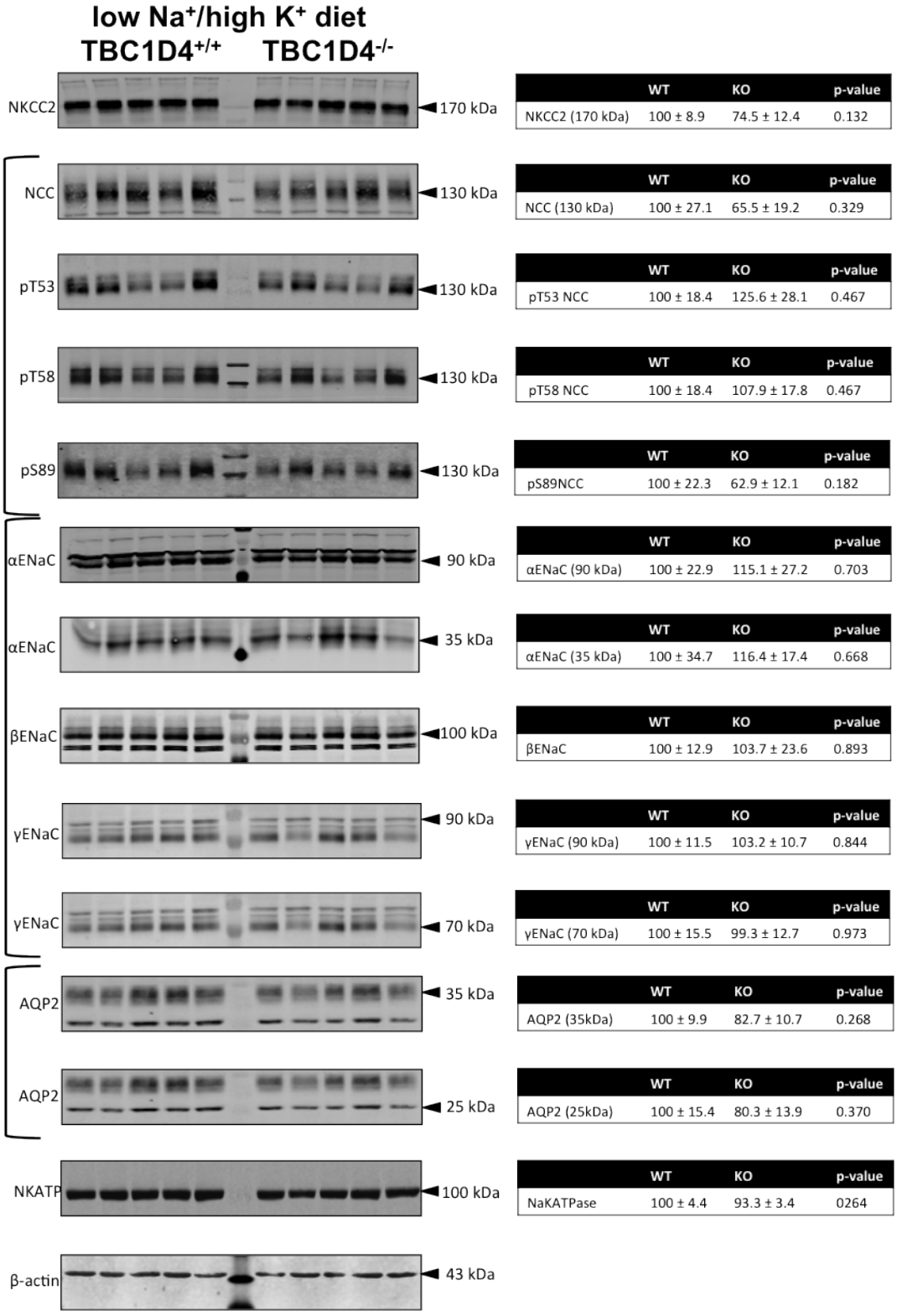

	WT	KO	p-value
NKCC2 (170 kDa)	100 ± 8.9	74.5 ± 12.4	0.132

	WT	KO	p-value
NCC (130 kDa)	100 ± 27.1	65.5 ± 19.2	0.329

	WT	KO	p-value
pT53 NCC	100 ± 18.4	125.6 ± 28.1	0.467

	WT	KO	p-value
pT58 NCC	100 ± 18.4	107.9 ± 17.8	0.467

	WT	KO	p-value
pS89NCC	100 ± 22.3	62.9 ± 12.1	0.182

	WT	KO	p-value
αENaC (90 kDa)	100 ± 22.9	115.1 ± 27.2	0.703

	WT	KO	p-value
αENaC (35 kDa)	100 ± 34.7	116.4 ± 17.4	0.668

	WT	KO	p-value
βENaC	100 ± 12.9	103.7 ± 23.6	0.893

	WT	KO	p-value
γENaC (90 kDa)	100 ± 11.5	103.2 ± 10.7	0.844

	WT	KO	p-value
γENaC (70 kDa)	100 ± 15.5	99.3 ± 12.7	0.973

	WT	KO	p-value
AQP2 (35kDa)	100 ± 9.9	82.7 ± 10.7	0.268

	WT	KO	p-value
AQP2 (25kDa)	100 ± 15.4	80.3 ± 13.9	0.370

	WT	KO	p-value
NaKATPase	100 ± 4.4	93.3 ± 3.4	0264

Figure 17: **Western blot analysis of important salt and water transporting proteins of WT and TBC1D4$^{-/-}$ mice under LNa/HKD** Left: Western blot analysis (WT and TBC1D4$^{-/-}$, n = 5), right: densitometric anaylses, values are ± SEM. Statistical significance was calculated using two-tailed and unpaired student's t test.

tion in vitro [Jung and Kwon, 2010; Kim et al., 2011], we challenged the mice with a mild 24 h water restriction (WR). A mild WR was performed in order to prevent a maximal stimulation of the vasopressin and renal collecting system, which could allow full compensation and mask subtle differences in the urinary concentrating mechanism. The relevance of this caveat has been demonstrated in previous studies [Zuber et al., 2007]. Therefore, the drinking bottle was removed, but the food was moisturized with 50 % of milliQ-water. When compared with the previous 48 h ad libitum food and water access, food intake slightly increased during 24 h WR in both genotypes but was not different between TBC1D4$^{-/-}$ and WT mice (Figure 18 A). WT as well as TBC1D4$^{-/-}$ littermates significantly reduced urine volumes during WR compared to the previous 48 h period ($p = 0.024$ and $p = 0.04$, respectively) (Figure 18 A). Furthermore, urine osmolarity was increased in the WT group ($p = 0.027$) and TBC1D4$^{-/-}$ mice showed a similar increase, although the increase did not reach statistical significance ($p = 0.14$) (Figure 18 A). Total water intake, calculated from drinking water and water content of the food, was slightly decreased confirming our aim to mildly deprive the mice from water (Figure 18 B). The urinary ion (Na^+, K^+, Mg^{2+}) excretion during WR was not different between WT and KO mice (Figure 18 C). Likewise, urinary aldosterone excretion was similar for WT and KO mice (Figure 18 D).

4.1.7 Similar protein levels of water and salt transporters and channels in TBC1D4$^{-/-}$ mice on high fat diet

In addition, we analyzed the abundance of renal Na^+-transporting proteins in kidneys of WT and TBC1D4$^{-/-}$ mice, when fed a high caloric fat-enriched diet. The Na^+-transporters present in the PT, NaPiIIa and NHE3, showed no dysregulation, as well as the Na^+-transporting proteins NKCC2, NCC, and ENaC in the distal tubule and the collecting system. Also the Na^+-K^+-ATPase was not differently abundant between WT and TBC1D4$^{-/-}$ mice, when compared to their WT littermates under a HFD (Figure 19).

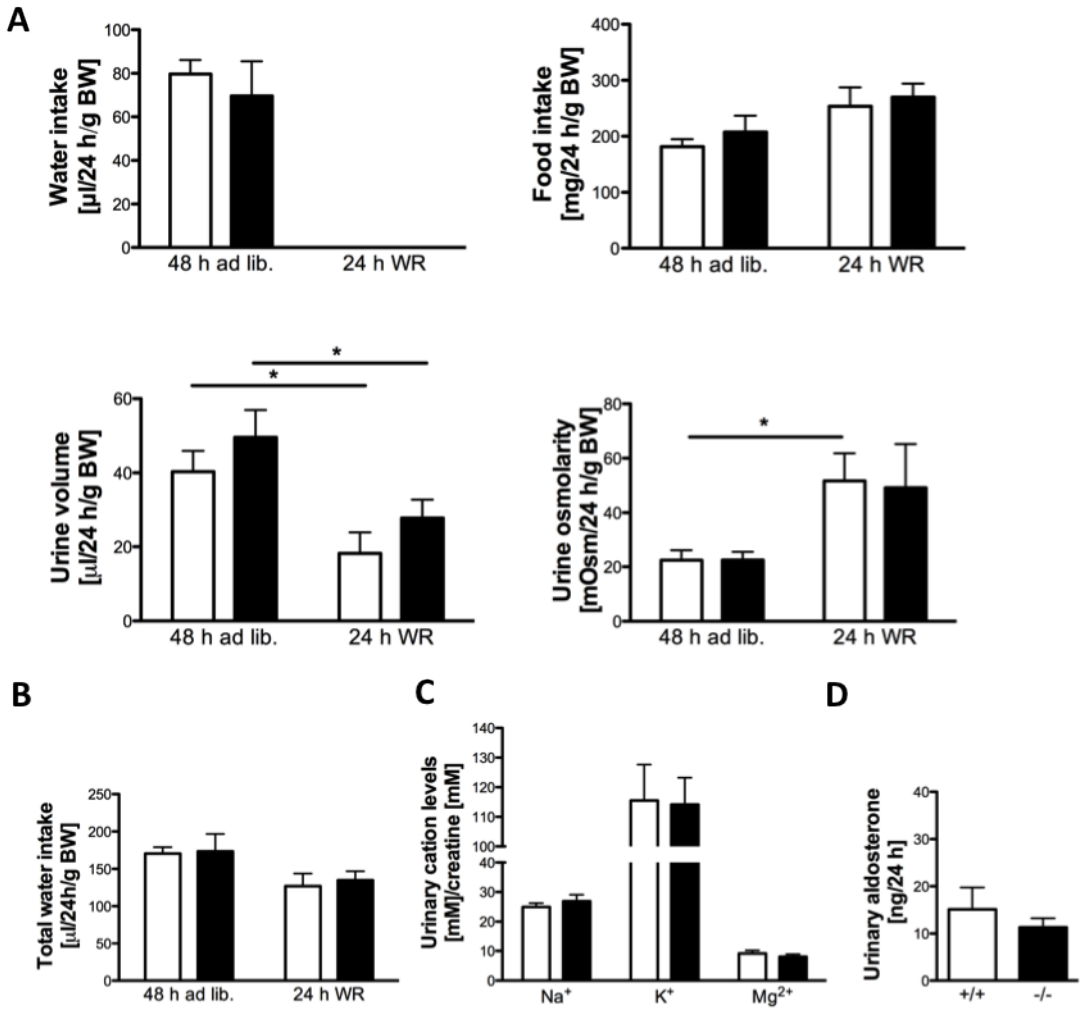

Figure 18: **Metabolic parameters of WT and TBC1D4$^{-/-}$ mice under water restriction (WR) A** Mice were restricted from water for 24 h. Food intake increased slightly but not significantly during WR in both groups. Urine volumes and osmolarity were similar before and after WR between the genotypes, but urine volumes were significantly reduced (WT, 48 h ad. lib. vs. 24 h WR, 40.3 ± 5.6 vs. 18.2 ± 5.6 μl/24 h/g BW, p = 0.024, TBC1D4$^{-/-}$ 49.6 ± 7.4 vs. 27.8 ± 4.9 μl/24 h/g BW, p = 0.04) and urine osmolarity increased in both groups (WT, 48 h ad. lib. vs. 24 h WR, 22.4 ± 3.6 vs. 51.7 ± 10.2 mOsm/24 h/g BW, p = 0.027, TBC1D4$^{-/-}$ 22.5 ± 3.0. vs. 49.2 ± 16.0 mOsm/24 h/g BW, p = 0.14). **B** Total water intake (calculated from water intake and water content in the food) was lowered as intended **C** Measurements of urinary cations did not show any difference in Na^+, K^+ and Mg^{2+} excretion **D** Urinary aldosterone levels were similar under WR between WT and TBC1D4$^{-/-}$ mice. White bars WT (TBC1D4$^{+/+}$), black bars TBC1D4$^{-/-}$ mice, n = 5, mean ± SEM, student's t test, *p ≤ 0.05

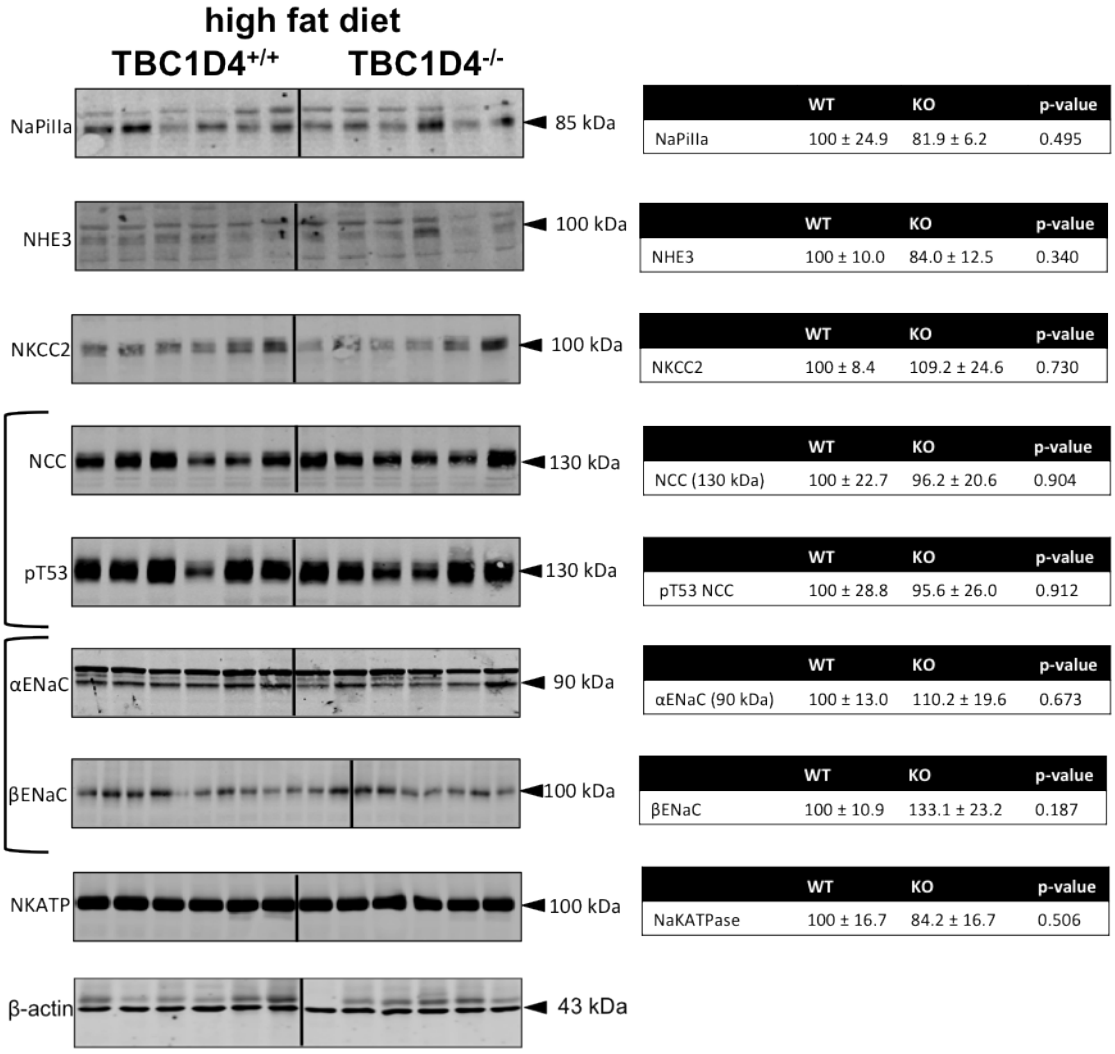

	WT	KO	p-value
NaPiIIa	100 ± 24.9	81.9 ± 6.2	0.495

	WT	KO	p-value
NHE3	100 ± 10.0	84.0 ± 12.5	0.340

	WT	KO	p-value
NKCC2	100 ± 8.4	109.2 ± 24.6	0.730

	WT	KO	p-value
NCC (130 kDa)	100 ± 22.7	96.2 ± 20.6	0.904

	WT	KO	p-value
pT53 NCC	100 ± 28.8	95.6 ± 26.0	0.912

	WT	KO	p-value
αENaC (90 kDa)	100 ± 13.0	110.2 ± 19.6	0.673

	WT	KO	p-value
βENaC	100 ± 10.9	133.1 ± 23.2	0.187

	WT	KO	p-value
NaKATPase	100 ± 16.7	84.2 ± 16.7	0.506

Figure 19: **Western blot analysis of important salt and water transporting proteins of WT and TBC1D4$^{-/-}$ mice under HFD** Left: Western blot analysis (WT and TBC1D4$^{-/-}$ n $\geq$ 6), right: densitometric anaylses, values are $\pm$ SEM. Statistical significance was calculated using two-tailed and unpaired student's t test.

4.2 Project 1, part II: TBC1D4-deficiency and systemic and renal glucose handling

4.2.1 TBC1D4$^{-/-}$ mice gain less body weight under HFD compared to WT littermates

The body weights (BW) of TBC1D4$^{-/-}$ and WT mice were monitored over 6 month on SD and HFD (Figure 20). Under SD, BWs increased significantly over a 6 month period (WT begin vs. after 6 months $p < 0.0005$ and KO begin vs. end $p < 0.0005$), but were not different between the genotypes (begin WT 19.94 g $\pm$ 0.43 g, n = 8 and TBC1D4$^{-/-}$ 21.11 g $\pm$ 1.52 g, n = 7, $p > 0.05$, after 6 months WT 31.94 $\pm$ 2.16 g, n = 8 and KO 30.89 $\pm$ 0.59 g, n = 7, $p > 0.05$). Interestingly, after 6 months on a HFD, TBC1D4$^{-/-}$ mice gained less BW in comparison to WT mice (begin WT 25.02 $\pm$ 2.5 g, n = 11 and KO 21.96 $\pm$ 1.18 g, n = 8, $p > 0.05$, after 6 months WT 41.44 $\pm$ 2.5 g, n = 11 and KO 32.89 $\pm$ 2.20 g, n = 8, $p < 0.05$). BW also increased with time in both genotypes under HFD (WT begin vs. after 6 months $p < 0.0001$ and KO begin vs. after 6 months $p < 0.0005$) (Figure 20 D).

4.2.2 TBC1D4$^{-/-}$ mice have an improved glucose tolerance under HFD compared to WT mice

As TBC1D4 is highly expressed in muscle and fat cells and is known to regulate glucose uptake into skeletal muscle and fat cells, we analyzed whole body glucose homeostasis in WT and TBC1D4$^{-/-}$ mice. Therefore, we performed a glucose tolerance test (GTT) (1.75 mg glucose/g BW) after an overnight fast (16 h). Interestingly, TBC1D4$^{-/-}$ mice had reduced blood glucose levels at the beginning of the GTT under SD and HFD (Figure 21). In general, TBC1D4$^{-/-}$ seemed to have an improved glucose tolerance shown by a faster glucose disposal over the 180 min measured, which was more pronounced under a HFD [area under the curve (AUC); SD WT 1347.19 $\pm$ 84.48, n = 8 vs. KO 1197.97 $\pm$ 54.11, n = 7, $p = 0.17$; HFD WT 1745.70 $\pm$ 60.25, n = 19 vs. KO 1420.36 $\pm$ 46.67, n = 16, $p < 0.0003$, only female mice were used]. These results are similar to what was shown by Wang et al. [2013], who used male mice, but contrast to the results of Lansey et al. [2012], in which glucose tolerance was impaired in female TBC1D4$^{-/-}$ mice, but normal in male mice (Table 1, 1.8.2).

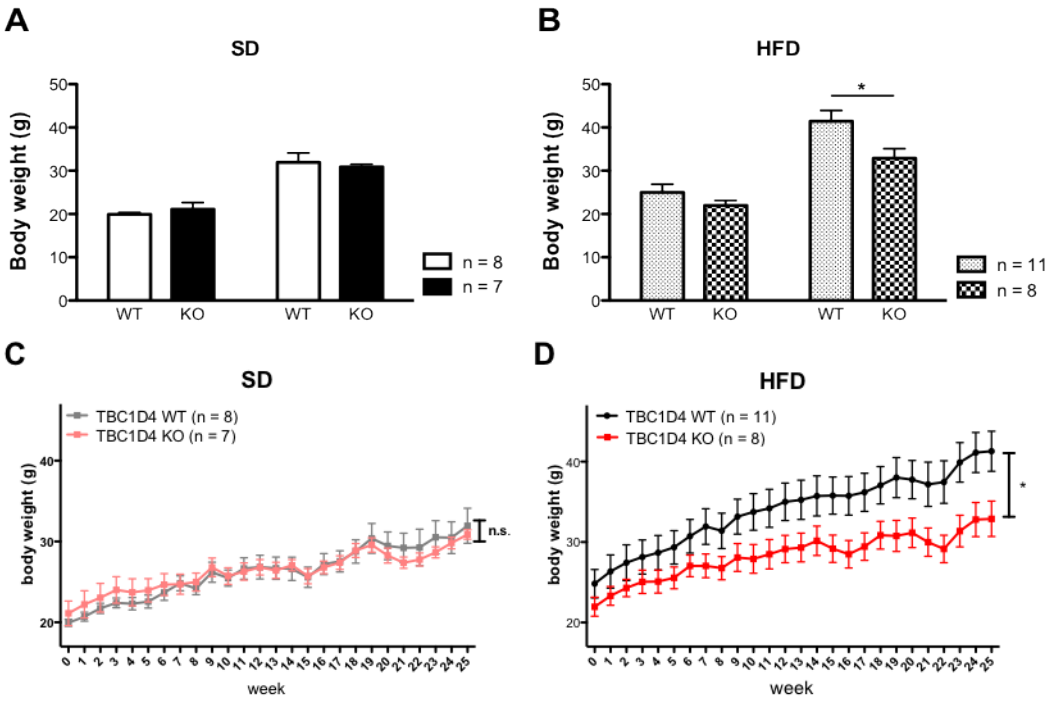

Figure 20: **Body weights of WT and TBC1D4$^{-/-}$ mice over 6 months on SD and HFD A + B** bar blots comparing start of the experiment and after 6 months **A** on SD, body weight was not different between the genotypes **B** on HFD, BW gain was significantly lower in TBC1D4$^{-/-}$ vs. WT mice **C + D** Line plots. BWs were not different over time under SD, but significantly changed over time on HFD between TBC1D4$^{-/-}$ vs. WT mice. Values are means ± SEM. BW was measured twice a week, two-way ANOVA with Bonferroni's Multiple Comparison Test, *p < 0.05

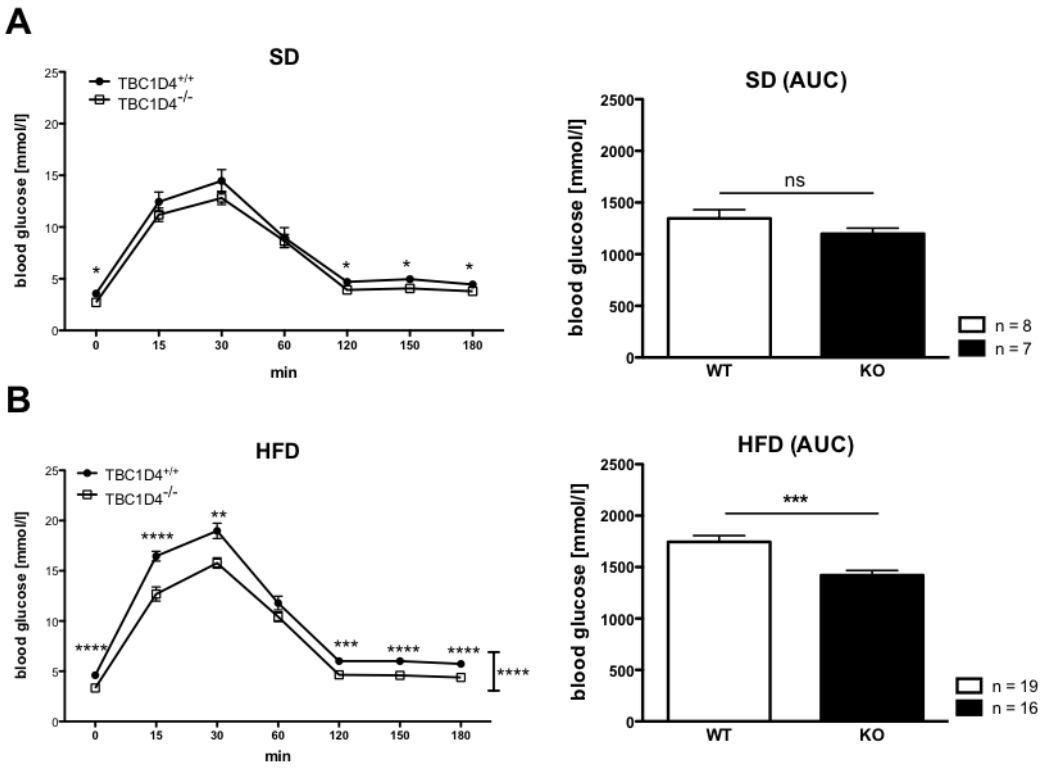

Figure 21: **Interperitonal glucose tolerance test (GTT)** TBC1D4$^{-/-}$ mice have an improved glucose tolerance under a HFD. The area under the curve (AUC) shows significantly decreased values for TBC1D4$^{-/-}$ (KO) mice. under HFD (***p < 0.0005) over 90 min compared to WT littermates. Values are $\pm$ SEM, student's t test, *p < 0.05, **p < 0.005, ****p < 0.0001.

4.2.3 TBC1D4$^{-/-}$ mice are insulin resistent

To determine whether the improved glucose tolerance was due to a higher insulin sensitivity, an insulin tolerance test (ITT) was performed. Mice were synchronized by starvation 3 h prior the i.p. insulin injection (0.75 mU/g BW). Unexpectedly, TBC1D4-deficient mice presented insulin resistance (Figure 22) [area under the curve (AUC); SD WT 230.98 ± 27.41, n = 6 vs. KO 303.8 ± 9.0, n = 6, $p < 0.03$; HFD WT 295.75 ± 32.13, n = 10 vs. KO 362.84 ± 20.80, n = 10, $p < 0.1$, over 90 min, only female mice]. The effect was even more pronounced, when only the period after insulin injection (15-90 min) was compared. (SD WT 162.85 ± 25.63, n = 6 vs. KO 244.82 ± 7.38, n = 6, p = 0.012; HFD WT 207.77 ± 27.94, n = 10 vs. KO 287.22 ± 16.61, n = 10, p = 0.025). Likewise, Lansey et al. [2012], and Wang et al. [2013], found insulin resistance in male and female TBC1D4$^{-/-}$ mice and in male TBC1D4$^{-/-}$ mice tested at different age. Again, in all our experiments, basal glucose levels were much lower in TBC1D4$^{-/-}$ mice compared to WT mice (see Table 9, 4.2.4, and Table 1, 1.8.2).

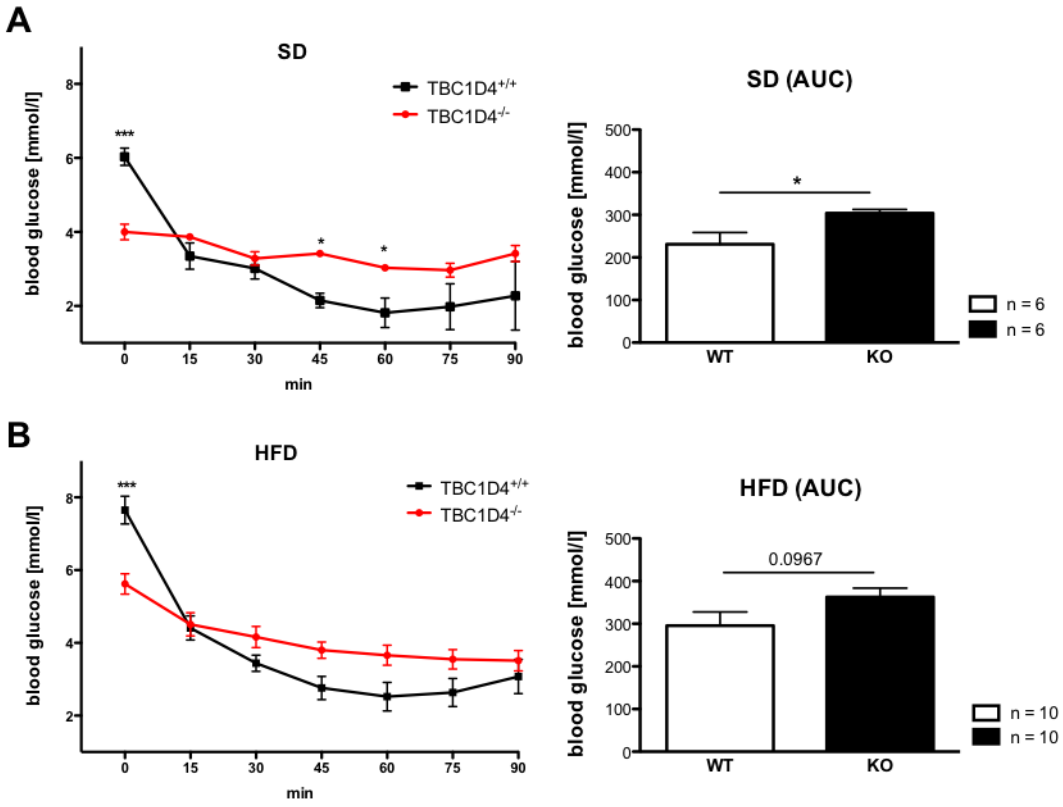

Figure 22: **Interperitonal insulin tolerance test (ITT)** TBC1D4$^{-/-}$ mice show an insulin resistance over a period of 90 min under SD and a tendency under HFD (p = 0.0967) compared to WT mice.

4.2.4 TBC1D4$^{-/-}$ mice are normoinsulemic but hypoglycemic under fasted conditions

From the results obtained from the ITT, the next question to address was whether the impaired insulin tolerance was due to an increased insulin secretion (Table 9). Under all three tested dietary conditions (SD, HFD, LNa/HKD) and under feeding ad lib., TBC1D4-deficient mice did not show any increased plasma insulin values when compared to WT mice. Nevertheless, TBC1D4$^{-/-}$ animals exhibited a slight hypoglycemia on SD and LNa/HKD and a strong hypoglycemia under starved conditions under SD and HFD compared to WT animals (Table 9). Thus, TBC1D4$^{-/-}$ mice compared to WT mice are not hyperinsulemic, but have constantly lowered blood glucose levels.

	SD				LNa/HKD				HFD			
	WT	**n**	**KO**	**n**	**WT**	**n**	**KO**	**n**	**WT**	**n**	**KO**	**n**
PInsulin (random fed)	0.4 ± 0.04	7	0.35 ±0.01	7	0.66 ±0.07	5	0.55 ±0.06	5	0.39 ±0.01	7	0.53 ±0.12	7
PGlucose (random fed)	8.72 ±0.46	5	7.43 ±0.32$	3	7.08 ±0.56	5	5.3 ±0.34*	5	8.54 ±0.21	5	8.17 ±0.49	5
PGlucose (starved GTT)	3.56 ±0.19	8	2.4 ±0.2*	7	3.72 ±0.39	5	3.6 ±0.35	5	4.61 ±0.14	19	3.33 ±0.19****	16
PGlucose (starved ITT)	6.03 ±0.23	6	4 ±0.21****	6	n.d.		n.d.		7.65 ±0.38	10	5.62 ±0.28***	10

Table 9: **Plasma insulin and glucose levels under random fed and starved conditions of TBC1D4$^{-/-}$ (KO) and wild-type (WT)** littermates on different diets Values are ± SEM, student's t test, *p < 0.05, ***p < 0.0005, ****p < 0.0001, \$p < 0.1, GTT = glucose tolerance test, ITT = insulin tolerance test, PInsulin = plasma insulin, PGlucose = plasma glucose, n.d. not determined

4.3 GLUT4 gene and protein expression analysis in kidney of WT mice

4.3.1 Analysis of GLUT4 gene expression in microdissected tubules of WT mice

The previous studies did not provide any evidence that TBC1D4 is involved in the regulation of renal ion and water transporting proteins. Therefore, we next tested the hypothesis that TBC1D4 might be involved in the regulation of renal glucose transporters, in particular GLUT4. Thus, it was first crucial to determine i) whether GLUT4 is expressed in the kidney and ii) where exactly the transporter

is found (cell type, intracellular localization). To approach this aim, we used free-hand renal tubule microdissection and subsequent mRNA expression analysis. qRT-PCR analysis revealed high GLUT4 gene levels in the TAL, which was therefore determined as reference segment for which expression levels were set to 100 %. GLUT4 expression in the glomerulus was 20 ± 4 %, but was very low in PCT and PST ($\leq$ 7 ± 1 %). Furthermore, the transporter was highly expressed in the DCT (74 ± 12 %) and modestly in CNT/CD (41 ± 5 %). This expression pattern nicely matched with the TBC1D4 expression levels along the nephron (Figure 23). Only the mRNA expression levels for TBC1D4 were slightly higher in the glomerulus compared to GLUT4 gene levels in this site (TBC1D4 mRNA 35 ± 10 % vs. WT mRNA 20 ± 4 %, p = 0.17). The qRT-PCR data were further confirmed by IHC (see next section).

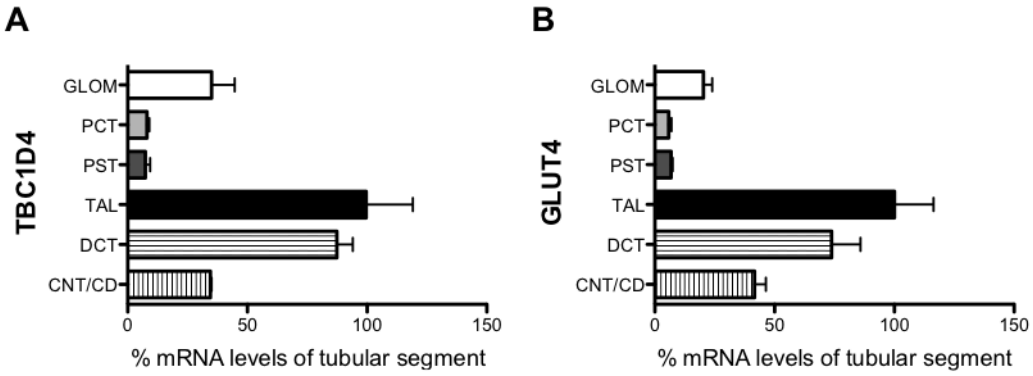

Figure 23: **TBC1D4 and GLUT4 mRNA expression along the nephron A + B** GLUT4 mRNA expression overlaps with TBC1D4 mRNA expression along the nephron (n $\geq$ 3 for each segment, mean ± SEM, normalized to GAPDH) of microdissected tubules from WT mice. **A** TBC1D4: Glom 35 ± 10 %, PCT 8 ± 1 %, PST 7 ± 2 %, TAL 100 ± 19 %, DCT 88 ± 7 %, CNT/CD 34 ± 1 % **B** GLUT4: Glom 20 ± 4 %, PCT 6 ± 1 %, PST 7 ± 1 %, TAL 100 ± 18 %, DCT 74 ± 12 %, CNT/CD 41 ± 5 %

4.3.2 Analysis of GLUT4 protein expression along the nephron via IHC in WT mice

We used two commercially available antibodies against GLUT4 (from Sigma Aldrich® and Millipore™ for immunohistochemistry on fixed kidney cryosections. GLUT4-immunostaining was detectable in the medullary and cortical TAL as shown by co-localization with the TAL specific NKCC2. Moreover, GLUT4 was shown by co-staining for with NCC (DCT-marker) and AQP2 (CNT/CD-marker) to be present at high levels in DCT, CNT and CD (Figure 24). In the latter two segments, GLUT4

protein expression levels were higher in intercalated cells than in the segment-specific CNT and CD cells. In the glomerulus, despite mRNA-results, no GLUT4-staining could be found. Instead, the close family member, GLUT1 stained parietal epithelial cells (PECs) in the glomerulus. One possible explanation might be that GLUT4-antibodies were not sensitive enough to stain for GLUT4 in the glomerulus, or that GLUT1 replaces GLUT4 in these cells, which might also be regulated by TBC1D4.

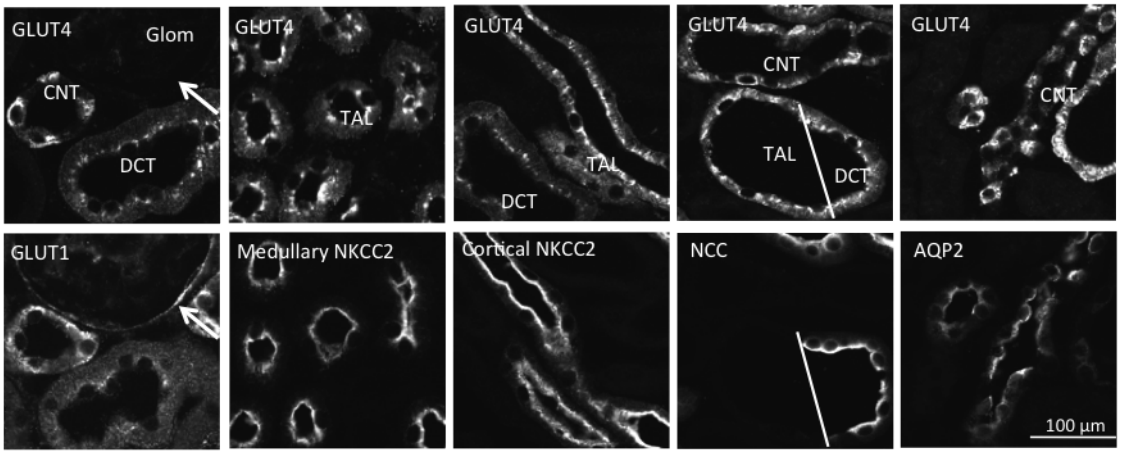

Figure 24: **Immunohistochemistry of GLUT4 protein expression along the nephron** GLUT4 is seen in NKCC2-positive TALs, NCC-positive DCTs, and AQP2 positive CNTs and CDs. The bar indicates the transition from TAL to DCT. GLUT4 is absent from the GLUT1-positive parietal epithelial cells (PECs, arrow). Consecutive sections, n $\geq$ 3.

4.3.3 Intracellular distribution of renal GLUT4 in WT mice

The intracellular localization of renal GLUT4 was analyzed by using IHC and confocal microscopy. In TAL and DCT, GLUT4 appeared to be localized below the apical membrane and in a perinuclear region (Figure 25). The latter possibly respresenting the GLUT4-storage vesicles (GSV). In the CNT/CD, especially in the intercalated cells, the staining for GLUT4 appeared to be most prominent at the cell basis. However, neither in TAL, DCT nor CNT/CD a clear apical or basolateral membrane staining was visible.

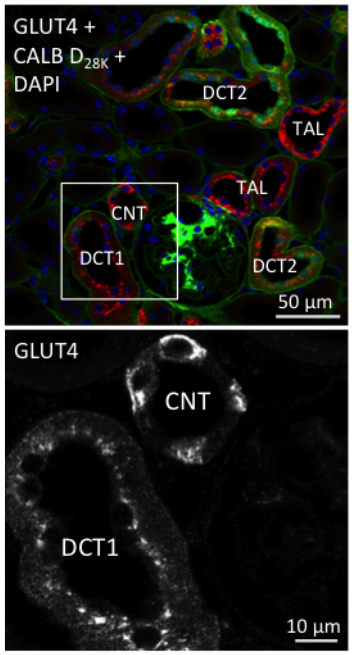

Figure 25: **Intracellular localization of GLUT4** GLUT4 seems to be localized below the apical membrane at perinuclear regions in the TAL/DCT. In the CNT, especially in the intercalated cells GLUT4 appears more pronounced at the basolateral cell side. CALB D28K (green); cytoplasmic Ca^{2+} binding protein, GLUT4 (red), DAPI (blue)

4.4 Renal GLUT4 protein levels are reduced in TBC1D4$^{-/-}$mice

When we analyzed by western blotting GLUT4 levels in the kidneys of WT vs. TBC1D4$^{-/-}$ mice, we found decreased GLUT4 expression in TBC1D4$^{-/-}$ mice, independent from the diet on which the mice were kept (Figure 26). Membrane-enriched GLUT4 as well as total GLUT4 protein levels were diminished by around 30 - 40 %. Both antibodies (S = from Sigma Aldrich® and M = from Millipore™) showed the same effect (Figure 27). This data indicates that the Rab GAP TBC1D4 may regulate GLUT4 not only in the previously shown fat and muscle tissue, but also in the kidney. Interestingly, also GLUT1 protein levels were found to be reduced in kidneys of TBC1D4$^{-/-}$ mice compared to TBC1D4 WT mice (Figure 27). To further analyze the effect of TBC1D4 on GLUT4, the distribution, localization and abundance of GLUT4 was also studied in kidneys of WT and TBC1D4$^{-/-}$ mice by IHC. Using an antibody dilution series, it was possible to clearly show that the GLUT4 signal vanished earlier and more in TBC1D4$^{-/-}$ mice than in WT litter-

mates (Figure 28). Although the protein abundance was clearly different between the genotypes, higher magnifications of TBC1D4-positive tubule segments did not reveal any differences in the subcellular localization of GLUT4 between renal tubules of WT and TBC1D4-deficient mice.

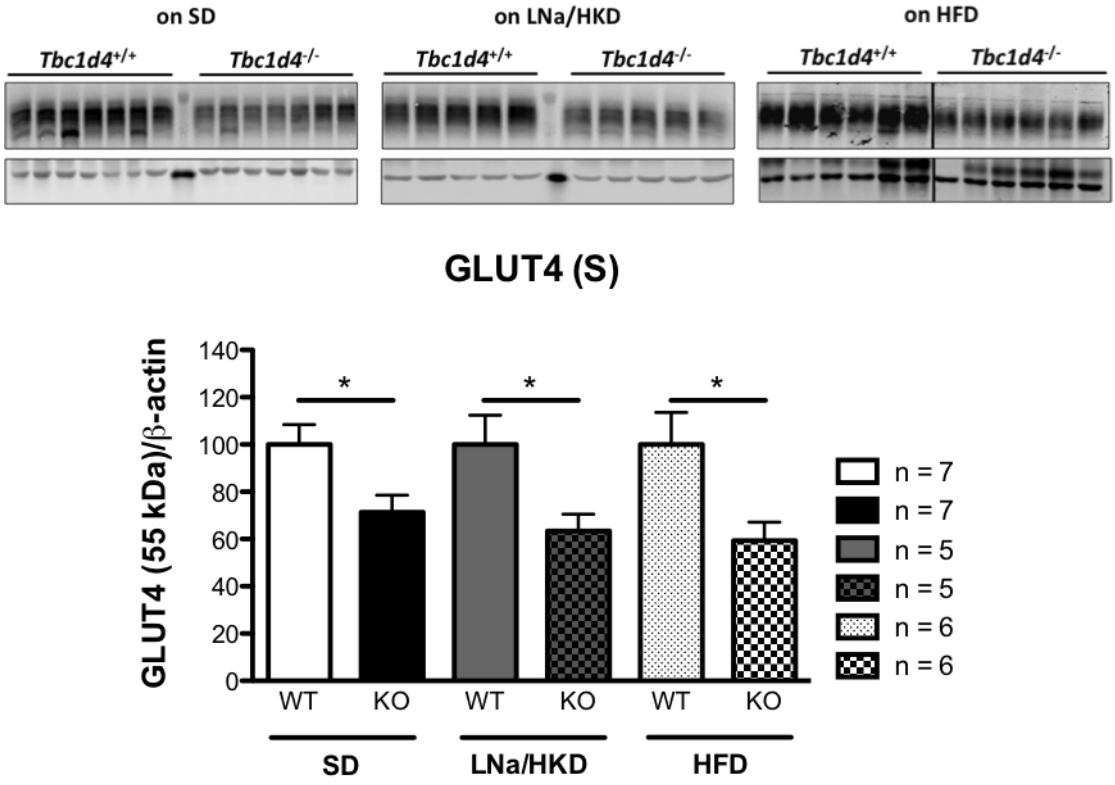

Figure 26: **Western blot analysis of renal GLUT4 of WT and TBC1D4$^{-/-}$ mice under different diets** SD, LNa/HKD and HFD show all a decrease of GLUT4 abundance of renal membrane enriched protein fractions (WT vs. KO: SD 100 ± 8.45 vs. 71.4 ± 7.18, p = 0.024; LNa/HKD 100 ± 12.45 vs. 63.38 ± 7.17, p = 0.034; HFD 100 ± 13.61 vs. 59.37 ± 7.81, p = 0.027). Normalized to β-actin. Densitometric analysis in bar graph, values are ± SEM, student's t test, *p < 0.05. GLUT4 Sigma (S) antibody

4.4.1 Upstream proteins and TBC1D1 proteins are not changed in TBC1D4$^{-/-}$ mice

To investigate whether upstream proteins of the insulin-TBC1D4-GLUT4 pathway were differentially regulated, immunoblotting was performed of kidney lysates from mice on SD and LNa/HKD. The phosphorylation level of the Akt kinase, which itself is activated through phosphorylation by the PI3K at Ser473 (pS473) after insulin binding, was analyzed (Figure 29). Under SD, Akt pS473 levels were not

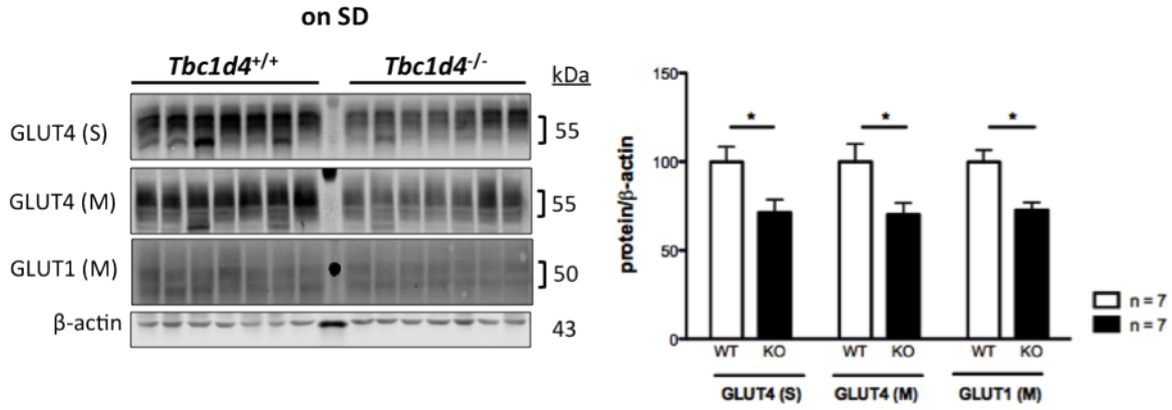

Figure 27: **Western blot analysis of renal GLUT4 and GLUT1 of WT and TBC1D4$^{-/-}$ mice under SD** GLUT4 levels of renal membrane enriched protein fractions were analyzed with two commercially availably antibodies (S = Sigma, M = Millipore). GLUT1 (M = Millipore) was further analyzed. Protein levels were all decreased [WT vs. KO: GLUT4 (S) 100 ± 8.45 vs. 71.4 ± 7.18, p = 0.024; GLUT4 (M) 100 ± 10.13 vs. 70.23 ± 6.48, p = 0.03; GLUT1 (M) 100 ± 6.58 vs. 72.74 ± 4.26, p = 0.004]. Densitometric analysis in bar graph, values are ± SEM, student's *t* test, *p < 0.05

different between WT and KO mice and slightly up-regulated under LNa/HKD in TBC1D4$^{-/-}$ mice (p = 0.083) (Figure 29). For the close homologue of TBC1D4, TBC1D1, no differential expression was observed in the kidneys of TBC1D4$^{-/-}$ mice under SD and LNa/HKD (p = 0.76 and p = 0.260, respectively) (Figure 29), suggesting that altered expression of TBC1D1 does not contribute to the compensation of the loss of TBC1D4 in knockout mice.

4.4.2 Increased basal glucose uptake in primary TAL cells of TBC1D4$^{-/-}$ mice

The data presented above suggests that GLUT4 protein abundance is reduced in the kidneys of TBC1D4$^{-/-}$ mice when compared to WT mice. To investigate the functional impact of altered GLUT4 abundance, an adequate assay system to measure GLUT4 function was needed. For this, we used the recently established primary TAL cell culture method [Glaudemans et al., 2013]. qRT-PCR of known genes in the insulin-signaling cascade of microdissected TAL tubules was performed, which

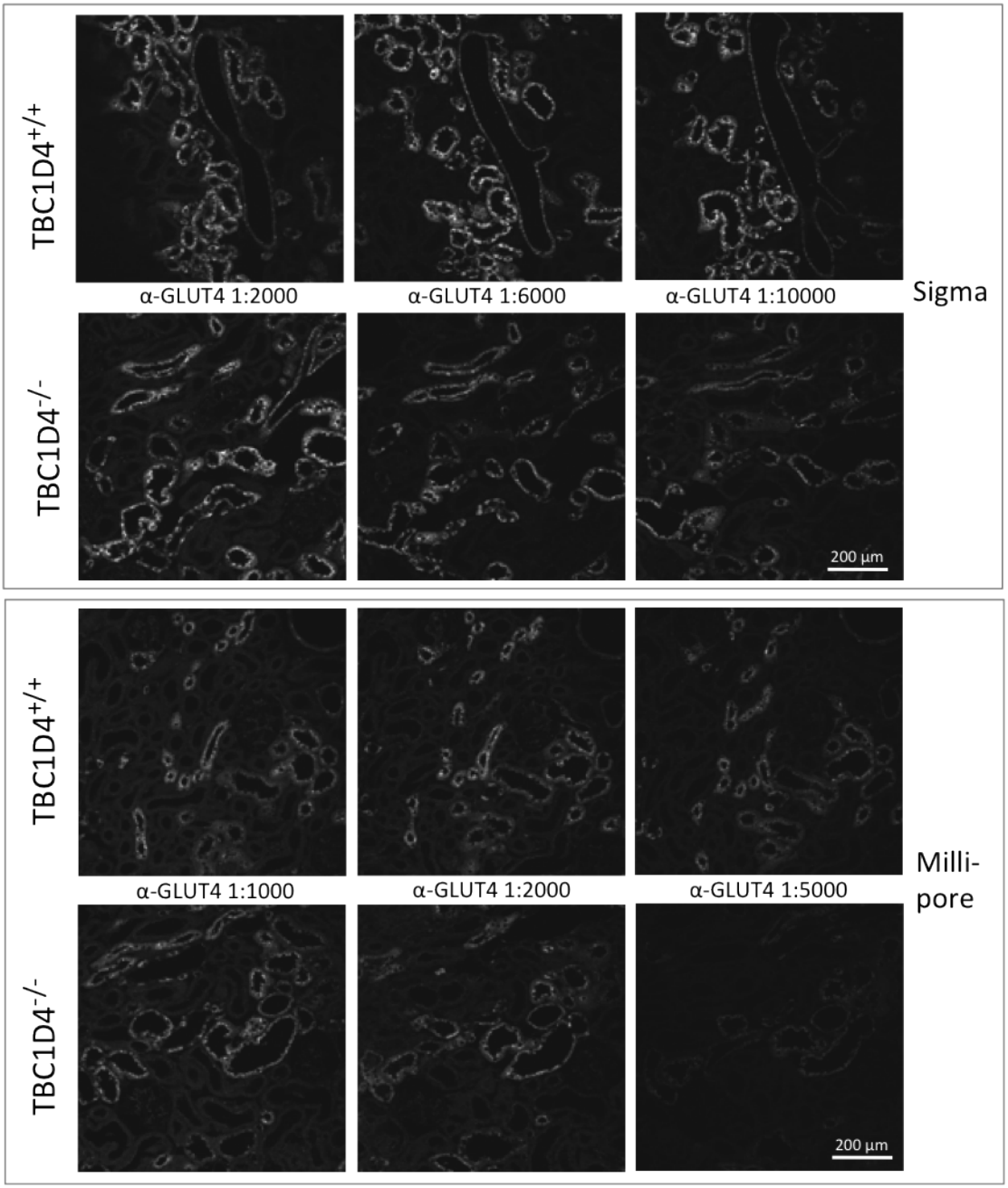

Figure 28: **GLUT4 IHC/antibody dilution series using two commercially available antibodies** GLUT4 staining disappears earlier in TBC1D4$^{-/-}$ compared to WT mice on higher antibody dilutions, tested with the antibody from Sigma and Millipore, n $\geq$ 3

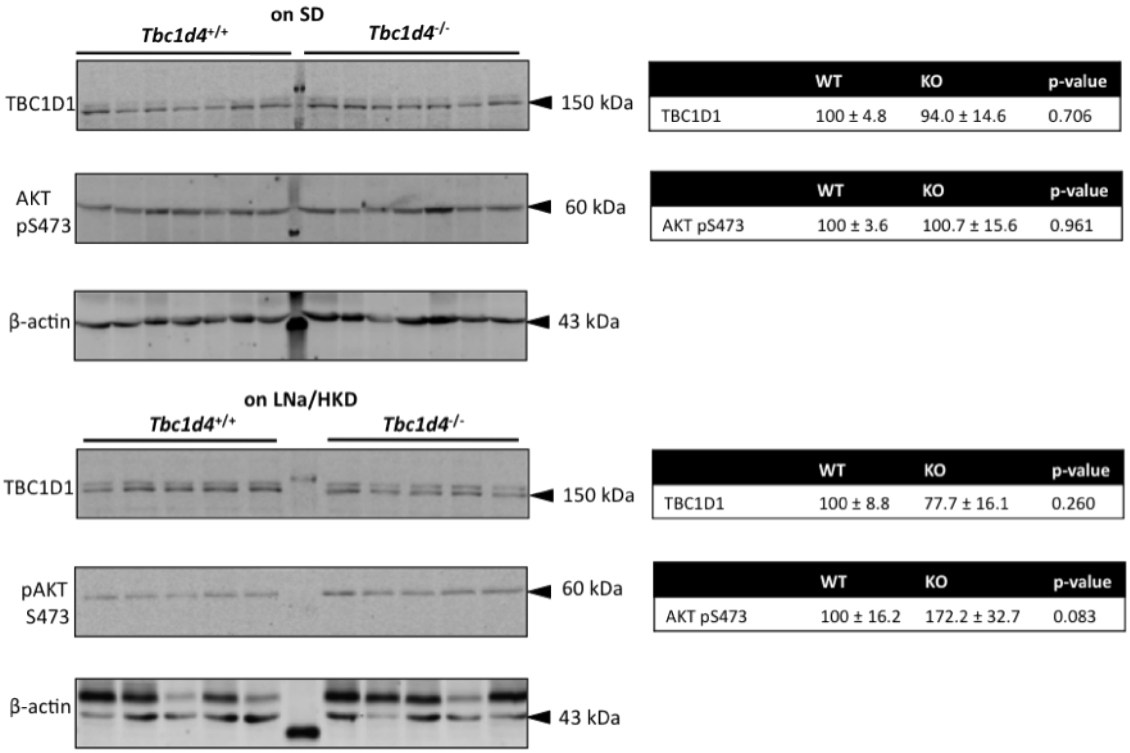

	WT	KO	p-value
TBC1D1	100 ± 4.8	94.0 ± 14.6	0.706

	WT	KO	p-value
AKT pS473	100 ± 3.6	100.7 ± 15.6	0.961

	WT	KO	p-value
TBC1D1	100 ± 8.8	77.7 ± 16.1	0.260

	WT	KO	p-value
AKT pS473	100 ± 16.2	172.2 ± 32.7	0.083

Figure 29: **Western blot analysis of TBC1D1 and Akt pS473 of WT and TBC1D4$^{-/-}$ (KO) mice under SD and LNa/HKD** Left: Western blot analysis (n = 5- 7), right: densitometric anaylsis, ± SEM, student's t test.

confirmed the presents of essential genes such as TBC1D4 and GLUT4 as well as the insulin receptor (IR), the Rab GAP TBC1D1 and the Rab GEF DENND4C (Table 10).

TAL genes	CT ± SEM
GLUT4	28.22 ± 0.085
TBC1D4	24.37 ± 0.22
TBC1D1	22.22 ± 0.035
IR	25.49 ± 0.064
Rab8A	23.49 ± 0.092
DENND4C	24.20 ± 0.085

Table 10: **qRT-PCR analysis of genes involved in the insulin-signaling pathway in lysates of microdissected TALs** Values are ± SEM. Triplicates were run.

Primary TAL cells were grown on permeable support for a proper differentiation and polarization (apical vs. basolateral) of the cells. After 14 days in primary culture, TAL cells taken from WT and TBC1D4$^{-/-}$ mice were analyzed for insulin-dependent glucose uptake measured by ^{3}H-deoxyglucose uptake. Glucose uptake under unstimulated conditions was significantly higher in TAL cells from TBC1D4$^{-/-}$ mice compared to TAL cells of WT mice (128.2 %, p = 0.018) (Figure 30 C). Insulin treatment (300 nM) increased glucose uptake to values seen in unstimulated TAL cells of TBC1D4$^{-/-}$ mice, when compared to unstimulated basal condition. In TAL cells of TBC1D4$^{-/-}$ mice, insulin did not stimulate glucose uptake at all (basal vs. insulin-stimulated: 128.2 % vs. 125.8 % p = 0.82). Indinavir, a reversible blocker of GLUT4 [Murata et al., 2002], lowered glucose uptake similarly in TAL cells of both, WT and TBC1D4$^{-/-}$ mice (WT: 101 %, p = 0.004, TBC1D4$^{-/-}$: 97 %, p = 0.027), suggesting that the insulin-mediated increase in glucose uptake is mediated, at least in part, by GLUT4. Cytochalasin B, an irreversible blocker of GLUT1-4 [Blodgett et al., 2011], reduced glucose uptake to over 99 % (Figure 30 B).

We also tried to determine the cell surface abundance of GLUT4 in TAL cells. To reach this aim, the apical and basolateral membrane of primary TAL cells grown on permeable supports were biotinylated. Subsequently, biotinylated proteins were purified by streptavidin-beats and then used for immunoblotting. While biotinylated Na^+-K^+-ATPase was well detectable, biotinylated NKCC2 and GLUT4 were not detectable, suggesting that their cell surface abundance is below the detection threshold (Figure 31). Detection of NKCC2 and GLUT4 in total kidneys and total TAL-cell protein samples served as positive controls. The intracellular β-actin was only detectable in total kidney and total TAL fractions, but not in the biotinylated fraction, confirming that only plasma membrane but not intracellular proteins had been biotinylated (Figure 31).

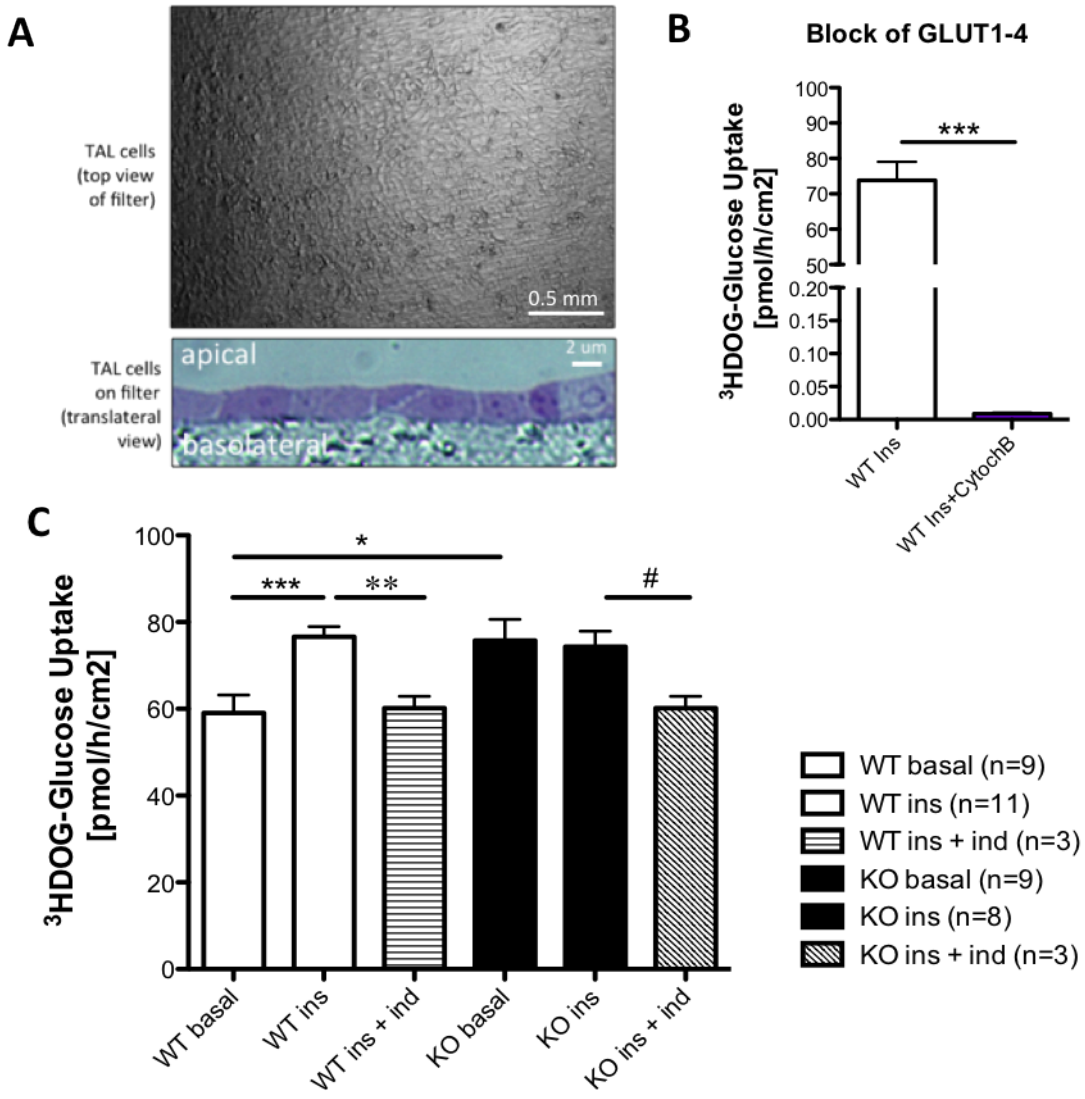

Figure 30: **Glucose uptake in primary TAL cells A** Top and tanslateral view of TAL cells grown on permeable supports. **B** Block with the irreversible GLUT1-4 blocker Cytochalasin B inhibited > 99 % of the glucose uptake in primary TAL cells. **C** Basal glucose uptake was increased in TAL cells of TBC1D4$^{-/-}$ mice and insulin response (300 nM insulin, 15 min) was abrogated in these cells compared to cells from WT mice. Block with the specific GLUT4 inhibitor indinavir (10 μM, 15 min) reduced glucose uptake levels to basal levels of TAL cells from WT mice in both genotypes. Ins = insulin, ind = indiniavir, * vs. WT basal *p < 0.05, ***p < 0.001, **p < 0.005, #vs. KO ins, #p < 0.05, n ≥ 3, mean $\pm$ SEM.

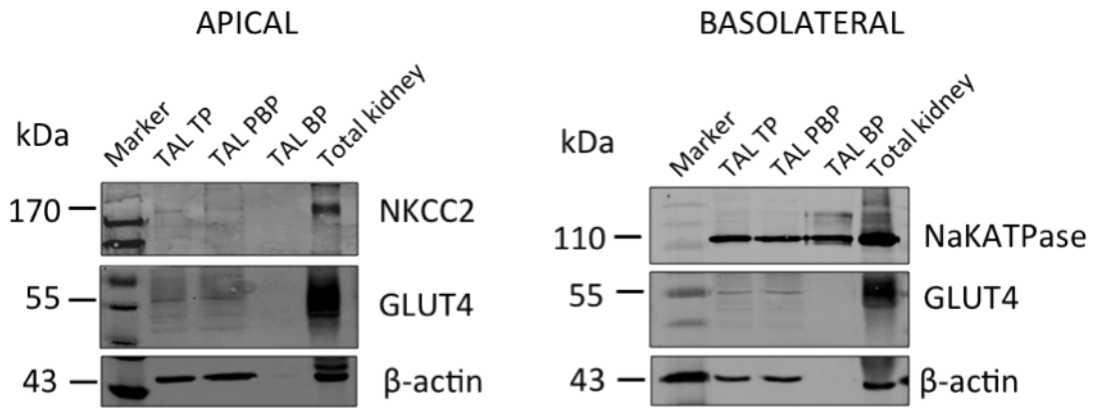

Figure 31: **Cell surface biotinylation of TAL cells Apical** No detection of the NKCC2 and GLUT4 in the biotinylated protein (BP) fraction. **Basolateral** The Na^+-K^+-ATPase was detectable in the BP fraction, but not GLUT4. The intracellular β-actin was not stained in the BP fraction. TP = total proteins, PBP = post-biotinylated proteins, BP = biotinylated proteins

4.5 Project 2: Microarray analysis to examine for compensatory mechanisms of TBC1D4-deficiency in COPAS-sorted DCT cells

The intensive phenotyping including various physiological challenges in project 1, did not reveal a severe impairment in renal water and salt handling, but rather showed a renal electrolyte handling that is not different between WT and TBC1D4-deficient mice. Therefore, we speculated a compensatory regulation of other genes (e.g. up-regulation of alternative RAB GAPs or down-regulation of counter-regulatory RAB GEFs) may explain the rather normal phenotype. To test this hypothesis, we used microarray analysis in order to investigate differently regulated mRNAs in COPAS-isolated DCTs of WT and TBC1D4-deficient mice. The DCT was chosen, because this tubule segment is one of the segments with the highest TBC1D4 expression levels. Moreover, it is rather short and composed by only one cell type, eliminating the risk of high variability between samples.

4.5.1 Confirmation of microarray analysis of TBC1D4 deficiency and the NF-κB inhibitor COMMD6 down-regulation by qRT-PCR

Microarray and qRT-PCR analysis confirmed loss of the TBC1D4 gene in DCT cells of TBC1D4 knockout mice (Figure 32 A). Interestingly, microarray analysis revealed also a loss of COMMD6 expression. COMMD6 is an inhibitor of tumor necrosis factor (TNF)-induced NF-κB. Remarkably, the gene is localized on the same chromosome as the TBC1D4 gene and both genes are directly adjacent (Figure 32 B). Therefore, we speculated that the loss of COMMD6 is due to an extended fusion transcript deletion of TBC1D4 and thus an artefact of the knockout technique. Indeed, when analyzing genomic DNA (gDNA), COMMD6 expression was not absent (Figure 32 C).

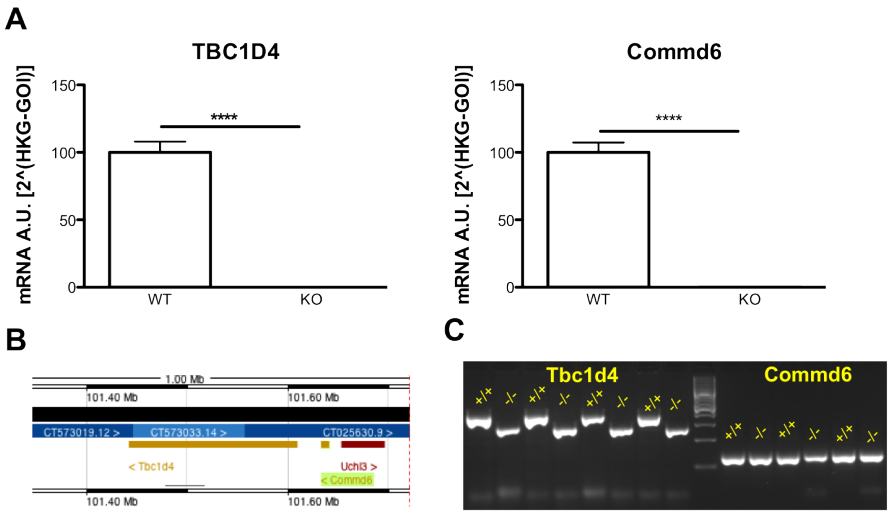

Figure 32: **Microarray analysis: Confirmation of TBC1D4 and COMMD6 knockdown in DCT lysate by qRT-PCR A** mRNA levels TBC1D4 and COMMD6 are significantly down-regulated in TBC1D4$^{-/-}$ vs. WT mice.**B** Adjacent localization of TBC1D4 and COMMD6 (green underlined) on chromosome 14 in mice (www.ensembl.org) **C** Expression of COMMD6 in genomic DNA.

4.5.2 qRT-PCR analysis of microarray data of possible genes interfering with TBC1D4-signaling

The microarray analysis revealed, in addition to COMMD6, a few other differently regulated genes (Table 11). Those that were most significantly regulated and/or

could be likely involved in compensation of the TBC1D4 loss were further analyzed by qRT-PCR. Reduced levels of Sprouty 2 (Spry2), which is able to inhibit Ras activity similarly to TBC1D4 and is involved in the endothelial growth factor (EGF) signaling, could not be confirmed by qRT-PCR to be differentially regulated between WT of TBC1D4$^{-/-}$ mice. Likewise, the mRNA levels of the protein tyrosine phosphatase 1 β, PTP-1B, or protein tyrosine phosphatase receptor type B (Ptpb1; Ptprb), being regulated by Spry2 and known to regulate IGF-1 signaling, were slightly but not significantly reduced in knockout mice compared to WT mice (Figure 33). Moreover, the TBC1 protein family member, TBC1D10a, and the Ras GTPase-activating like protein IQGAP1 were not differentially expressed between WT and TBC1D4-deficient mice as shown by qRT-PCR (Figure 34).

Gene		Chr	Ratio	p-value	ØWT	ØKO	KO1	WT1	KO2	WT2	KO3	WT3	KO4	WT4
Tbc1d4	TBC1 domain family, member 4	chr14	0.05129	6.60E-012	6.752	2.467	2.509	6.695	2.724	6.807	2.455	6.582	2.178	6.924
Commd6	COMM domain containing 6	chr14	1.285	0.0001085	7.403	7.765	7.851	7.424	7.806	7.402	7.733	7.366	7.67	7.42
Ptprb	protein tyrosine phosphatase, receptor type B	chr10	0.6894	0.002328	4.104	3.567	3.262	4.216	3.784	3.977	3.86	4.12	3.364	4.103
Spry2	sprouty homolog 2 (Drosophila)	chr14	1.217	0.007187	4.367	4.65	4.834	4.446	4.634	4.431	4.565	4.187	4.566	4.402
Itpripl1	inositol 1,4,5-triphosphate receptor interacting protein-like 1	chr2	0.7876	0.007899	4.219	3.874	3.799	3.911	3.939	4.194	3.835	4.37	3.925	4.401
Scd1	stearoyl-Coenzyme A desaturase 1	chr19	0.4913	0.02288	4.962	3.937	4.133	5.347	4.6	3.796	3.571	5.613	3.443	5.093
Hbegf	heparin-binding EGF-like growth factor	chr18	0.7806	0.02747	4.804	4.447	4.522	5.16	4.52	4.951	4.244	4.535	4.501	4.592
Iqgap1	IQ motif containing GTPase activating protein 1	chr7	1.112	0.01762	7.889	8.041	8.041	7.926	8.102	7.895	8.044	7.884	7.978	7.85
Tbc1d10a	TBC1 domain family, member 10a	chr11	1.142	0.05076	4.674	4.865	5.023	4.634	4.938	4.778	4.752	4.759	4.746	4.524
Acadm	acyl-Coenzyme A dehydrogenase, medium chain	chr3	1.011	0.8038	9.628	9.644	9.658	9.534	9.545	9.655	9.726	9.629	9.646	9.694
Ehhadh	enoyl-Coenzyme A, hydratase/3-hydroxyacyl Coenzyme A dehydrogenase	chr16	1.005	0.9725	6.907	6.914	6.526	6.619	7.4	6.656	6.966	7.109	6.763	7.244
Hadh	hydroxyacyl-Coenzyme A dehydrogenase	chr3	1.001	0.9876	10.52	10.52	10.66	10.46	10.48	10.49	10.5	10.56	10.45	10.58
Ppargc1a	peroxisome proliferative activated receptor, gamma, coactivator 1 alpha	chr5	1.055	0.4514	9.402	9.479	9.482	9.465	9.586	9.617	9.557	9.302	9.291	9.222
Ppargc1a	peroxisome proliferative activated receptor, gamma, coactivator 1 alpha	chr5	1.033	0.5558	8.476	8.524	8.572	8.513	8.608	8.551	8.602	8.419	8.313	8.422
Ppargc1b	peroxisome proliferative activated receptor, gamma, coactivator 1 beta	chr18	1.04	0.6976	5.604	5.661	5.768	5.772	6.063	5.501	5.453	5.603	5.36	5.542
Insr	insulin receptor	chr8	1.042	0.4396	7.181	7.241	7.23	7.274	7.178	7.21	7.338	7	7.217	7.242
Rab8a	RAB8A, member RAS oncogene family	chr8	0.9975	0.9514	8.277	8.273	8.305	8.264	8.222	8.268	8.205	8.261	8.36	8.315
Dennd4c	DENN/MADD domain containing 4C	chr4	1.003	0.9505	7.168	7.172	7.237	7.176	7.281	7.207	7.152	7.085	7.018	7.202
Slc2a4	solute carrier family 2 (facilitated glucose transporter), member 4	chr11	1.001	0.9801	7.71	7.712	7.706	7.801	7.694	7.746	7.649	7.766	7.798	7.527
Slc12a1	solute carrier family 12, member 1	chr2	0.9341	0.4817	7.541	7.443	7.223	7.675	7.709	7.511	7.57	7.734	7.269	7.244
Scnn1a	sodium channel, nonvoltage-gated 1 alpha	chr6	1.103	0.06993	9.901	10.04	9.989	9.851	10	10.07	10.11	9.83	10.06	9.849
Scnn1b	sodium channel, nonvoltage-gated 1 beta	chr7	0.8982	0.1281	7.604	7.449	7.519	7.722	7.633	7.499	7.202	7.601	7.444	7.596
Scnn1g	sodium channel, nonvoltage-gated 1 gamma	chr7	0.9541	0.6009	7.378	7.31	7.485	7.336	7.531	7.324	6.941	7.564	7.285	7.288

Table 11: **Microarray analysis: list of genes of DCT cells from WT and TBC1D4 $^{-/-}$ mice**

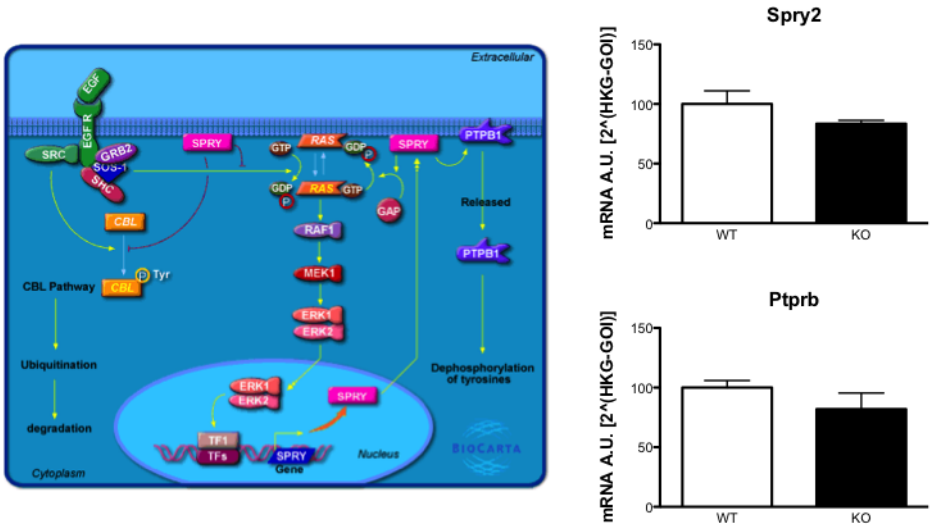

Figure 33: **Microarray analysis: Analysis of Spry2 and Ptprb in DCT lysates by qRT-PCR** Left: Schematic depiction of the Spry2 and Ptprb (also named PTPB1) pathways (www.biocarta.com). Right: Differential regulation of the Spry2 and Ptprb gene could not be confirmed by qRT-PCR.

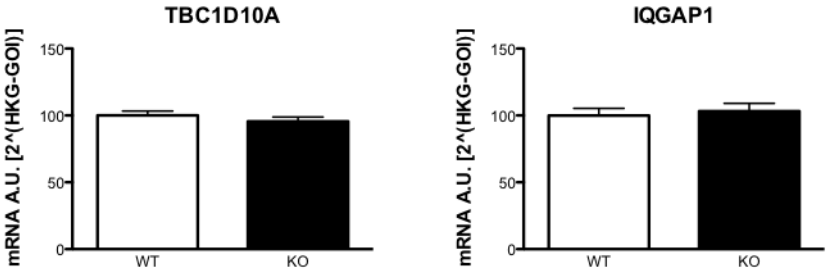

Figure 34: **Microarray analysis: Analysis of TBC1D10A and IQGAP1 in DCT lysates by qRT-PCR** The TBC1D10a and IQGAP1 genes were not differentially expressed between WT and TBC1D4$^{-/-}$ (KO) mice in DCT lysates as shown by qRT-PCR.

In contrast, the stearoyl-CoA desaturase 1 (Scd1), which is a rate-limiting enzyme in the biosynthesis of mono-unsaturated fatty acids, was confirmed to be reduced by over 50 % (Figure 35). Dobrzyn and coworkers have shown that Scd1 knockout mice have increased energy expenditure, reduced adiposity, and increased insulin sensitivity. Furthermore, Scd1-deficiency decreases the activity of PTP-1B, which leads to an increase in phosphorylation of IR and IRS-1 and -2 with subsequent augmentation of Akt activity and finally increased GLUT4 membrane translocation and enhanced glucose transport. Likewise, Scd1-KO mice showed increase in the expression of enzymes involved in fatty acid oxidation [Dobrzyn and Ntambi, 2005;

Dobrzyn et al., 2010]. Additionally, Chadt et al. showed an increased basal palmitate oxidation in EDL muscle of TBC1D4$^{-/-}$ mice [Chadt et al., 2015]. However, when we analyzed mRNA levels of genes involved in fatty acid oxidation, such as the acyl-Coenzyme A dehydrogenase medium chain (MCAD; Acadm), the enoyl-Coenzyme A hydratase/3-hydroxylacyl Coenzyme A dehydrogenase (HD; Ehhadh), and the 3-hydroxyacyl-Coenzyme A dehydrogenase (HCDH; Hadh) as well as the transcriptional activators PGC-1α and PGC1β (peroxisome proliferative activated receptor gamma, coactivator 1; Ppargc1a and Ppargc1b), we found no evidence for any differential regulation of these genes at the transcriptional level in renal DCT cells of WT and TBC1D4$^{-/-}$ mice (Figure 36). Therefore, the functional impact of the deregulated Scd1 expression for fatty acid oxidation in particular and metabolism in general remains elusive.

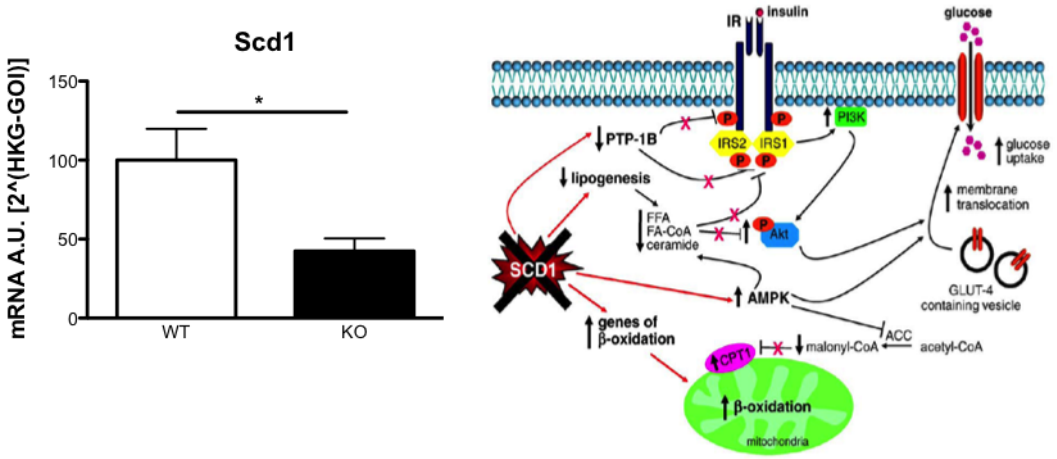

Figure 35: **Microarray analysis: Confirmation of reduced Scd1 gene expression in TBC1D4$^{-/-}$ (KO) mouse qRT-PCR** Left: The Scd1 gene expression was decreased in DCT cell lysates of TBC1D4$^{-/-}$ compared to WT mice. student's t test, n =4, *p < 0.05. Right: impact of Scd1 deletion on multiple intracellular pathways [Dobrzyn and Ntambi, 2005].

4.6 Establishing a cell culture system with functional NCC expression as a tool to study the role of TBC1D4 in NCC regulation

The aim of this subproject was to establish an in vitro system with stable NCC expression in which by co-expression the role of TBC1D4 on NCC regulation could

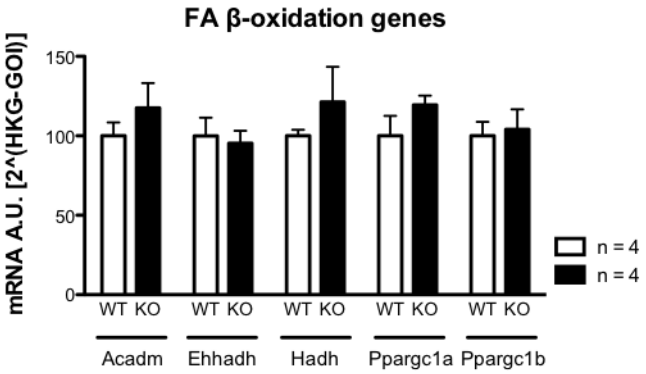

Figure 36: **Microarray analysis: Genes of the fatty acid (FA)-β oxidation** Gene levels of the acyl-Coenzyme A dehydrogenase medium chain (Acadm), enoyl-Coenzyme A hydratase/3-hydroxylacyl Coenzyme A dehydrogenase (Ehhadh), 3-hydroxyacyl-Coenzyme A dehydrogenase (Hadh), and the peroxisome proliferative activated receptor gamma, coactivator 1 β and α (Ppargc1a and Ppargc1b) were similar. qRT-PCR of DCT lysates of WT and TBC1D4$^{-/-}$ (KO) mice, student's t test

be studied. To date, no ex vivo/in vitro system has been found suitable to study the molecular regulation of NCC. The only two available DCT cell line so far, the mpkDCT [Gesek and Friedman, 1992; Diepens et al., 2004] and native mDCT cells [Gesek and Friedman, 1995; Dai et al., 1997a,b, 1998], both form a polarized epithelium, yet have either a very low NCC expression or lose their NCC expression rapidly with time in cell culture.

4.6.1 HEK293 cells with stably inserted hNCC

Human embryonic kidney (HEK293) cells were transfected with either the linearized pcDNA3.1-hNCC plasmid or with the pEGFP-C3-NCC plasmid for monitoring transfection efficiency (Figure 37). Only cell cultures showing a transfection efficiency > 50 % were kept for antibiotic selection (gentamycin; G-418) of stably transfected cells (Figure 37). Further on, cell lines with NCC expression maintained for more than 2 passages under antibiotic selections were considered to stably express NCC and were used for further experiments.

We tested mRNA expression of transfected HEK cells, which were starved for 24 h or 48 h prior to RNA extraction, with two different primer pairs, amplifying the initial region (N-terminus) and the end region (C-terminus) of NCC. The latter primer

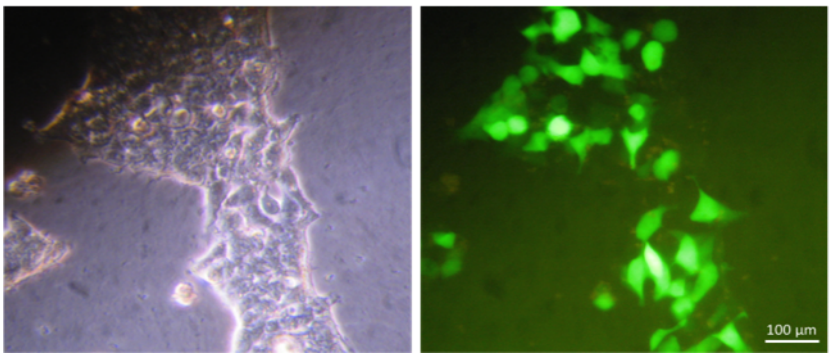

Figure 37: **Transfection of HEK293 with pEGFP-C3-NCC** HEK293 cells were transfected with the pEGFP-C3-NCC in order to estimate transfection efficiency, cell cultures with > 50 % transfection rate were used.

pair was used in order to confirm complete integration of the linearized plasmid in the cells' genome and thus intact NCC-expression (Figure 38 A). With both primer sets, strong NCC expression could be detected in transfected HEK293 cells, but not in untransfected HEK293 and mCCD cells, confirming successful stable expression of full-length NCC in the transfected HEK293 cells. These results were reflected on the protein level (Figure 38 B). Untransfected HEK293 cells and mCCD cells showed no NCC expression. The total kidney lysate showed a slight smear at around 130 kDa, which is well known to represent glycosylated NCC and a band at around 110 kDa representing core-glycosylated NCC [de Jong et al., 2003; Hoorn et al., 2011]. Transfected HEK293 cells strongly expressed the 110 kDa-NCC band. Next to transcriptional and proteomic studies, immunofluorescence of transfected HEK293 cells revealed a strong NCC-staining, whereas untransfected HEK293 cells only showed background staining. The arrow points to possible membrane localization of NCC (Figure 38 C). The amount of transfected NCC-cells was around 40-50 %.

4.6.2 Analyzing the phosphorylation levels of hNCC in stably transfected HEK cells using in cell western

NCC function critically depends on phosphorylation of NCC at several serine and threonine residues in the N-terminal tail of NCC [Richardson et al., 2008]. To assess if NCC phosphorylation can be modulated in stably transfected NCC cells, cells were treated with calyculin A (CA), a strong serine/threonine protein phosphatase inhibitor, in an in cell western (ICW). Total NCC abundance, using an antibody recognizing the C-terminus of NCC (total NCC = tNCC), was similar compared

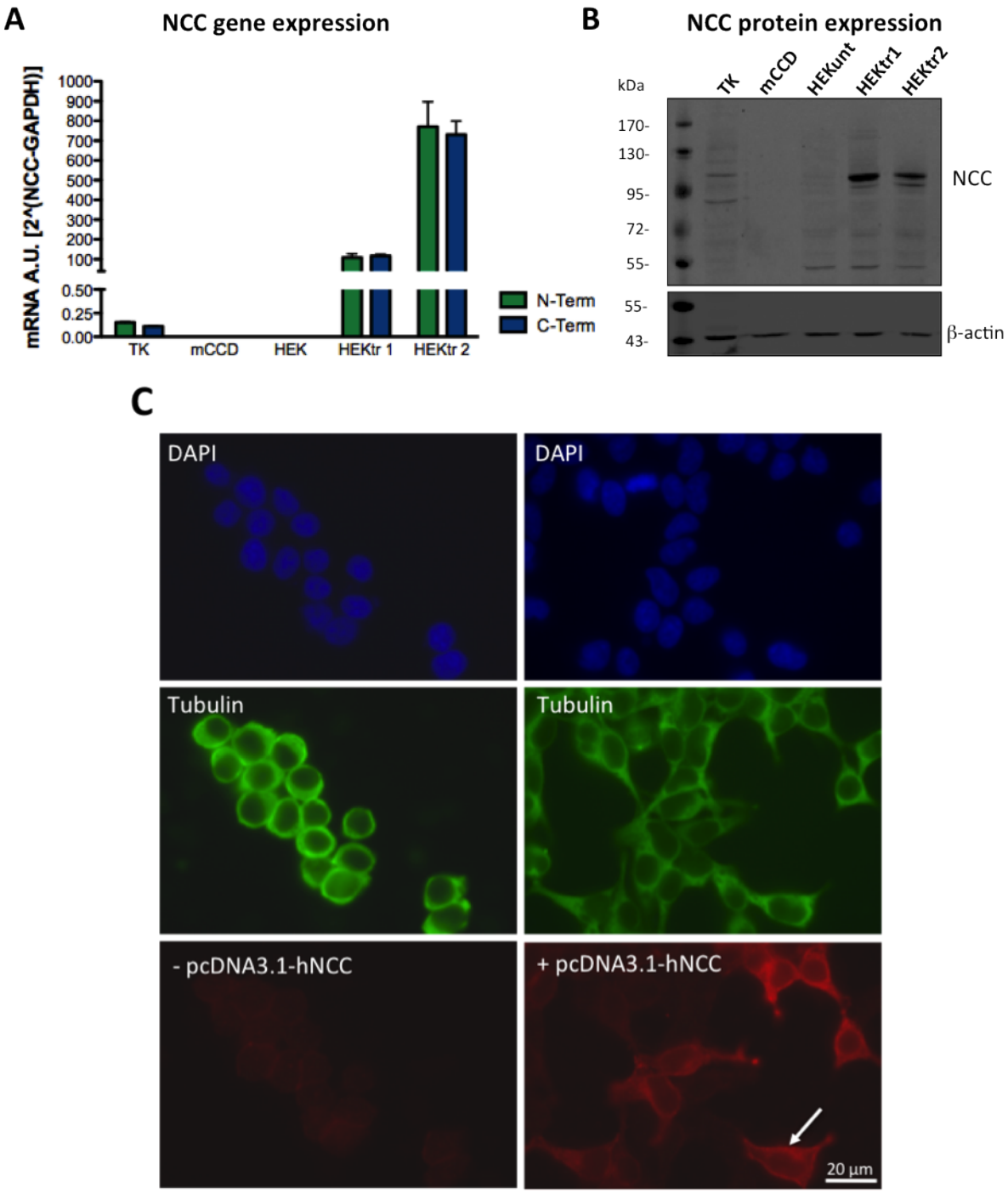

Figure 38: **Stable transfection of HEK293 with pcDNA3.1-hNCC A** Analysis of NCC gene expression in total kidney (TK), mCCD cells, untransfected HEK293 and HEK293 transfected and starved for 24 h/48 h (HEKtr 1/HEKtr 2), with two primer pairs, N-terminal (N-Term) and C-terminal (C-Term). **B** NCC protein expression (HEKunt = HEK293 untransfected). **C** Immunocytochemistry of untransfected and transfected HEK293 with the pcDNA3.1-hNCC with NCC (red). Detection of nuclei with DAPI (blue), of cytoskeleton with α-tubulin (green). Arrow points to a possible membrane staining of NCC.

to control and vehicle treated HEK293-hNCC-cells (Figure 39). Total NCC abundance, using an antibody recognizing an extracellular loop of NCC (extracellular total NCC = etNCC), was strongly reduced after CA treatment compared to control and vehicle cells. All 4 phosphorylation sites (pT53, pT58, pS71 and pS89) were highly phosphorylated. In conclusion, the phosphatase-inhibitor CA is able to modulate phosphorylation of hNCC in transfected HEK293 cells. Further characterization of the HEK-hNCC-cell line (e.g. NCC sequencing, NCC trafficking, NCC cell surface expression, Na^+ and Cl^- uptake) was the objective of the master thesis of Dario Ruppli [Ruppli, 2012], that I oversaw under the supervision of Prof. Johannes Loffing and Dr. Urs Ziegler. The thesis showed that HEK293 cells, though expressing significant levels of NCC, do not export NCC to the cell surface and hence show no measurable NCC cell surface abundance and activity. Likewise, other research groups were not able to achieve significant cell surface activity in transfected HEK293 cells (O. Staub and D. Ellison, personal communication). Therefore, this approach was abandoned.

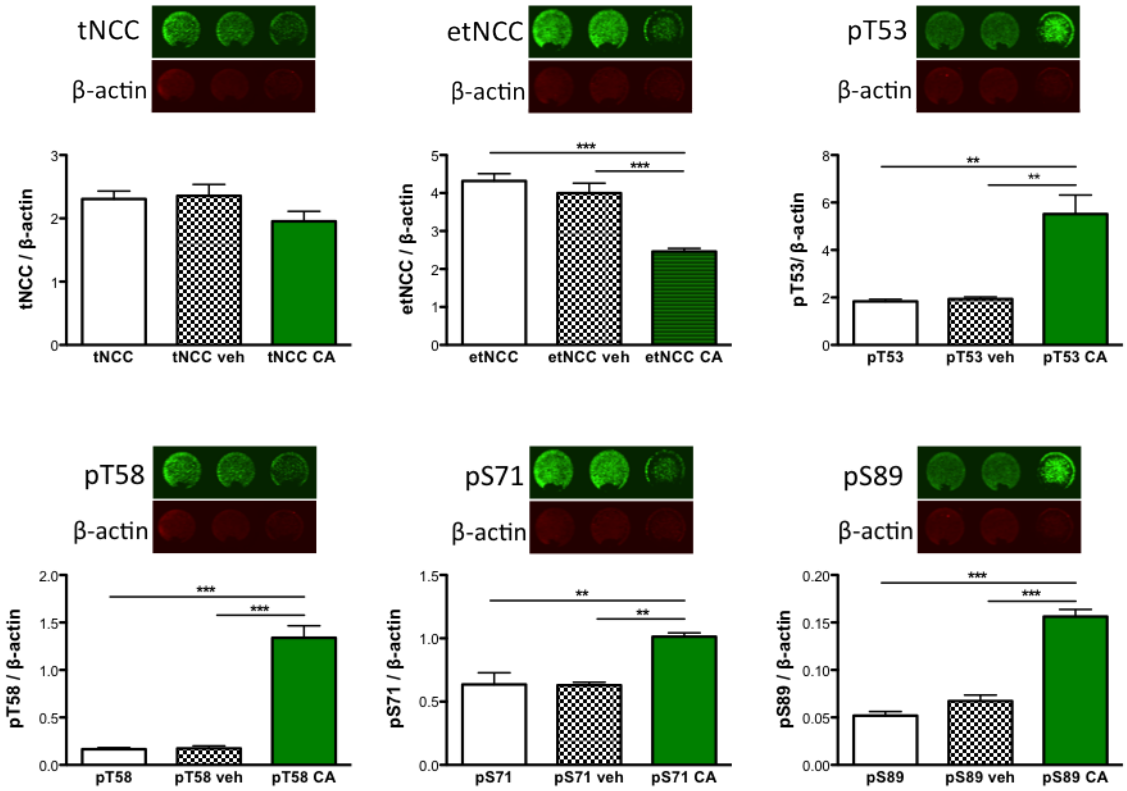

Figure 39: **NCC phosphorylation by ICW** HEK293-hNCC cells were treated for 30 min with either 50 nM CA or vehicle. An additional control without any treatment was used, n = 4. CA-treatment increased NCC-phosphorylation at pT53, pT58, pS71 and pS89, extracellular NCC was decreased (etNCC). tNCC = total NCC, student's t test, ** $p < 0.005$, *** $p < 0.0005$

5 Discussion

By using a complete knockout mouse model, this thesis investigated the role of the Rab GAP TBC1D4 with a special focus on the role of TBC1D4 on renal electrolyte and fluid homeostasis. By immunohistochemistry analyses, TBC1D4 expression was found in distinct nephron segments; the parietal epithelial cells (PECs) of Bowman's capscule, the thin and thick limbs of Henle's loop, the DCT, CNT and CD, but its function in these segments remained elusive. Based on in vitro studies showing modulation by TBC1D4 of ENaC, AQP2 and Na^+-K^+-ATPase abundance, cell surface localization and function, we hypothesized that TBC1D4 might be involved in the regulation of these salt and water transporting proteins in the kidney and thus that TBC1D4 controls renal ion and water handling and hence extracellular fluid homeostasis. The experiments presented in this thesis showed that a loss of TBC1D4 in the kidney in vivo does not impair renal ion and water handling but reduces the abundance of the glucose transporter GLUT4 in the renal distal tubule. The latter may affect glucose uptake into these renal epithelia and hence interfere with their glycolytic capacity. Microarray analysis of COPAS-isolated DCTs from WT and TBC1D4$^{-/-}$ mice did not provide any conclusive proof regarding the differential expression of other gene products compensating for the loss of TBC1D4. However, Scd1, an enzyme involved in fatty acid metabolism was significantly down-regulated in TBC1D4$^{-/-}$ mice on transcriptional levels. The functional relevance of Scd1 in the kidney remains to be analyzed.

5.1 TBC1D4 and the control of renal salt and water reabsorption in vivo

One of the most pivotal tasks of the kidneys is to adjust ion and water balance and hence blood volume and blood pressure. To fulfill this task, the nephron is equipped with specific ion transporters and ion and water channels such as NKCC2, NCC, ENaC, AQP2 and the Na^+-K^+-ATPase. Recent in vitro studies suggested that the Rab GAP TBC1D4 is a key protein regulating the trafficking of the Na^+-K^+-ATPase

[Alves et al., 2010], ENaC [Liang et al., 2010], and AQP2 [Jung and Kwon, 2010; Kim et al., 2011]. In MDCK and COS cells, Alves and coworkers demonstrated that TBC1D4 promotes intercellular retention of the Na^+-K^+-ATPase [Alves et al., 2010]. Likewise, Liang and coworkers showed that knockdown of TBC1D4 in mpkCCD cells increases apical ENaC abundance and amiloride-sensitive Na^+ transport [Liang et al., 2010]. Thus, these in vitro studies suggested that TBC1D4 retains the Na^+-K^+-ATPase and ENaC inside the cell and reduces transepithelial Na^+ transport. Conversely, we found in another mouse CCD cell line (mCCD cells), that a TBC1D4 knockdown reduced both, baseline as well as aldosterone-stimulated ENaC cell surface abundance and activity [Gresko, 2011], suggesting that TBC1D4 is a positive regulator of Na^+ transport in the renal collecting system. Based on the results of Liang, we expected that TBC1D4$^{-/-}$ mice would have a sodium retaining phenotype with arterial hypertension, hypokalemia and suppressed plasma aldosterone levels (Liddle's syndrome-like phenotype), while based on our results, we expected the opposite phenotype with arterial hypotension, hyperkalemia, and increased plasma aldosterone levels (pseudohypoaldosteronism type I-like phenotype).

5.1.1 Effects of renal TBC1D4 loss on salt homeostasis under standard conditions

In contrast to the profound effects of TBC1D4 on ENaC and the Na^+-K^+-ATPase in vitro, TBC1D4$^{-/-}$ mice were neither hyper- nor hypotensive, independent of any dietary challenge (high-fat diet or high salt-high fat diet). For blood pressure recordings, we used the non-invasive tail cuff method, which has a lower sensitivity in detecting blood pressure differences compared to the invasive, more costly radiotelemetry. The disadvantage of the tail cuff method compared with the radiotelemetry is, that it does not allow monitoring of blood pressure over 24 hours. Hence, we lack blood pressure-measurements during the active night period, where differences between mouse lines may become more pronounced as shown for example in Ronzaud et al. [2013]. Nevertheless, we did not find any evidence by further analyzes, that TBC1D4$^{-/-}$ mice display a dysfunction of ENaC. The TBC1D4$^{-/-}$ mice did not show any abnormalities in plasma aldosterone and renin levels, plasma ion levels (Na^+, K^+), acid-base status, urinary ion excretion (Na^+, K^+), and urinary aldosterone excretion. Moreover, the protein abundance of the most important distal tubule Na^+ proteins (NKCC2, NCC, ENaC, AQP2 and the Na^+-K^+-ATPase) were not different between the genotypes. Likewise, no difference in the phosphorylation level of NCC was observed. Taken together, these results strongly suggest that TBC1D4$^{-/-}$ mice do not have any dysregulation in renal Na^+ transporting

proteins and renal Na^+ handling, which does also likely explain the normal blood pressure in the knockout mice.

5.1.2 Effects of renal TBC1D4 loss on salt homeostasis under challenging conditions

Gene knockout mice do often show no or a rather mild renal phenotype under standard conditions, but reveal severe adaptive impairments when challenged, e.g. by dietary ion restriction or loading. Only on a high Na^+ diet, mice with a nephron-specific deletion of the E3-ubiquitin protein ligase Nedd4-2 reveal increased blood pressure and elevated ENaC (β and γ), ROMK, total and phosphorylated NCC levels [Ronzaud et al., 2013]. Similarly, in nephron-specific $SGK1^{-/-}$ mice reduced blood pressure, lowered Nedd4-2 phosphorylation, decreased NCC levels and Na^+ loss only became apparent under a low Na^+ diet [Faresse et al., 2012]. Likewise, $NCC^{-/-}$ mice developed hypokalemia, a common feature of Gitelman's syndrome, only after exposure to a low K^+ diet only [Morris et al., 2006]. A main task of the TBC1D4-positive distal tubule is to adapt renal Na^+ and K^+ excretion to the dietary intake. A maximal stimulation of the distal tubule can be achieved by a low Na^+ and high K^+ diet, that also profoundly stimulates the aldosterone system [Kaissling and Le Hir, 1982; Le Hir et al., 1982]. Therefore, WT and $TBC1D4^{-/-}$ mice were given a low Na^+/high K^+ diet (LNa/HKD) for 14 days. This diet drastically increased urinary and plasma aldosterone levels in both genotypes, confirming the efficacy of the diet. However, plasma aldosterone levels were not different between the genotypes and also other metabolic parameters, blood values, renal renin mRNA levels and the renal protein abundance of NKCC2, NCC, ENaC, AQP2 or the Na^+-K^+-ATPase were not different between WT and $TBC1D4^{-/-}$mice (4.1.4 and 4.1.5). Thus, even under conditions of a maximally challenged aldosterone system, we could find no evidence for a disturbed regulation of one of the tested Na^+ and water transporting proteins and renal Na^+ and K^+ handling. Hence, despite the strong role of TBC1D4 for the regulation of ENaC and the Na^+-K^+-ATPase in vitro [Alves et al., 2010; Liang et al., 2010], we did not find any evidence for a similar role of TBC1D4 in vivo.

5.2 TBC1D4 and the control of renal water reabsorption in vivo

Based on in vitro experiments showing how TBC1D4 siRNA knockdown is associated with increased AQP2 cell surface abundance in mpkCCD cells [Kim et al., 2011], we wanted to investigate whether the vasopressin-dependent regulation of AQP2 abundance and trafficking and thus water balance (i.e. urine volumes and urine osmolarity) is disturbed in TBC1D4$^{-/-}$ mice. Therefore, mice were challenged by a mild water restriction in order to stimulate vasopressin release, but to avoid an over-compensatory response induced by maximum water depletion [Zuber et al., 2007]. To do so, mice had ad libitum access to moisturized food (50 %), but not to a water bottle for 24 hours. In response to water restriction, both WT and knockout mice were able to decrease urinary output significantly (4.1.6, Figure 18 A). The urine osmolarity was also increased in WT and KO mice. Likewise, urinary ion (Na^+, K^+, Mg^{2+}) excretion remained similar in both genotypes, suggesting normal vasopressin-dependent regulation of renal water handling. The final effector for vasopressin-dependent regulation of renal water handling is the water channel AQP2 localized in the apical membrane of the segment-specific cells of the CNT and CD. Vasopressin was shown to stimulate via binding to vasopressin V2 receptors intracellular cAMP levels, which activate protein kinase A (PKA) and finally increase the phosphorylation of AQP2 at multiple sites [Fenton et al., 2013; Hoffert et al., 2008, 2006; Katsura et al., 1997; Rice et al., 2012]. The phosphorylation level of AQP2 is eventually decisive for the trafficking of AQP2 to the cell surface and hence for the activity of AQP2 and water transport [Katsura et al., 1997; Rice et al., 2012]. In our study, we did not analyze AQP2 phosphorylation levels, as TBC1D4 is supposed to interfere with AQP2 trafficking, but not with vasopressin-signaling and AQP2-phosphorylation. Using immunoblotting and immunohistochemistry, we did not obtain any evidence that AQP2 regulation is disturbed, even not under challenging conditions such as water restriction. Together with the unaffected urinary concentration ability in TBC1D4$^{-/-}$ mice, our data suggest that the loss of TBC1D4 does not affect renal AQP2 activity in vivo, which contrasts to the strong effect seen in in vitro-experiments [Jung and Kwon, 2010; Kim et al., 2011].

5.3 Discrepancy between in vitro and in vivo data

Our renal phenotyping experiments did not reveal any striking renal disturbance (especially in regard to Na^+ handling, blood pressure control and water homeostasis)

in mice lacking the Rab GAP TBC1D4 (whole section 4.1). This contrasts to several in vitro studies, which consistently reported that TBC1D4 regulates salt and water transporting proteins in renal cells. Kwon and colleagues observed i) decreased phosphorylation of TBC1D4 in Akt1-siRNA M1 cells with or without dDAVP stimulation and ii) in the absence of dDAVP, increased plasma membrane expression of AQP2 in both TBC1D4 knockdown-M1 cells [Jung and Kwon, 2010] and -mpkCCDc14 cells [Kim et al., 2011] by semi-quantitative immunocytochemistry. Furthermore, cell surface biotinylation assays also showed increased AQP2 expression in transfected TBC1D4-siRNA compared with non-targeting control-siRNA mpkCCDc14 cells. Notably, the experiments were performed on non-polarized M1 and mpkCCDc14 cells, which do not resemble the situation found in vivo, in which cells are well differentiated and polarized. The mechanism of regulation of membrane proteins may differ between non-polarized and polarized cells [Lavialle et al., 2000]. On the other hand, Liang and coworkers used polarized mCCD cells, which better resemble the normal physiological properties of tubular cells in vivo. They observed, that the knockdown of TBC1D4 resulted in increased ENaC activity [Liang et al., 2010]. In the same year, Alves et al. showed intracellular retention of the Na^+-K^+-ATPase in COS cells, a monkey kidney-derived cell line, when co-transfected with the Na^+-K^+-ATPase and TBC1D4 [Alves et al., 2010]. However, also these cells do not form a polarized epithelium, questioning the relevance of this model for the in vivo situation. In experiments with polarized MDCK cells, Alves and coworkers found that silencing of TBC1D4 mediated Na^+-K^+-ATPase endocytosis, when treated with compound C, an inhibitor of AMPK. This led to the suggestion that phosphorylation of TBC1D4 might be important for Na^+-K^+-ATPase trafficking and retention at the cell surface. Overall, the discrepancy between the profound role of TBC1D4 on ENaC, the Na^+-K^+-ATPase and AQP2 seen in vitro and the lack of any clear effect seen in vivo might be related to:

1. The cell culture systems. Cell physiology as well as cell culture environment might lack or differ in important cellular and systemic features (e.g. hormonal composition, free fatty acids content, gene expression, and level of cell differentiation).

2. Compensatory mechanisms. As a consequence of the congenital deletion of TBC1D4, compensation may occur, whereby essential renal functions are taken over by other, yet to be determined, mechanisms leading to no overt renal phenotype.

3. Indirect stimulation. The effects seen in vitro might reflect an indirect stimulation leading to an unspecific increased or decreased trafficking and/or activity of membrane transporters and channels.

To 3): the effect seen by the knockdown of TBC1D4 in vitro might reflect an indirect stimulation, e.g. by the lack of GLUT4-storage vesicles, which are typically regulated by TBC1D4, other cargo-vesicles containing e.g. ENaC, AQP2 or the Na^+-K^+-ATPase might be transported in a more unspecific way via Rab proteins to the cell membrane. One other possibility might be, that by interfering with the insulin-signaling cascade, for instance by repressing TBC1D4 in these cells, the trafficking of GLUT4 and thus glucose uptake and energy availability is increased leading to a (secondary/indirect) increase in trafficking and activity of membrane proteins such as ENaC, APQ2 and the Na^+-K^+-ATPase. Indeed, several group have suggested that insulin is thought to regulate ENaC, AQP2, the Na^+-K^+-ATPase as well as NCC not only in vitro but also in vivo. However, the molecular mechanisms and whether this regulation occurs via GLUT4 are still unexplored. Song and coworkers observed increased activity of NCC (most likely via WNK4) and ENaC during chronic insulin infusion in rats [Song et al., 2006]. Several studies have demonstrated that insulin induces the phosphorylation of NCC in heterologous expression systems [Chávez-Canales et al., 2013], in mpkDCT cells [Sohara et al., 2011] as well as in vivo, in Zucker obese (ZO) rats [Komers et al., 2012] and in mice [Sohara et al., 2011]. Interestingly, this specific NCC phosphorylation is associated with a concomitant increase in the phosphorylation of SPAK and OSR1 [Chávez-Canales et al., 2013; Komers et al., 2012; Sohara et al., 2011]. Furthermore, insulin is known to increase renal salt reabsorption in the distal nephron and hyperinsulemia is proposed to cause hypertension [Song et al., 2006]. In mammals (men, dogs and mice), insulin leads to the reduction of fractional Na^+ excretion [DeFronzo et al., 1975, 1976] related to increased ENaC abundance, trafficking and activity [Tiwari et al., 2007]. Furthermore, the Na^+-K^+-ATPase is activated, phosphorylated, and trafficked from intracellular vesicles to the cell surface by insulin stimulation [Comellas et al., 2010; McGill and Guidotti, 1991]. This insulin-dependent Na^+-K^+-ATPase regulation has been demonstrated in adipocytes [McGill, 1991], human [Al-Khalili et al., 2004] and rat skeletal muscle cells [Al-Khalili et al., 2003], and in lungs [Comellas et al., 2010] and is linked to ERK1/2 and PI3K signaling ([Al-Khalili et al., 2004; Comellas et al., 2010]. Likewise, insulin has been shown to increase AQP2 expression via MAPK, PI3K, and ERK1/2 in mouse mpkCCD [Bustamante et al., 2005] and rat native IMCD cells [Pisitkun et al., 2008]. However, it seems in this case that the loss of TBC1D4 is redundant in vivo as no effect on renal ion and water handling as well

as in the abundance, subcellular localization and activity of renal Na^+ and water transporting proteins was seen with mice fed different diets like the high fat diet known to affect insulin signaling. However, when interfering more upstream in the insulin-signaling cascade, e.g. knockout of the insulin receptor (IR), effects on ENaC trafficking and regulation were observed in vivo (Li et al., 2013; Pavlov et al., 2013) (further discussed in 5.5).

5.4 TBC1D4 and whole body glucose homeostasis

5.4.1 Loss of TBC1D4 and body weight regulation

As mentioned previously, TBC1D4 was linked to the insulin-dependent regulation of glucose homeostasis. Moreover, members of the TBC1 domain family were related to the control of body weight. Chadt and coworkers reported for example a protection against diet-induced obesity in mice bearing a naturally-occurring mutation in TBC1D1 [Chadt et al., 2008]. A lower BW was also seen in TBC1D1/TBC1D4 double knockout mice, even when fed an ad libitum standard diet [Chadt et al., 2015]. Likewise, a reduced gain in BW gain was observed in the TBC1D4-Thr649Ala knockin mice [Chen et al., 2011]. Overall, these examples are in line with our findings that TBC1D4$^{-/-}$ mice increase their body weight (BW) less than their WT littermates following a 6-month period on a HFD. Interestingly, this weakened increase in BW was not driven by food intake, which was similar in both mice genotypes [data not shown, but see [Wang et al., 2013]]. In addition, TBC1D1$^{-/-}$ and TBC1D4$^{-/-}$ mice had increased fatty acid uptake and oxidation, reflected by a lower respiratory quotient, which implies a higher energy supply from fatty acids [Chadt et al., 2015, 2008]. Wang and coworker could further demonstrate that TBC1D4$^{-/-}$ mice have a normal physical activity, but a lower energy expenditure rate, evident from a lower oxygen consumption and heat production [Wang et al., 2013]. Chadt and coworkers suggested that the lower BW in TBC1D1$^{-/-}$ and TBC1D4$^{-/-}$ mice results from a higher lipid oxidation and hence from a lowered adipose tissue mass [Chadt et al., 2015]. Conclusively, our finding of a reduced body weight gain further confirms that also TBC1D4 might control body weight.

5.4.2 Effects on glucose tolerance and insulin sensitivity in TBC1D4$^{-/-}$ mice

We found a normal to a slightly improved glucose tolerance and impaired insulin sensitivity in TBC1D4$^{-/-}$ mice. These effects may appear surprising, given that an impaired insulin sensitivity and an improved glucose tolerance are usually opposing effects. However, similar observations were made by others; in TBC1D4 knockout mouse models, which are different from ours [Lansey et al., 2012; Wang et al., 2013], and in the Thr649Ala knockin mouse model [Chen et al., 2011]. In contrast to the knockout models, the TBC1D4 Thr649Ala model has an impaired glucose tolerance, whereas the knockout models show either a normal or slightly improved glucose tolerance [Wang et al., 2013]. Interestingly, all knockout models did not show any hyperinsulemia during the glucose tolerance test [Chadt et al., 2015; Chen et al., 2011; Wang et al., 2013]. Our TBC1D4$^{-/-}$ mice had constantly lower blood glucose levels under non-starved conditions and significantly lower levels after starvation (see 4.2.4). Remarkably, the TBC1D4$^{-/-}$ mice had also lower plasma insulin levels, which could be the consequence of the slight hypoglycemia (see section 4.2.4 and [Wang et al., 2013]). The cellular and molecular mechanisms underlying these findings deserve further elucidation. This thesis focused on the renal role of TBC1D4. Underlying mechanisms for the metabolic phenotype are currently being addressed elsewhere. The discrepancies observed between the different TBC1D4-knockout and -knockin models regarding glucose metabolism (Table 1, 1.8.2) may dependent on several factors, such as strain differences, targeting strategy for knockout/knockin generation, age and sex of the animals, etc. These discrepancies also warrant further investigations, as they might be informative about the role of TBC1D4 in different genetic backgrounds and may offer explanations for gender differences.

5.5 GLUT4 expression in the kidney

As mentioned above, TBC1D4 was previously demonstrated to regulate the intracellular trafficking of the glucose transporters GLUT4 [Kane et al., 2002; Sano et al., 2003; Treebak et al., 2010] and GLUT1 [Ngo et al., 2009] in fat and skeletal muscles cells. Both transporters were also shown to be expressed in the human and rat kidney, though slightly discrepant results on the precise intracellular localization were reported. Now, we analyzed mouse kidneys of WT mice and found by qRT-PCR analysis of free-hand microdissected nephron segments GLUT4 mRNA expression in the glomerulus, the TAL, DCT and CNT/CD (see 4.3.1). Using two

different GLUT4 antibodies, immunohistochemistry confirmed the high abundance of GLUT4 in distal tubules and the collecting system (4.3.2). However, in the glomerulus, GLUT4 protein could not be detected by IHC. This divergence to the mRNA data could be explained by several not mutually exclusive reasons:

1. The sensitivity of qRT-PCR is usually higher than the sensitivity of IHC. Thus, it is possible that the protein abundance of GLUT4 in the glomerulus is below the detection limit of IHC, while the mRNA is already well detectable by qRT-PCR. In fact, the glomerular GLUT4 mRNA expression was lower than in distal tubules and collecting ducts.

2. mRNA and protein abundance do not necessarily correlate, due to posttranscriptional and posttranslational mechanisms, which control protein abundance independent from altered transcription [Gygi et al., 1999].

3. The detection of GLUT4 in the glomerular preparation could be due to a contamination with distal tubular epithelia cells. In fact, the macula densa of the TAL is firmly attached to the vascular pole of the glomerulus (see 1.1). However, previous studies using the detection of tubule marker genes confirmed that contaminations are negligible [Glaudemans et al., 2013].

While there was a close correlation between GLUT4 and TBC1D4 expression throughout the renal tubular system, GLUT4 mRNA expression in the glomerulus was rather weak compared with the prominent TBC1D4 expression at this site. This suggests, that there might be an additional target protein for TBC1D4 expressed in the glomerulus. In fact, IHC demonstrated that the parietal epithelial cells (PECs) of the mouse glomerulus, previously shown by us to be the glomerular site of TBC1D4 expression [Lier et al., 2012], do also express GLUT1. Similarly, Heilig and coworkers found GLUT1 staining in PECs by using immunogold staining [Heilig et al., 1995]. Moreover, Clarke and collaborators suggested an insulin-regulated transport of GLUT1 similar to GLUT4 [Clarke et al., 1994], which was reinforced by the finding of Mendes et al., who showed GLUT1 cell surface expression in response to WNK1-phosphorylation of TBC1D4 in HEK293 cells [Mendes et al., 2010]. There is increasing evidence that cells of the glomerulus and the distal tubule are insulin-sensitive, as shown by the presence of proteins of the insulin-signaling cascade, including the insulin receptor (IR) [Butlen et al., 1988; Hale and Coward, 2013] and PKB/Akt [Chabardès-Garonne et al., 2003; Pradervand et al., 2010]. As mentioned

in 5.3, previous studies suggested that insulin regulates distal tubule ion transporting proteins including NCC, ENaC and the Na^+-K^+-ATPase [Féraille et al., 1995; Sohara et al., 2011; Tiwari et al., 2007]. Consistently, recent studies demonstrated the localization of the IR on the basolateral plasma membrane of the distal tubule and collecting duct of WT mice [Li et al., 2013; Pavlov et al., 2013]. Mice with a CD-specific deletion of the IR have a reduced apical ENaC activity and an abated blood pressure [Li et al., 2013]. These observations were interpreted to further support a direct regulation of ENaC by insulin. However, given the striking high abundance of GLUT4 in the distal tubule and collecting duct another link between the IR and ENaC activity is conceivable. Insulin may regulate GLUT4-dependent glucose uptake into the distal tubular and collecting duct epithelial cells, which could be used for glycolytic ATP production, which drives the activity of the Na^+-K^+-ATPase and hence indirectly also ENaC activity. Indeed, the distal tubules require a lot of energy, especially the TAL and the DCT, which do also have the highest expression of GLUT4 and TBC1D4. Furthermore, these nephron segments do have the highest density of mitochondria and basolateral membrane infoldings bearing the Na^+-K^+-ATPase, which drives active transport processes [Giebisch and Stanton, 1979; Jorgensen, 1985]. In contrast to the proximal tubule cells, the distal tubule cells possess glycolytic enzymes, which are capable to oxidize glucose and produce ATP in response to insulin during high energy requirements [Mitrakou, 2011]. The GLUT4-mediated glucose uptake and the glycolytic capacity of these cells might contribute to their more pronounced hypoxic/ischemic tolerance compared to the strictly aerobic proximal tubule cells [Bastin et al., 1987; Gamboa et al., 2011; Sun et al., 1994]. Nevertheless, GLUT4 localization at the basolateral side, where the glucose is hypothesized to enter the renal cells, has yet to be confirmed. From our IHC-pictures, GLUT4 appears to be localized in a perinuclear, cytoplasmic region (4.3.2 and 4.3.3), which is consistent to previous reports by Heilig [Heilig et al., 1995]. Only in intercalated cells (ICCs), where GLUT4 as well as TBC1D4 [Lier et al., 2012] are highly abundant, GLUT4 appears to be preferentially localized towards the basolateral plasma membrane. Further experiments and specialized methods are needed (e.g. cell-impermeable GLUT4 photolabeled-biotin ATB-BMPA, high-resolution microscopy, etc.), to reveal the precise localization of GLUT4 expression in kidney cells.

5.6 GLUT4 expression in kidneys and glucose uptake in TAL cells of TBC1D4$^{-/-}$ mice

By western blot analysis and by performing IHC, GLUT4 levels in the kidney were found to be decrease in TBC1D4$^{-/-}$ mice (4.4). Since TBC1D4 down-regulates GLUT4 activity, we expected that the loss of TBC1D4 would increase (and not decrease) GLUT4 abundance, trafficking and membrane insertion. However, also in adipocytes and skeletal muscle cells of TBC1D4$^{-/-}$ mice, GLUT4 levels were reported to be reduced [Lansey et al., 2012; Wang et al., 2013]. A surprising inconsistency was observed when comparing adipocytes with soleus muscle cells in TBC1D4$^{-/-}$ mice. Specifically, basal glucose uptake and the GLUT4-ratio (the ratio between cell surface GLUT4 versus total GLUT4) was increased in adipocytes, whereas is soleus muscle these values were unaltered and decreased, respectively, in TBC1D4$^{-/-}$ versus WT mice [Lansey et al., 2012]. Therefore, global predictions of GLUT4-ratios and glucose uptake cannot be reliably made. Given the fact that renal GLUT4 mRNA levels were not different between our TBC1D4$^{-/-}$ and WT mice, posttranslational effects (e.g. reduced translocation, increased degradation) likely explain the reduced GLUT4 abundance in TBC1D4$^{-/-}$ mice. Moreover, due to the possibility of a higher intrinsic activity of cell surface GLUT4, abundance might be reduced as a compensatory effect in TBC1D4$^{-/-}$ mice. Since GLUT4 abundance and GLUT4 (transport) activity do not necessary correlate, we tried to set-up an ex vivo assay system to measure glucose uptake into renal epithelia of TBC1D4-WT and -deficient mice. For this purpose, we took advantage of the previously developed technique of primary culture of TAL cells from mouse kidneys [Glaudemans et al., 2013]. A further advantage of TAL cells was the high expression of TBC1D4 and GLUT4 and genes involved in the insulin-signaling cascade (see 4.4.2). Using different inhibitors, we confirmed the reliability of our ex vivo assay and to the best of our knowledge, this assay is the first cell culture assay for GLUT4-mediated glucose uptake in polarized renal cells. In these ex vivo-experiments using TAL cells derived from WT and TBC1D4-deficient mice, we found an increased basal glucose uptake in TAL cells of TBC1D4$^{-/-}$ mice. Upon stimulation of TAL cells with insulin, glucose uptake was increased in TAL cells of WT but not in KO mice, suggesting that in TBC1D4-deficient TAL cells glucose uptake was already maximally stimulated (see 4.4.2). Interestingly, the increased basal glucose uptake and the lack of any response to insulin in TAL cells matches well with the hypoglycemic status of TBC1D4$^{-/-}$ mice on basal conditions and the abrogated response to insulin in the insulin tolerance test (ITT). Nevertheless, the observed changes to whole-body glucose homeostasis are unlikely to be related solely to the kidneys. They are most likely

a consequence of the whole body deletion of TBC1D4, but especially in adipocytes and muscle cells. It is however conceivable that the kidneys contribute to the observed systemic effect. Insulin-dependent uptake of glucose into renal distal tubule epithelia may suit the requirements of the cells: provide substrates (e.g. glucose), replenish energy and cover metabolic needs for the increasing workload in e.g. postprandial states. Western blot analysis did also reveal reduced GLUT1 protein levels in kidneys of TBC1D4$^{-/-}$ mice, which further underlines, that GLUT1 might be also regulated by TBC1D4. Similar to the previous results of other research groups [Lansey et al., 2012; Wang et al., 2013] on adipocytes and skeletal muscle cells of TBC1D4$^{-/-}$ mice, we did not find any evidence for any consistent dysregulation of PKB/Akt, suggesting that the observed effects on GLUT4 abundance and activity are independent from or down-stream of Akt.

5.7 Microarray analysis of differentially regulated genes in DCT1 cell of TBC1D4$^{-/-}$ mice

Given the rather mild renal phenotype of the TBC1D4$^{-/-}$ mice (see 4.1), we addressed the question whether the up- or down-regulation of other genes may compensate for the loss of TBC1D4. Therefore, we performed a microarray analysis to seek differentially expressed genes in COPAS-isolated DCT cells from WT and TBC1D4$^{-/-}$ mice. The DCT was chosen, because previous data established that the DCT expresses very high levels of TBC1D4 (our data and Lier et al. [2012]). Moreover, the DCT is, in contrast to the CNT and CD, composed by only one single cell type, reducing the risk of high variability of these results due to cellular heterogeneity in the isolated preparation. The microarray mRNA analysis of COPAS-sorted DCTs corroborated the loss of TBC1D4. Moreover, microarray data showed an almost complete loss of the expression of COMMD6, an inhibitor of NF-κB-dependent immunity and inflammation [Bartuzi et al., 2013]. COMMD6 is localized directly adjacent and down-stream of the TBC1D4 gene on chromosome 14. Although the analyzes of genomic DNA indicated that the COMMD6 gene locus is intact in TBC1D4$^{-/-}$ mice, it is possible that the almost complete decrease of COMMD6 mRNA levels might reflect the loss of an extended fusion transcript with TBC1D4 and/or an artefact by the applied knockout technique. In as much the concomitant loss of COMMD6 interfered with the effect of the loss of TBC1D4 is unclear and a caveat that needs to be considered for the interpretation of the presented data in this thesis. In addition, several other genes (e.g. Spry2, Ptpb1, Scd1, TBC1D10a, IQGAP1) were found to be differently regulated between DCTs of WT

and TBC1D4-deficient mice in the microarray data. However, only dysregulation the stearoylCoA-desaturase-1 (Scd1) could be confirmed by qRT-PCR. Scd1 is a key enzyme in fatty acid metabolism. Interestingly, DCT-Scd1 mRNA levels were decreased in TBC1D4$^{-/-}$ mice. Scd1-KO mice show enhanced insulin-signaling with increased insulin sensitivity together with higher phosphorylation of downstream proteins, such as the IR, insulin receptor substrate (IRS) 1 and 2, and Akt. Consequently, Scd1-deficiency leads to enhanced glucose transport [Dobrzyn and Ntambi, 2005; Rahman et al., 2003]. The loss of TBC1D4 might favor an increase of Scd1 protein levels in order to avoid uncontrolled glucose uptake, thus decreasing Scd1-mRNA levels as a feedback mechanism. Indeed, similarly to TBC1D4$^{-/-}$ mice, which are insulin-resistant, increased Scd1 protein levels have been related to insulin-resistance in humans and animals (reviewed in Dobrzyn et al. [2010]). In addition, Scd1 has been shown to modulate membrane fluidity by the production of oleate, a major monounsaturated fatty acid. By the knockdown of Scd1, the ratio between oleate and membrane phospholipids might change, leading to alterations in the membrane fluidity [Dobrzyn et al., 2010]. The DCT segment is highly plastic and Scd1 loss might influence membrane integrity, having implications on absorptive and secretory transport mechanisms of the DCT. However, a clear role for Scd1 in the DCT and in the kidneys in general is not known. Overall, Scd1 seems promising in unravel further mechanisms in the complex regulation of glucose homeostasis through a putative interference with the TBC1D4-signaling pathway, what could be investigated in a double knockout mouse model. Furthermore, Scd1 has been demonstrated to modulate enzymes involved in fatty acid β-oxidation and Chadt and coworkers showed increased palmitate oxidation in the Rab GAP-deficient mice [Chadt et al., 2008]. We therefore analyzed additional genes, especially involved in fatty acid β-oxidation, although a priori microarray data did not show any specific changes. None of five genes (**Acadm, Ehhadh, Hadh, Ppargc1a, Ppargc1b**) tested by qRT-PCR was either up- or downregulated. Although microarray analysis revealed some contamination of isolated DCTs by NKCC2 (*Slc12a1*)-positive TALs and ENaC (*Scnn1*)-positive late DCTs/CNTs, the expression did not differ between samples from TBC1D4 WT and KO mice. As TBC1D4 as well as GLUT4 (*Slc2a4*) are highly expressed in these adjacent segments, the contamination through mRNAs of these segments was not believed to interfere with the regulatory mechanisms on gene levels in DCTs. However, if genes of the TAL and late DCT/CNT segment would have an impact, the compensatory regulation would most probably be similar in the GLUT4/TBC1D4-positive adjacent segments as in the DCT.

6 General Conclusion/Perspectives

With the finding of TBC1D4 expression in specific segments of the nephron [Lier et al., 2012], this study was devoted to unravel the physiological role of TBC1D4 in the kidneys. In vitro observations suggested a role of TBC1D4 in the control of the ENaC, AQP2 and Na^+-K^+-ATPase. However, this thesis shows that in the kidney in vivo, the regulation of these sodium and water transporting proteins is not affected by a constitutive TBC1D4 deletion. Instead, this thesis provides conclusive evidence from in vivo and in vitro experiments that TBC1D4 controls the glucose transporter GLUT4 in renal distal tubule cells. RT-PCR and immunohistochemistry demonstrated a prominent co-expression of TBC1D4 and GLUT4 along the distal tubule and the collecting system. Loss of TBC1D4 reduces total protein abundance of renal GLUT4, but increases glucose uptake into distal tubules cells to such extent that it cannot be further stimulated by insulin. As such, the data are consistent with the role of TBC1D4 in adipocytes and skeletal muscle cells and suggest that renal TBC1D4 mainly controls renal GLUT4 and glucose metabolism, but not directly renal ion and water handling. Future studies will have to further determine the precise function of TBC1D4 and in particular GLUT4 in the kidney. The distinct localization of TBC1D4 and GLUT4 in the distal tubule is striking. In contrast to proximal tubules, distal tubules do not only rely on aerobic metabolism, but are also enabled for anaerobic glycolysis, which however requires the uptake of large quantities of substrates such as glucose. Given the fact that the tubular fluid in distal tubules is glucose-free, glucose uptake can be only achieved via the basolateral cell side, where it is likely facilitated by GLUT4. The ability for GLUT4-mediated glucose uptake may explain the lower vulnerability to ischemic damage of distal tubules compared with proximal tubules. In line with this, we would expect that the kidneys of TBC1D4-deficient mice may better tolerate ischemia than kidneys of wild-type mice. In fact, preliminary data of collaborators in Yale point in this direction. Moreover, in WT mice insulin-dependent phosphorylation of TBC1D4 may release GLUT4 from intracellular retention in order to provide glucose and energy via glycolysis at times of high requirements/working load (e.g. in the postprandial state) (Figure 40). Moreover, the higher glucose and hence energy supply may indirectly improve energy consuming transepithelial ion and water transport, driven by

the Na^+-K^+-ATPase and mediated by ENaC and AQP2, respectively (Figure 40). Future studies using wild-type, TBC1D4-, and kidney-specific GLUT4-deficient mice will have to further address these hypothesis.

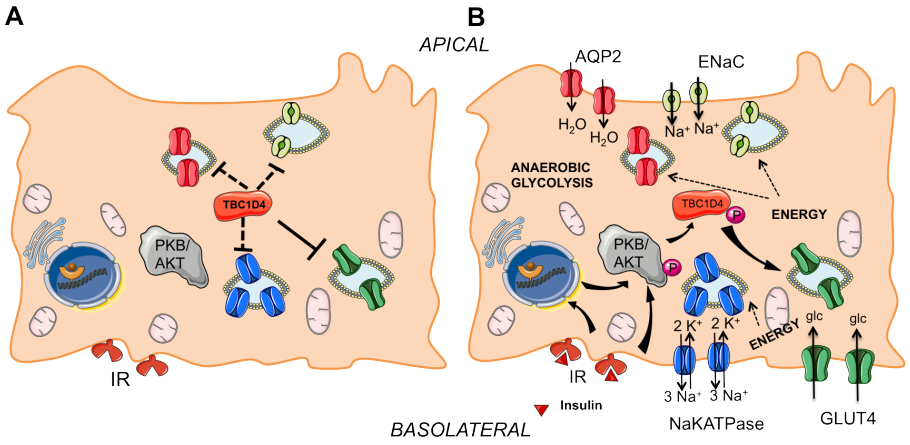

Figure 40: **Hypothetical role of TBC1D4 in renal epithelial cells A** In its non-phosphorylated state, TBC1D4 might inhibit GLUT4-trafficking to the basolateral membrane, as well as indirectly inhibit trafficking of ENaC, AQP2 and the Na^+-K^+-ATPase. **B** After binding of insulin to the basolateral insulin receptor (IR), e.g. at postprandial states, the intracellular phosphorylation cascade might phosphorylate TBC1D4, leading to GLUT4-transport to the membrane and increased glucose uptake. Via (aerobic or anaerobic) glycolysis, the energy in the cell rises favoring the transport of other vesicles containing renal transporters and channels (e.g. ENaC, AQP2 and the Na^+-K^+-ATPase) to the membrane.

In summary, TBC1D4 is not directly crucial for the regulation of renal electrolyte and water transport, but may play a role as part of the renal insulin-signaling cascade in which GLUT4-mediated basolateral glucose uptake may improve the anaerobic glycolytic capacity of distal tubules cells relevant during renal hypoxia and/or during enhanced workload in e.g. postprandial states.

7 References

L. Al-Khalili, M. Yu, and A. V. Chibalin. Na+,K+-ATPase trafficking in skeletal muscle: insulin stimulates translocation of both alpha 1- and alpha 2-subunit isoforms. *FEBS letters*, 536 (1-3):198–202, Feb. 2003. ISSN 0014-5793. URL `http://www.ncbi.nlm.nih.gov/pubmed/12586363`.

L. Al-Khalili, O. Kotova, H. Tsuchida, I. Ehrén, E. Féraille, A. Krook, and A. V. Chibalin. ERK1/2 mediates insulin stimulation of Na(+),K(+)-ATPase by phosphorylation of the alpha-subunit in human skeletal muscle cells. *The Journal of biological chemistry*, 279(24): 25211–8, June 2004. ISSN 0021-9258. doi: 10.1074/jbc.M402152200. URL `http://www.ncbi.nlm.nih.gov/pubmed/15069082`.

S. Albert, E. Will, and D. Gallwitz. Identification of the catalytic domains and their functionally critical arginine residues of two yeast GTPase-activating proteins specific for Ypt/Rab transport GTPases. *The EMBO journal*, 18(19):5216–25, Oct. 1999. ISSN 0261-4189. doi: 10.1093/emboj/18.19.5216. URL `http://www.pubmedcentral.nih.gov/articlerender.fcgi?artid=1171592&tool=pmcentrez&rendertype=abstract`.

A. L. Albiston, H. R. Yeatman, V. Pham, S. J. Fuller, S. Diwakarla, R. N. Fernando, and S. Y. Chai. Distinct distribution of GLUT4 and insulin regulated aminopeptidase in the mouse kidney. *Regulatory peptides*, 166(1-3):83–9, Jan. 2011. ISSN 1873-1686. doi: 10.1016/j.regpep.2010.09.003. URL `http://www.ncbi.nlm.nih.gov/pubmed/20851149`.

R. J. Alpern, O. W. Moe, and M. J. Caplan. *Seldin and Giebisch's The kidney: physiology and pathophysiology*. Elsevier/Academic Press, 5th edition, 2013. ISBN 978-0-12-381462-3.

D. S. Alves, G. A. Farr, P. Seo-Mayer, and M. J. Caplan. AS160 associates with the Na+,K+-ATPase and mediates the adenosine monophosphate-stimulated protein kinase-dependent regulation of sodium pump surface expression. *Molecular biology of the cell*, 21(24):4400–8, Dec. 2010. ISSN 1939-4586. doi: 10.1091/mbc.E10-06-0507. URL `http://www.pubmedcentral.nih.gov/articlerender.fcgi?artid=3002392&tool=pmcentrez&rendertype=abstract`.

T. J. Anderson, S. Martin, J. L. Berka, D. E. James, J. W. Slot, and J. L. Stow. Distinct localization of renin and GLUT-4 in juxtaglomerular cells of mouse kidney. *The American journal of physiology*, 274(1 Pt 2):F26–33, Jan. 1998. ISSN 0002-9513.

J. P. Arroyo, D. Lagnaz, C. Ronzaud, N. Vázquez, B. S. Ko, L. Moddes, D. Ruffieux-Daidié, P. Hausel, R. Koesters, B. Yang, J. B. Stokes, R. S. Hoover, G. Gamba, and O. Staub. Nedd4-2 modulates renal Na+-Cl- cotransporter via the aldosterone-SGK1-Nedd4-2 pathway. *Journal of the American Society of Nephrology : JASN*, 22(9):1707–19, Sept. 2011. ISSN

1533-3450. doi: 10.1681/ASN.2011020132. URL http://www.pubmedcentral.nih.gov/articlerender.fcgi?artid=3171941&tool=pmcentrez&rendertype=abstract.

D. Bacic, C. A. Wagner, N. Hernando, B. Kaissling, J. Biber, and H. Murer. Novel aspects in regulated expression of the renal type IIa Na/Pi-cotransporter. *Kidney international. Supplement*, (91):S5–S12, Oct. 2004. ISSN 0098-6577. doi: 10.1111/j.1523-1755.2004.09102.x. URL http://www.ncbi.nlm.nih.gov/pubmed/15461703.

L. Bai, Y. Wang, J. Fan, Y. Chen, W. Ji, A. Qu, P. Xu, D. E. James, and T. Xu. Dissecting multiple steps of GLUT4 trafficking and identifying the sites of insulin action. *Cell metabolism*, 5(1):47–57, Jan. 2007. ISSN 1550-4131. doi: 10.1016/j.cmet.2006.11.013. URL http://www.ncbi.nlm.nih.gov/pubmed/17189206.

C. Bailly. Transducing pathways involved in the control of NaCl reabsorption in the thick ascending limb of Henle's loop. *Kidney international. Supplement*, 65:S29–35, Apr. 1998. ISSN 0098-6577. URL http://www.ncbi.nlm.nih.gov/pubmed/9551429.

C. Barlet-Bas, C. Khadouri, S. Marsy, and A. Doucet. Enhanced intracellular sodium concentration in kidney cells recruits a latent pool of Na-K-ATPase whose size is modulated by corticosteroids. *The Journal of biological chemistry*, 265(14):7799–803, May 1990. ISSN 0021-9258. URL http://www.ncbi.nlm.nih.gov/pubmed/2159458.

P. Bartuzi, M. H. Hofker, and B. van de Sluis. Tuning NF-κB activity: a touch of COMMD proteins. *Biochimica et biophysica acta*, 1832(12):2315–21, Dec. 2013. ISSN 0006-3002. doi: 10.1016/j.bbadis.2013.09.014. URL http://www.ncbi.nlm.nih.gov/pubmed/24080195.

J. Bastin, N. Cambon, M. Thompson, O. H. Lowry, and H. B. Burch. Change in energy reserves in different segments of the nephron during brief ischemia. *Kidney international*, 31(6): 1239–47, June 1987. ISSN 0085-2538. URL http://www.ncbi.nlm.nih.gov/pubmed/3613402.

G. I. Bell, T. Kayano, J. B. Buse, C. F. Burant, J. Takeda, D. Lin, H. Fukumoto, and S. Seino. Molecular biology of mammalian glucose transporters. *Diabetes care*, 13(3):198–208, Mar. 1990. ISSN 0149-5992. URL http://www.ncbi.nlm.nih.gov/pubmed/2407475.

D. J. Benos. Amiloride: a molecular probe of sodium transport in tissues and cells. *The American journal of physiology*, 242(3):C131–45, Mar. 1982. ISSN 0002-9513. URL http://www.ncbi.nlm.nih.gov/pubmed/7039345.

M. J. Birnbaum. The insulin-sensitive glucose transporter. *International review of cytology*, 137: 239–97, Jan. 1992. ISSN 0074-7696. URL http://www.ncbi.nlm.nih.gov/pubmed/1428672.

O. Björkman, P. Felig, and J. Wahren. The contrasting responses of splanchnic and renal glucose output to gluconeogenic substrates and to hypoglucagonemia in 60-h-fasted humans. *Diabetes*, 29(8):610–6, Aug. 1980. ISSN 0012-1797. URL http://www.ncbi.nlm.nih.gov/pubmed/6108272.

A. B. Blodgett, R. K. Kothinti, I. Kamyshko, D. H. Petering, S. Kumar, and N. M. Tabatabai. A fluorescence method for measurement of glucose transport in kidney cells. *Diabetes technology & therapeutics*, 13(7):743–51, July 2011. ISSN 1557-8593. doi: 10.1089/dia.2011.0041. URL http://www.pubmedcentral.nih.gov/articlerender.fcgi?artid=3118926&tool=pmcentrez&rendertype=abstract.

W. F. Boron and E. L. Boulpaep. *Medical Physiology, 2nd edition.* Saunders Elsevier, 2009. ISBN 978-1-4160-3115-4.

M. Bostanjoglo, W. B. Reeves, R. F. Reilly, H. Velázquez, N. Robertson, G. Litwack, P. Morsing, J. Dø rup, S. Bachmann, D. H. Ellison, and M. Bostonjoglo. 11Beta-hydroxysteroid dehydrogenase, mineralocorticoid receptor, and thiazide-sensitive Na-Cl cotransporter expression by distal tubules. *Journal of the American Society of Nephrology : JASN*, 9(8): 1347–58, Aug. 1998. ISSN 1046-6673. URL http://www.ncbi.nlm.nih.gov/pubmed/9697656.

K. Bouzakri, P. Ribaux, A. Tomas, G. Parnaud, K. Rickenbach, and P. A. Halban. Rab GTPase-activating protein AS160 is a major downstream effector of protein kinase B/Akt signaling in pancreatic beta-cells. *Diabetes*, 57(5):1195–204, May 2008. ISSN 1939-327X. doi: 10.2337/db07-1469. URL http://diabetes.diabetesjournals.org/content/57/5/1195.long.

B. M. Brenner and F. C. Rector. *Brenner & Rector's The kidney.* Saunders Philadelphia, 7th edition, 2004.

F. C. Brosius and C. W. Heilig. Glucose transporters in diabetic nephropathy. *Pediatric nephrology (Berlin, Germany)*, 20(4):447–51, Apr. 2005. ISSN 0931-041X. doi: 10.1007/s00467-004-1748-x. URL http://www.ncbi.nlm.nih.gov/pubmed/15717166.

F. C. Brosius, J. P. Briggs, R. G. Marcus, M. Barac-Nieto, and M. J. Charron. Insulin-responsive glucose transporter expression in renal microvessels and glomeruli. *Kidney international*, 42 (5):1086–92, Nov. 1992. ISSN 0085-2538.

R. Brown, J. Quirk, and P. Kirkpatrick. Eplerenone. *Nature reviews. Drug discovery*, 2(3):177–8, Mar. 2003. ISSN 1474-1776. doi: 10.1038/nrd1039. URL http://www.ncbi.nlm.nih.gov/pubmed/12619638.

S. M. Busque and C. a. Wagner. Potassium restriction, high protein intake, and metabolic acidosis increase expression of the glutamine transporter SNAT3 (Slc38a3) in mouse kidney. *American journal of physiology. Renal physiology*, 297(2):F440–50, Aug. 2009. ISSN 1522-1466. doi: 10.1152/ajprenal.90318.2008. URL http://www.ncbi.nlm.nih.gov/pubmed/19458124.

M. Bustamante, U. Hasler, O. Kotova, A. V. Chibalin, D. Mordasini, M. Rousselot, A. Vandewalle, P.-Y. Martin, and E. Féraille. Insulin potentiates AVP-induced AQP2 expression in cultured renal collecting duct principal cells. *American journal of physiology. Renal physiology*, 288(2):F334–44, Feb. 2005. ISSN 1931-857X. doi: 10.1152/ajprenal.00180.2004. URL http://www.ncbi.nlm.nih.gov/pubmed/15494547.

D. Butlen, S. Vadrot, S. Roseau, and F. Morel. Insulin receptors along the rat nephron: [125I] insulin binding in microdissected glomeruli and tubules. *Pflügers Archiv : European journal of physiology*, 412(6):604–12, Oct. 1988. ISSN 0031-6768. URL http://www.ncbi.nlm.nih.gov/pubmed/3211711.

D. Q. Cai, M. Li, K. K. Lee, K. M. Lee, L. Qin, and K. M. Chan. Parvalbumin expression is downregulated in rat fast-twitch skeletal muscles during aging. *Archives of biochemistry and biophysics*, 387(2):202–8, Mar. 2001. ISSN 0003-9861. doi: 10.1006/abbi.2001.2231. URL http://www.ncbi.nlm.nih.gov/pubmed/11370842.

D. M. Calderhead, K. Kitagawa, L. I. Tanner, G. D. Holman, and G. E. Lienhard. Insulin regulation of the two glucose transporters in 3T3-L1 adipocytes. *The Journal of biological chemistry*, 265(23):13801–8, Aug. 1990. ISSN 0021-9258. URL http://www.ncbi.nlm.nih.gov/pubmed/2199443.

C. M. Canessa, L. Schild, G. Buell, B. Thorens, I. Gautschi, J. D. Horisberger, and B. C. Rossier. Amiloride-sensitive epithelial Na+ channel is made of three homologous subunits. *Nature*, 367 (6462):463–7, Feb. 1994. ISSN 0028-0836. doi: 10.1038/367463a0. URL http://www.ncbi.nlm.nih.gov/pubmed/8107805.

G. D. Cartee and K. Funai. Exercise and insulin: Convergence or divergence at AS160 and TBC1D1? *Exercise and sport sciences reviews*, 37(4):188–95, Oct. 2009. ISSN 1538-3008. doi: 10.1097/JES.0b013e3181b7b7c5. URL http://www.pubmedcentral.nih.gov/articlerender.fcgi?artid=2789346&tool=pmcentrez&rendertype=abstract.

G. D. Cartee and J. r. F. P. Wojtaszewski. Role of Akt substrate of 160 kDa in insulin-stimulated and contraction-stimulated glucose transport. *Applied physiology, nutrition, and metabolism = Physiologie appliquée, nutrition et métabolisme*, 32(3):557–66, June 2007. ISSN 1715-5312. doi: 10.1139/H07-026. URL http://www.ncbi.nlm.nih.gov/pubmed/17510697.

D. Chabardès-Garonne, A. Mejéan, J.-C. Aude, L. Cheval, A. Di Stefano, M.-C. Gaillard, M. Imbert-Teboul, M. Wittner, C. Balian, V. Anthouard, C. Robert, B. Ségurens, P. Wincker, J. Weissenbach, A. Doucet, and J.-M. Elalouf. A panoramic view of gene expression in the human kidney. *Proceedings of the National Academy of Sciences of the United States of America*, 100(23):13710–5, Nov. 2003. ISSN 0027-8424. doi: 10.1073/pnas.2234604100. URL http://www.pubmedcentral.nih.gov/articlerender.fcgi?artid=263878&tool=pmcentrez&rendertype=abstract.

A. Chadt, K. Leicht, A. Deshmukh, L. Q. Jiang, S. Scherneck, U. Bernhardt, T. Dreja, H. Vogel, K. Schmolz, R. Kluge, J. R. Zierath, C. Hultschig, R. C. Hoeben, A. Schürmann, H.-G. Joost, and H. Al-Hasani. Tbc1d1 mutation in lean mouse strain confers leanness and protects from diet-induced obesity. *Nature genetics*, 40(11):1354–9, Nov. 2008. ISSN 1546-1718. doi: 10.1038/ng.244.

A. Chadt, A. Immisch, C. de Wendt, C. Springer, Z. Zhou, T. Stermann, G. D. Holman, D. Loffing-Cueni, J. Loffing, H.-G. Joost, and H. Al-Hasani. Deletion of Both Rab-GTPase-Activating Proteins TBC14KO and TBC1D4 in Mice Eliminates Insulin- and AICAR-Stimulated Glucose Transport. *Diabetes*, 64(3):746–59, Mar. 2015. ISSN 1939-327X. doi: 10.2337/db14-0368. URL http://www.ncbi.nlm.nih.gov/pubmed/25249576.

M. Chávez-Canales, J. P. Arroyo, B. Ko, N. Vázquez, R. Bautista, M. Castañeda Bueno, N. A. Bobadilla, R. S. Hoover, and G. Gamba. Insulin increases the functional activity of the renal NaCl cotransporter. *Journal of hypertension*, 31(2):303–11, Feb. 2013. ISSN 1473-5598. doi: 10.1097/HJH.0b013e32835bbb83. URL http://www.pubmedcentral.nih.gov/articlerender.fcgi?artid=3781588&tool=pmcentrez&rendertype=abstract.

S. Chen, J. Murphy, R. Toth, D. G. Campbell, N. A. Morrice, and C. Mackintosh. Complementary regulation of TBC1D1 and AS160 by growth factors, insulin and AMPK activators. *The Biochemical journal*, 409(2):449–59, Jan. 2008. ISSN 1470-8728. doi: 10.1042/BJ20071114. URL http://www.ncbi.nlm.nih.gov/pubmed/17995453.

S. Chen, D. H. Wasserman, C. MacKintosh, and K. Sakamoto. Mice with AS160/TBC1D4-Thr649Ala knockin mutation are glucose intolerant with reduced insulin sensitivity and altered GLUT4 trafficking. *Cell metabolism*, 13(1):68–79, Jan. 2011. ISSN 1932-7420. doi: 10.1016/j.cmet.2010.12.005. URL http://www.pubmedcentral.nih.gov/articlerender.fcgi?artid=3081066&tool=pmcentrez&rendertype=abstract.

Y. Chen and J. Lippincott-Schwartz. Rab10 delivers GLUT4 storage vesicles to the plasma membrane. *Communicative & integrative biology*, 6(3):e23779, May 2013a. ISSN 1942-0889. doi: 10.4161/cib.23779. URL http://www.pubmedcentral.nih.gov/articlerender.fcgi?artid=3656013&tool=pmcentrez&rendertype=abstract.

Y. Chen and J. Lippincott-Schwartz. Insulin triggers surface-directed trafficking of sequestered GLUT4 storage vesicles marked by Rab10. *Small GTPases*, 4(3):193–197, July 2013b. ISSN 2154-1256. doi: 10.4161/sgtp.26471. URL http://www.pubmedcentral.nih.gov/articlerender.fcgi?artid=3976978&tool=pmcentrez&rendertype=abstract.

A. V. Chibalin, G. Ogimoto, C. H. Pedemonte, T. A. Pressley, A. I. Katz, E. Féraille, P. O. Berggren, and A. M. Bertorello. Dopamine-induced endocytosis of Na+,K+-ATPase is initiated by phosphorylation of Ser-18 in the rat alpha subunit and Is responsible for the decreased activity in epithelial cells. *The Journal of biological chemistry*, 274(4):1920–7, Jan. 1999. ISSN 0021-9258. URL http://www.ncbi.nlm.nih.gov/pubmed/9890946.

E. Chin, J. Zhou, and C. Bondy. Anatomical and developmental patterns of facilitative glucose transporter gene expression in the rat kidney. *The Journal of clinical investigation*, 91(4): 1810–5, Apr. 1993. ISSN 0021-9738. doi: 10.1172/JCI116392. URL http://www.jci.org/articles/view/116392.

H. Cho, J. Mu, J. K. Kim, J. L. Thorvaldsen, Q. Chu, E. B. Crenshaw, K. H. Kaestner, M. S. Bartolomei, G. I. Shulman, and M. J. Birnbaum. Insulin resistance and a diabetes mellitus-like syndrome in mice lacking the protein kinase Akt2 (PKB beta). *Science (New York, N.Y.)*, 292 (5522):1728–31, July 2001. ISSN 0036-8075. doi: 10.1126/science.292.5522.1728. URL http://www.ncbi.nlm.nih.gov/pubmed/11387480.

B. M. n. Christensen, W. Wang, J. r. Frø kiaer, and S. r. Nielsen. Axial heterogeneity in basolateral AQP2 localization in rat kidney: effect of vasopressin. *American journal of physiology. Renal physiology*, 284(4):F701–17, Apr. 2003. ISSN 1931-857X. doi: 10.1152/ajprenal.00234.2002. URL http://www.ncbi.nlm.nih.gov/pubmed/12453871.

J. F. Clarke, P. W. Young, K. Yonezawa, M. Kasuga, and G. D. Holman. Inhibition of the translocation of GLUT1 and GLUT4 in 3T3-L1 cells by the phosphatidylinositol 3-kinase inhibitor, wortmannin. *The Biochemical journal*, 300 (Pt 3:631–5, June 1994. ISSN 0264-6021. URL http://www.pubmedcentral.nih.gov/articlerender.fcgi?artid=1138214&tool=pmcentrez&rendertype=abstract.

A. P. Comellas, A. M. Kelly, H. E. Trejo, A. Briva, J. Lee, J. I. Sznajder, and L. A. Dada. Insulin regulates alveolar epithelial function by inducing Na+/K+-ATPase translocation to the plasma membrane in a process mediated by the action of Akt. *Journal of cell science*, 123(Pt 8):1343–51, Apr. 2010. ISSN 1477-9137. doi: 10.1242/jcs.066464. URL http://www.pubmedcentral.nih.gov/articlerender.fcgi?artid=2848117&tool=pmcentrez&rendertype=abstract.

R. J. M. Coward, G. I. Welsh, G. D. Holman, D. Kerjaschki, J. M. Tavare, P. W. Mathieson, M. A. Saleem, and Web-support@bath.ac.uk. Human podocytes rapidly utilize glucose by both GLUT1 and GLUT4 in response to insulin; with significant differences in glucose transporter levels occurring in diabetic nephropathy, Oct. 2003. URL http://opus.bath.ac.uk/4112/.

R. J. M. Coward, G. I. Welsh, J. Yang, C. Tasman, R. Lennon, A. Koziell, S. Satchell, G. D. Holman, D. Kerjaschki, J. M. Tavaré, P. W. Mathieson, and M. A. Saleem. The human glomerular podocyte is a novel target for insulin action. *Diabetes*, 54(11):3095–102, Nov. 2005. ISSN 0012-1797. URL http://www.ncbi.nlm.nih.gov/pubmed/16249431.

N. P. Curthoys and O. W. Moe. Proximal Tubule Function and Response to Acidosis. *Clinical journal of the American Society of Nephrology : CJASN*, Mar. 2014. ISSN 1555-905X. doi: 10.2215/CJN.10391012. URL http://www.ncbi.nlm.nih.gov/pubmed/23908456.

L. J. Dai, P. A. Friedman, and G. A. Quamme. Cellular mechanisms of chlorothiazide and cellular potassium depletion on Mg2+ uptake in mouse distal convoluted tubule cells. *Kidney international*, 51(4):1008–17, Apr. 1997a. ISSN 0085-2538. URL http://www.ncbi.nlm.nih.gov/pubmed/9083264.

L. J. Dai, L. Raymond, P. A. Friedman, and G. A. Quamme. Mechanisms of amiloride stimulation of Mg2+ uptake in immortalized mouse distal convoluted tubule cells. *The American journal of physiology*, 272(2 Pt 2):F249–56, Feb. 1997b. ISSN 0002-9513. URL http://www.ncbi.nlm.nih.gov/pubmed/9124403.

L. J. Dai, G. Ritchie, B. Bapty, and G. A. Quamme. Aldosterone potentiates hormone-stimulated Mg2+ uptake in distal convoluted tubule cells. *The American journal of physiology*, 274(2 Pt 2):F336–41, Feb. 1998. ISSN 0002-9513. URL http://www.ncbi.nlm.nih.gov/pubmed/9486228.

S. Dash, H. Sano, J. J. Rochford, R. K. Semple, G. Yeo, C. S. S. Hyden, M. A. Soos, J. Clark, A. Rodin, C. Langenberg, C. Druet, K. A. Fawcett, Y. C. L. Tung, N. J. Wareham, I. Barroso, G. E. Lienhard, S. O'Rahilly, and D. B. Savage. A truncation mutation in TBC1D4 in a family with acanthosis nigricans and postprandial hyperinsulinemia. *Proceedings of the National Academy of Sciences of the United States of America*, 106(23):9350–5, June 2009. ISSN 1091-6490. doi: 10.1073/pnas.0900909106. URL http://www.pubmedcentral.nih.gov/articlerender.fcgi?artid=2695078&tool=pmcentrez&rendertype=abstract.

J. H. F. de Baaij, M. J. Groot Koerkamp, M. Lavrijsen, F. van Zeeland, H. Meijer, F. C. P. Holstege, R. J. Bindels, and J. G. J. Hoenderop. Elucidation of the distal convoluted tubule transcriptome identifies new candidate genes involved in renal magnesium handling. *American journal of physiology. Renal physiology*, (286), Oct. 2013. ISSN 1522-1466. doi: 10.1152/ajprenal.00322.2013. URL http://www.ncbi.nlm.nih.gov/pubmed/24089412.

J. C. de Jong, P. H. G. M. Willems, L. P. W. J. van den Heuvel, N. V. A. M. Knoers, and R. J. M. Bindels. Functional expression of the human thiazide-sensitive NaCl cotransporter in Madin-Darby canine kidney cells. *Journal of the American Society of Nephrology : JASN*, 14 (10):2428–35, Oct. 2003. ISSN 1046-6673. URL http://www.ncbi.nlm.nih.gov/pubmed/14514720.

R. A. DeFronzo, C. R. Cooke, R. Andres, G. R. Faloona, and P. J. Davis. The effect of insulin on renal handling of sodium, potassium, calcium, and phosphate in man. *The Journal of clinical investigation*, 55(4):845–55, Apr. 1975. ISSN 0021-9738. doi: 10.1172/JCI107996. URL http://www.pubmedcentral.nih.gov/articlerender.fcgi?artid=301822&tool=pmcentrez&rendertype=abstract.

R. A. DeFronzo, M. Goldberg, and Z. S. Agus. The effects of glucose and insulin on renal electrolyte transport. *The Journal of clinical investigation*, 58(1):83–90, July 1976. ISSN 0021-9738. doi: 10.1172/JCI108463. URL http://www.pubmedcentral.nih.gov/articlerender.fcgi?artid=333158&tool=pmcentrez&rendertype=abstract.

E. Delpire and K. B. E. Gagnon. Genome-wide analysis of SPAK/OSR1 binding motifs. *Physiological genomics*, 28(2):223–31, Jan. 2007. ISSN 1531-2267. doi: 10.1152/physiolgenomics.00173.2006. URL http://www.ncbi.nlm.nih.gov/pubmed/17032814.

N. Denef, Y. Chen, S. D. Weeks, G. Barcelo, and T. Schüpbach. Crag regulates epithelial architecture and polarized deposition of basement membrane proteins in Drosophila. *Developmental cell*, 14(3):354–64, Mar. 2008. ISSN 1878-1551. doi: 10.1016/j.devcel.2007.12.012. URL http://www.pubmedcentral.nih.gov/articlerender.fcgi?artid=2278040&tool=pmcentrez&rendertype=abstract.

P. S. Denker and V. E. Pollock. Fasting serum insulin levels in essential hypertension. A meta-analysis. *Archives of internal medicine*, 152(8):1649–51, Aug. 1992. ISSN 0003-9926. URL http://www.ncbi.nlm.nih.gov/pubmed/1386725.

R. J. W. Diepens, E. den Dekker, M. Bens, A. F. Weidema, A. Vandewalle, R. J. M. Bindels, and J. G. J. Hoenderop. Characterization of a murine renal distal convoluted tubule cell line for the study of transcellular calcium transport. *American journal of physiology. Renal physiology*, 286(3):F483–9, Mar. 2004. ISSN 1931-857X. doi: 10.1152/ajprenal.00231.2003. URL http://www.ncbi.nlm.nih.gov/pubmed/14625201.

H. Dimke, P. San-Cristobal, M. de Graaf, J. W. Lenders, J. Deinum, J. G. J. Hoenderop, and R. J. M. Bindels. γ-Adducin stimulates the thiazide-sensitive NaCl cotransporter. *Journal of the American Society of Nephrology : JASN*, 22(3):508–17, Mar. 2011. ISSN 1533-3450. doi: 10.1681/ASN.2010060606. URL http://www.pubmedcentral.nih.gov/articlerender.fcgi?artid=3060444&tool=pmcentrez&rendertype=abstract.

A. Dobrzyn and J. M. Ntambi. The role of stearoyl-CoA desaturase in the control of metabolism. *Prostaglandins, leukotrienes, and essential fatty acids*, 73(1):35–41, July 2005. ISSN 0952-3278. doi: 10.1016/j.plefa.2005.04.011. URL http://www.ncbi.nlm.nih.gov/pubmed/15941655.

P. Dobrzyn, M. Jazurek, and A. Dobrzyn. Stearoyl-CoA desaturase and insulin signaling–what is the molecular switch? *Biochimica et biophysica acta*, 1797(6-7):1189–94, 2010. ISSN 0006-3002. doi: 10.1016/j.bbabio.2010.02.007. URL http://www.ncbi.nlm.nih.gov/pubmed/20153289.

J. Dokas, A. Chadt, T. Nolden, H. Himmelbauer, J. R. Zierath, H.-G. Joost, and H. Al-Hasani. Conventional knockout of Tbc1d1 in mice impairs insulin- and AICAR-stimulated glucose

uptake in skeletal muscle. *Endocrinology*, 154(10):3502–14, Oct. 2013. ISSN 1945-7170. doi: 10.1210/en.2012-2147. URL http://www.ncbi.nlm.nih.gov/pubmed/23892475.

S. Ducommun, H. Y. Wang, K. Sakamoto, C. MacKintosh, and S. Chen. Thr649Ala-AS160 knock-in mutation does not impair contraction/AICAR-induced glucose transport in mouse muscle. *American journal of physiology. Endocrinology and metabolism*, 302(9):E1036–43, May 2012. ISSN 1522-1555. doi: 10.1152/ajpendo.00379.2011. URL http://www.ncbi.nlm.nih.gov/pubmed/22318952.

L. Eguez, A. Lee, J. A. Chavez, C. P. Miinea, S. Kane, G. E. Lienhard, and T. E. McGraw. Full intracellular retention of GLUT4 requires AS160 Rab GTPase activating protein. *Cell metabolism*, 2(4):263–72, Oct. 2005. ISSN 1550-4131. doi: 10.1016/j.cmet.2005.09.005. URL http://www.ncbi.nlm.nih.gov/pubmed/16213228.

Z. Ergonul, G. Frindt, and L. G. Palmer. Regulation of maturation and processing of ENaC subunits in the rat kidney. *American journal of physiology. Renal physiology*, 291(3):F683–93, Sept. 2006. ISSN 1931-857X. doi: 10.1152/ajprenal.00422.2005. URL http://www.ncbi.nlm.nih.gov/pubmed/16554417.

N. Faresse, D. Lagnaz, A. Debonneville, A. Ismailji, M. Maillard, G. Fejes-Toth, A. Náray-Fejes-Tóth, and O. Staub. Inducible kidney-specific Sgk1 knockout mice show a salt-losing phenotype. *American journal of physiology. Renal physiology*, 302(8):F977–85, Apr. 2012. ISSN 1522-1466. doi: 10.1152/ajprenal.00535.2011. URL http://ajprenal.physiology.org/content/302/8/F977.full-text.pdf+html.

R. A. Fenton, C. N. Pedersen, and H. B. Moeller. New insights into regulated aquaporin-2 function. *Current opinion in nephrology and hypertension*, 22(5):551–8, Sept. 2013. ISSN 1473-6543. doi: 10.1097/MNH.0b013e328364000d. URL http://www.ncbi.nlm.nih.gov/pubmed/23852332.

E. Féraille, M. Rousselot, R. Rajerison, and H. Favre. Effect of insulin on Na(+),K(+)-ATPase in rat collecting duct. *The Journal of physiology*, 488 (Pt 1:171–80, Oct. 1995. ISSN 0022-3751. URL http://www.pubmedcentral.nih.gov/articlerender.fcgi?artid=1156710&tool=pmcentrez&rendertype=abstract.

E. Féraille, D. Mordasini, S. Gonin, G. Deschênes, M. Vinciguerra, A. Doucet, A. Vandewalle, V. Summa, F. Verrey, and P.-Y. Martin. Mechanism of control of Na,K-ATPase in principal cells of the mammalian collecting duct. *Annals of the New York Academy of Sciences*, 986: 570–8, Apr. 2003. ISSN 0077-8923. URL http://www.ncbi.nlm.nih.gov/pubmed/12763891.

Y. Fischer, J. Thomas, L. Sevilla, P. Muñoz, C. Becker, G. Holman, I. J. Kozka, M. Palacín, X. Testar, H. Kammermeier, and A. Zorzano. Insulin-induced recruitment of glucose transporter 4 (GLUT4) and GLUT1 in isolated rat cardiac myocytes. Evidence of the existence of different intracellular GLUT4 vesicle populations. *The Journal of biological chemistry*, 272(11):7085–92, Mar. 1997. ISSN 0021-9258. URL http://www.ncbi.nlm.nih.gov/pubmed/9054401.

M. Fukuda. TBC proteins: GAPs for mammalian small GTPase Rab? *Bioscience reports*, 31(3): 159–68, June 2011. ISSN 1573-4935. doi: 10.1042/BSR20100112. URL http://www.ncbi.nlm.nih.gov/pubmed/21250943.

G. Gamba. Regulation of the renal Na+-Cl- cotransporter by phosphorylation and ubiquitylation. *American journal of physiology. Renal physiology*, 303(12):F1573–83, Dec. 2012. ISSN 1522-1466. doi: 10.1152/ajprenal.00508.2012. URL http://ajprenal.physiology.org/content/303/12/F1573.

J. L. Gamboa, M. L. Garcia-Cazarin, and F. H. Andrade. Chronic hypoxia increases insulin-stimulated glucose uptake in mouse soleus muscle. *American journal of physiology. Regulatory, integrative and comparative physiology*, 300(1):R85–91, Jan. 2011. ISSN 1522-1490. doi: 10.1152/ajpregu.00078.2010. URL http://www.pubmedcentral.nih.gov/articlerender.fcgi?artid=3023279&tool=pmcentrez&rendertype=abstract.

K. Geering. Subunit assembly and functional maturation of Na,K-ATPase. *The Journal of membrane biology*, 115(2):109–21, May 1990. ISSN 0022-2631. URL http://www.ncbi.nlm.nih.gov/pubmed/2162391.

R. C. Gentleman, V. J. Carey, D. M. Bates, B. Bolstad, M. Dettling, S. Dudoit, B. Ellis, L. Gautier, Y. Ge, J. Gentry, K. Hornik, T. Hothorn, W. Huber, S. Iacus, R. Irizarry, F. Leisch, C. Li, M. Maechler, A. J. Rossini, G. Sawitzki, C. Smith, G. Smyth, L. Tierney, J. Y. H. Yang, and J. Zhang. Bioconductor: open software development for computational biology and bioinformatics. *Genome biology*, 5(10):R80, Jan. 2004. ISSN 1465-6914. doi: 10.1186/gb-2004-5-10-r80. URL http://www.pubmedcentral.nih.gov/articlerender.fcgi?artid=545600&tool=pmcentrez&rendertype=abstract.

K. M. Geraghty, S. Chen, J. E. Harthill, A. F. Ibrahim, R. Toth, N. A. Morrice, F. Vandermoere, G. B. Moorhead, D. G. Hardie, and C. MacKintosh. Regulation of multisite phosphorylation and 14-3-3 binding of AS160 in response to IGF-1, EGF, PMA and AICAR. *The Biochemical journal*, 407(2):231–41, Oct. 2007. ISSN 1470-8728. doi: 10.1042/BJ20070649. URL http://www.pubmedcentral.nih.gov/articlerender.fcgi?artid=2049023&tool=pmcentrez&rendertype=abstract.

F. A. Gesek and P. A. Friedman. Mechanism of calcium transport stimulated by chlorothiazide in mouse distal convoluted tubule cells. *The Journal of clinical investigation*, 90(2):429–38, Aug. 1992. ISSN 0021-9738. doi: 10.1172/JCI115878. URL http://www.pubmedcentral.nih.gov/articlerender.fcgi?artid=443118&tool=pmcentrez&rendertype=abstract.

F. A. Gesek and P. A. Friedman. Sodium entry mechanisms in distal convoluted tubule cells. *The American journal of physiology*, 268(1 Pt 2):F89–98, Jan. 1995. ISSN 0002-9513. URL http://www.ncbi.nlm.nih.gov/pubmed/7840252.

G. Giebisch and B. Stanton. Potassium transport in the nephron. *Annual review of physiology*, 41:241–56, Jan. 1979. ISSN 0066-4278. doi: 10.1146/annurev.ph.41.030179.001325. URL http://www.ncbi.nlm.nih.gov/pubmed/373590.

B. Glaudemans, S. Terryn, N. Gölz, M. Brunati, A. Cattaneo, A. Bachi, L. Al-Qusairi, U. Ziegler, O. Staub, L. Rampoldi, and O. Devuyst. A primary culture system of mouse thick ascending limb cells with preserved function and uromodulin processing. *Pflugers Archiv : European journal of physiology*, July 2013. ISSN 1432-2013.

M. Glover, A. Mercier Zuber, N. Figg, and K. M. O'Shaughnessy. The activity of the thiazide-sensitive Na(+)-Cl(-) cotransporter is regulated by protein phosphatase PP4.

Canadian journal of physiology and pharmacology, 88(10):986–95, Oct. 2010. ISSN 1205-7541. doi: 10.1139/y10-080. URL http://www.ncbi.nlm.nih.gov/pubmed/20962898.

S. Gonin, G. Deschênes, F. Roger, M. Bens, P. Y. Martin, J. L. Carpentier, A. Vandewalle, A. Doucet, and E. Féraille. Cyclic AMP increases cell surface expression of functional Na,K-ATPase units in mammalian cortical collecting duct principal cells. *Molecular biology of the cell*, 12(2):255–64, Feb. 2001. ISSN 1059-1524. URL http://www.pubmedcentral.nih.gov/articlerender.fcgi?artid=30941&tool=pmcentrez&rendertype=abstract.

C. J. Gottardi and M. J. Caplan. Delivery of Na+,K(+)-ATPase in polarized epithelial cells. *Science (New York, N.Y.)*, 260(5107):552–4; author reply 554–6, Apr. 1993. ISSN 0036-8075. URL http://www.ncbi.nlm.nih.gov/pubmed/8386395.

N. Gresko. *Regulation of Epithelial Sodium Channel (ENaC) Trafficking and Function in Mouse Cortical Collecting Duct Cells - Importance of Golgi Apparatus, Microtubules and TBC1D4 Rab-GAP Protein*. PhD thesis, 2011.

C. A. Grillo, G. G. Piroli, R. M. Hendry, and L. P. Reagan. Insulin-stimulated translocation of GLUT4 to the plasma membrane in rat hippocampus is PI3-kinase dependent. *Brain research*, 1296:35–45, Nov. 2009. ISSN 1872-6240. doi: 10.1016/j.brainres.2009.08.005. URL http://www.pubmedcentral.nih.gov/articlerender.fcgi?artid=2997526&tool=pmcentrez&rendertype=abstract.

S. P. Gygi, Y. Rochon, B. R. Franza, and R. Aebersold. Correlation between protein and mRNA abundance in yeast. *Molecular and cellular biology*, 19(3):1720–30, Mar. 1999. ISSN 0270-7306. URL http://www.pubmedcentral.nih.gov/articlerender.fcgi?artid=83965&tool=pmcentrez&rendertype=abstract.

L. J. Hale and R. J. M. Coward. Insulin signalling to the kidney in health and disease. *Clinical science (London, England : 1979)*, 124(6):351–70, Mar. 2013. ISSN 1470-8736. doi: 10.1042/CS20120378. URL http://www.ncbi.nlm.nih.gov/pubmed/23190266.

R. A. Hall, R. T. Premont, C. W. Chow, J. T. Blitzer, J. A. Pitcher, A. Claing, R. H. Stoffel, L. S. Barak, S. Shenolikar, E. J. Weinman, S. Grinstein, and R. J. Lefkowitz. The beta2-adrenergic receptor interacts with the Na+/H+-exchanger regulatory factor to control Na+/H+ exchange. *Nature*, 392(6676):626–30, Apr. 1998. ISSN 0028-0836. doi: 10.1038/33458. URL http://www.ncbi.nlm.nih.gov/pubmed/9560162.

U. Hasler, D. Mordasini, M. Bianchi, A. Vandewalle, E. Féraille, and P.-Y. Martin. Dual influence of aldosterone on AQP2 expression in cultured renal collecting duct principal cells. *The Journal of biological chemistry*, 278(24):21639–48, June 2003. ISSN 0021-9258. doi: 10.1074/jbc.M212388200. URL http://www.ncbi.nlm.nih.gov/pubmed/12660245.

U. Hasler, M. Vinciguerra, A. Vandewalle, P.-Y. Martin, and E. Féraille. Dual effects of hypertonicity on aquaporin-2 expression in cultured renal collecting duct principal cells. *Journal of the American Society of Nephrology : JASN*, 16(6):1571–82, June 2005. ISSN 1046-6673. doi: 10.1681/ASN.2004110930. URL http://www.ncbi.nlm.nih.gov/pubmed/15843469.

U. Hasler, V. Leroy, P.-Y. Martin, and E. Féraille. Aquaporin-2 abundance in the renal collecting duct: new insights from cultured cell models. *American journal of physiology. Renal physiology*, 297(1):F10–8, July 2009. ISSN 1522-1466. doi: 10.1152/ajprenal.00053.2009. URL http://www.ncbi.nlm.nih.gov/pubmed/19244407.

S. S. Hegde, A. L. Jadhav, and M. F. Lokhandwala. Role of kidney dopamine in the natriuretic response to volume expansion in rats. *Hypertension*, 13(6 Pt 2):828–34, June 1989. ISSN 0194-911X. URL http://www.ncbi.nlm.nih.gov/pubmed/2661432.

C. Heilig, C. Zaloga, M. Lee, X. Zhao, B. Riser, F. Brosius, and P. Cortes. Immunogold localization of high-affinity glucose transporter isoforms in normal rat kidney. *Laboratory investigation; a journal of technical methods and pathology*, 73(5):674–84, Nov. 1995. ISSN 0023-6837. URL http://www.ncbi.nlm.nih.gov/pubmed/7474941.

C. W. Heilig, Y. Liu, R. L. England, S. O. Freytag, J. D. Gilbert, K. O. Heilig, M. Zhu, L. A. Concepcion, and F. C. Brosius. D-glucose stimulates mesangial cell GLUT1 expression and basal and IGF-I-sensitive glucose uptake in rat mesangial cells: implications for diabetic nephropathy. *Diabetes*, 46(6):1030–9, June 1997. ISSN 0012-1797. URL http://www.ncbi.nlm.nih.gov/pubmed/9166676.

N. Hernando, I. C. Forster, J. Biber, and H. Murer. Molecular characteristics of phosphate transporters and their regulation. *Experimental nephrology*, 8(6):366–75, 2000. ISSN 1018-7782. doi: 20691. URL http://www.ncbi.nlm.nih.gov/pubmed/11014934.

J. G. Hoenderop, D. Müller, A. W. Van Der Kemp, A. Hartog, M. Suzuki, K. Ishibashi, M. Imai, F. Sweep, P. H. Willems, C. H. Van Os, and R. J. Bindels. Calcitriol controls the epithelial calcium channel in kidney. *Journal of the American Society of Nephrology : JASN*, 12(7): 1342–9, July 2001. ISSN 1046-6673. URL http://www.ncbi.nlm.nih.gov/pubmed/11423563.

J. D. Hoffert, T. Pisitkun, G. Wang, R.-F. Shen, and M. A. Knepper. Quantitative phosphoproteomics of vasopressin-sensitive renal cells: regulation of aquaporin-2 phosphorylation at two sites. *Proceedings of the National Academy of Sciences of the United States of America*, 103(18):7159–64, May 2006. ISSN 0027-8424. doi: 10.1073/pnas.0600895103. URL http://www.pubmedcentral.nih.gov/articlerender.fcgi?artid=1459033&tool=pmcentrez&rendertype=abstract.

J. D. Hoffert, R. A. Fenton, H. B. Moeller, B. Simons, D. Tchapyjnikov, B. W. McDill, M.-J. Yu, T. Pisitkun, F. Chen, and M. A. Knepper. Vasopressin-stimulated increase in phosphorylation at Ser269 potentiates plasma membrane retention of aquaporin-2. *The Journal of biological chemistry*, 283(36):24617–27, Sept. 2008. ISSN 0021-9258. doi: 10.1074/jbc.M803074200. URL http://www.pubmedcentral.nih.gov/articlerender.fcgi?artid=2528999&tool=pmcentrez&rendertype=abstract.

E. J. Hoorn, S. B. Walsh, J. A. McCormick, A. Fürstenberg, C.-L. Yang, T. Roeschel, A. Paliege, A. J. Howie, J. Conley, S. Bachmann, R. J. Unwin, and D. H. Ellison. The calcineurin inhibitor tacrolimus activates the renal sodium chloride cotransporter to cause hypertension. *Nature medicine*, 17(10):1304–9, Oct. 2011. ISSN 1546-170X. doi: 10.1038/nm.2497. URL http://www.pubmedcentral.nih.gov/articlerender.fcgi?artid=3192268&tool=pmcentrez&rendertype=abstract.

J. D. Horisberger and B. C. Rossier. Aldosterone regulation of gene transcription leading to control of ion transport. *Hypertension*, 19(3):221–7, Mar. 1992. ISSN 0194-911X. URL http://www.ncbi.nlm.nih.gov/pubmed/1372288.

M. Imbert, D. Chabardès, M. Montegut, A. Clique, and F. Morel. Vasopressin dependent adenylate cyclase in single segments of rabbit kidney tubule. *Pflügers Archiv : European journal of physiology*, 357(3-4):173–86, June 1975. ISSN 0031-6768. URL http://www.ncbi.nlm.nih.gov/pubmed/172859.

R. A. Irizarry, B. Hobbs, F. Collin, Y. D. Beazer-Barclay, K. J. Antonellis, U. Scherf, and T. P. Speed. Exploration, normalization, and summaries of high density oligonucleotide array probe level data. *Biostatistics (Oxford, England)*, 4(2):249–64, Apr. 2003. ISSN 1465-4644. doi: 10.1093/biostatistics/4.2.249. URL http://www.ncbi.nlm.nih.gov/pubmed/12925520.

L. Jiang, J. Fan, L. Bai, Y. Wang, Y. Chen, L. Yang, L. Chen, and T. Xu. Direct quantification of fusion rate reveals a distal role for AS160 in insulin-stimulated fusion of GLUT4 storage vesicles. *The Journal of biological chemistry*, 283(13):8508–16, Mar. 2008. ISSN 0021-9258. doi: 10.1074/jbc.M708688200. URL http://www.pubmedcentral.nih.gov/articlerender.fcgi?artid=2417169&tool=pmcentrez&rendertype=abstract.

P. L. Jorgensen. Molecular basis for active Na,K-transport by Na,K-ATPase from outer renal medulla. *Biochemical Society symposium*, 50:59–79, Jan. 1985. ISSN 0067-8694. URL http://www.ncbi.nlm.nih.gov/pubmed/2428372.

H. J. Jung and T.-H. Kwon. Membrane Trafficking of Collecting Duct Water Channel Protein AQP2 Regulated by Akt/AS160. *Electrolyte & blood pressure : E & BP*, 8(2):59–65, Dec. 2010. ISSN 2092-9935. doi: 10.5049/EBP.2010.8.2.59. URL http://www.pubmedcentral.nih.gov/articlerender.fcgi?artid=3043758&tool=pmcentrez&rendertype=abstract.

K. T. Kahle, J. Rinehart, and R. P. Lifton. Phosphoregulation of the Na-K-2Cl and K-Cl cotransporters by the WNK kinases. *Biochimica et biophysica acta*, 1802(12):1150–8, Dec. 2010. ISSN 0006-3002. doi: 10.1016/j.bbadis.2010.07.009. URL http://www.pubmedcentral.nih.gov/articlerender.fcgi?artid=3529164&tool=pmcentrez&rendertype=abstract.

B. Kaissling and M. Le Hir. Distal tubular segments of the rabbit kidney after adaptation to altered Na- and K-intake. I. Structural changes. *Cell and tissue research*, 224(3):469–92, Jan. 1982. ISSN 0302-766X. URL http://www.ncbi.nlm.nih.gov/pubmed/7116409.

E. J. Kamsteeg, T. A. Wormhoudt, J. P. Rijss, C. H. van Os, and P. M. Deen. An impaired routing of wild-type aquaporin-2 after tetramerization with an aquaporin-2 mutant explains dominant nephrogenic diabetes insipidus. *The EMBO journal*, 18(9):2394–400, May 1999. ISSN 0261-4189. doi: 10.1093/emboj/18.9.2394. URL http://www.pubmedcentral.nih.gov/articlerender.fcgi?artid=1171322&tool=pmcentrez&rendertype=abstract.

E. J. Kamsteeg, I. Heijnen, C. H. van Os, and P. M. Deen. The subcellular localization of an aquaporin-2 tetramer depends on the stoichiometry of phosphorylated and nonphosphorylated monomers. *The Journal of cell biology*, 151(4):919–30, Nov. 2000. ISSN 0021-9525. URL http://www.pubmedcentral.nih.gov/articlerender.fcgi?artid=2169442&tool=pmcentrez&rendertype=abstract.

E.-J. Kamsteeg, G. Hendriks, M. Boone, I. B. M. Konings, V. Oorschot, P. van der Sluijs, J. Klumperman, and P. M. T. Deen. Short-chain ubiquitination mediates the regulated endocytosis of the aquaporin-2 water channel. *Proceedings of the National Academy of Sciences of the United States of America*, 103(48):18344–9, Nov. 2006. ISSN 0027-8424. doi: 10.1073/pnas.0604073103. URL `http://www.pubmedcentral.nih.gov/articlerender.fcgi?artid=1838753&tool=pmcentrez&rendertype=abstract`.

S. Kane, H. Sano, S. C. H. Liu, J. M. Asara, W. S. Lane, C. C. Garner, and G. E. Lienhard. A method to identify serine kinase substrates. Akt phosphorylates a novel adipocyte protein with a Rab GTPase-activating protein (GAP) domain. *The Journal of biological chemistry*, 277(25): 22115–8, June 2002. ISSN 0021-9258. doi: 10.1074/jbc.C200198200. URL `http://www.ncbi.nlm.nih.gov/pubmed/11994271`.

H. k. K. R. Karlsson, J. R. Zierath, S. Kane, A. Krook, G. E. Lienhard, and H. Wallberg-Henriksson. Insulin-stimulated phosphorylation of the Akt substrate AS160 is impaired in skeletal muscle of type 2 diabetic subjects. *Diabetes*, 54(6):1692–7, June 2005. ISSN 0012-1797. URL `http://www.ncbi.nlm.nih.gov/pubmed/15919790`.

H. k. K. R. Karlsson, M. Ahlsén, J. R. Zierath, H. Wallberg-Henriksson, and H. A. Koistinen. Insulin signaling and glucose transport in skeletal muscle from first-degree relatives of type 2 diabetic patients. *Diabetes*, 55(5):1283–8, May 2006. ISSN 0012-1797. URL `http://www.ncbi.nlm.nih.gov/pubmed/16644684`.

T. Katsura, C. E. Gustafson, D. A. Ausiello, and D. Brown. Protein kinase A phosphorylation is involved in regulated exocytosis of aquaporin-2 in transfected LLC-PK1 cells. *The American journal of physiology*, 272(6 Pt 2):F817–22, June 1997. ISSN 0002-9513. URL `http://www.ncbi.nlm.nih.gov/pubmed/9227644`.

D. S. Kempe, G. Siraskar, H. Fröhlich, A. T. Umbach, M. Stübs, F. Weiss, T. F. Ackermann, H. Völkl, M. J. Birnbaum, D. Pearce, M. Föller, and F. Lang. Regulation of renal tubular glucose reabsorption by Akt2/PKBβ. *American journal of physiology. Renal physiology*, 298 (5):F1113–7, May 2010. ISSN 1522-1466. doi: 10.1152/ajprenal.00592.2009. URL `http://www.ncbi.nlm.nih.gov/pubmed/20164156`.

H.-Y. Kim, H.-J. Choi, J.-S. Lim, E.-J. Park, H. J. Jung, Y.-J. Lee, S.-Y. Kim, and T.-H. Kwon. Emerging role of Akt substrate protein AS160 in the regulation of AQP2 translocation. *American journal of physiology. Renal physiology*, 301(1):F151–61, July 2011. ISSN 1522-1466. doi: 10.1152/ajprenal.00519.2010. URL `http://www.ncbi.nlm.nih.gov/pubmed/21511697`.

L. S. King, M. Choi, P. C. Fernandez, J. P. Cartron, and P. Agre. Defective urinary-concentrating ability due to a complete deficiency of aquaporin-1. *The New England journal of medicine*, 345(3):175–9, July 2001. ISSN 0028-4793. doi: 10.1056/NEJM200107193450304. URL `http://www.ncbi.nlm.nih.gov/pubmed/11463012`.

M. Kiroytcheva, L. Cheval, M. L. Carranza, P. Y. Martin, H. Favre, A. Doucet, and E. Féraille. Effect of cAMP on the activity and the phosphorylation of Na+,K(+)-ATPase in rat thick ascending limb of Henle. *Kidney international*, 55(5):1819–31, May 1999. ISSN 0085-2538. doi: 10.1046/j.1523-1755.1999.00414.x. URL `http://www.ncbi.nlm.nih.gov/pubmed/10231444`.

T. R. Kleyman and E. J. Cragoe. The mechanism of action of amiloride. *Seminars in nephrology*, 8(3):242–8, Sept. 1988. ISSN 0270-9295. URL http://www.ncbi.nlm.nih.gov/pubmed/2849182.

M. A. Knepper, G.-H. Kim, P. Fernandez-Llama, and C. A. Ecelbarger. Regulation of Thick Ascending Limb Transport by Vasopressin. *J. Am. Soc. Nephrol.*, 10(3):628–634, Mar. 1999. URL http://jasn.asnjournals.org/content/10/3/628.long.

R. Komers, S. Rogers, T. T. Oyama, B. Xu, C.-L. Yang, J. McCormick, and D. H. Ellison. Enhanced phosphorylation of Na(+)-Cl- co-transporter in experimental metabolic syndrome: role of insulin. *Clinical science (London, England : 1979)*, 123(11):635–47, Dec. 2012. ISSN 1470-8736. doi: 10.1042/CS20120003. URL http://www.pubmedcentral.nih.gov/articlerender.fcgi?artid=3943429&tool=pmcentrez&rendertype=abstract.

M. L. A. Kortenoeven, N. B. Pedersen, R. L. Miller, A. Rojek, and R. A. Fenton. Genetic ablation of aquaporin-2 in the mouse connecting tubules results in defective renal water handling. *The Journal of physiology*, 591(Pt 8):2205–19, Apr. 2013. ISSN 1469-7793. doi: 10.1113/jphysiol.2012.250852. URL http://www.pubmedcentral.nih.gov/articlerender.fcgi?artid=3634529&tool=pmcentrez&rendertype=abstract.

H. A. Krebs and T. Yoshida. Renal Gluconeogensis. 2. The Gluconeogenic Capacity of The Kidney Cortex of Various Species. *The Biochemical journal*, 89:398–400, Nov. 1963. ISSN 0264-6021. URL http://www.pubmedcentral.nih.gov/articlerender.fcgi?artid=1202371&tool=pmcentrez&rendertype=abstract.

J. H. Krege, J. B. Hodgin, J. R. Hagaman, and O. Smithies. A Noninvasive Computerized Tail-Cuff System for Measuring Blood Pressure in Mice. *Hypertension*, 25(5):1111–1115, May 1995. ISSN 0194-911X. doi: 10.1161/01.HYP.25.5.1111. URL http://hyper.ahajournals.org/cgi/content/long/25/5/1111.

M. Kroiher, M. A. Miller, and R. E. Steele. Deceiving appearances: signaling by "dead" and "fractured" receptor protein-tyrosine kinases. *BioEssays : news and reviews in molecular, cellular and developmental biology*, 23(1):69–76, Jan. 2001. ISSN 0265-9247. doi: 10.1002/1521-1878(200101)23:1⟨69::AID-BIES1009⟩3.0.CO;2-K. URL http://www.ncbi.nlm.nih.gov/pubmed/11135311.

L. Lai, X. Feng, D. Liu, J. Chen, Y. Zhang, B. Niu, Y. Gu, and H. Cai. Dietary salt modulates the sodium chloride cotransporter expression likely through an aldosterone-mediated WNK4-ERK1/2 signaling pathway. *Pflügers Archiv : European journal of physiology*, 463(3): 477–85, Mar. 2012. ISSN 1432-2013. doi: 10.1007/s00424-011-1062-y. URL http://www.ncbi.nlm.nih.gov/pubmed/22200850.

M. N. Lansey, N. N. Walker, S. R. Hargett, J. R. Stevens, and S. R. Keller. Deletion of Rab GAP AS160 modifies glucose uptake and GLUT4 translocation in primary skeletal muscles and adipocytes and impairs glucose homeostasis. *American journal of physiology. Endocrinology and metabolism*, 303(10):E1273–86, Nov. 2012. ISSN 1522-1555. doi: 10.1152/ajpendo.00316.2012. URL http://www.ncbi.nlm.nih.gov/pubmed/23011063.

M. Larance, G. Ramm, J. Stöckli, E. M. van Dam, S. Winata, V. Wasinger, F. Simpson, M. Graham, J. R. Junutula, M. Guilhaus, and D. E. James. Characterization of the role of the

Rab GTPase-activating protein AS160 in insulin-regulated GLUT4 trafficking. *The Journal of biological chemistry*, 280(45):37803–13, Nov. 2005. ISSN 0021-9258. doi: 10.1074/jbc.M503897200. URL http://www.ncbi.nlm.nih.gov/pubmed/16154996.

F. Lavialle, D. Rainteau, D. Massey-Harroche, and F. Metz. Establishment of plasma membrane polarity in mammary epithelial cells correlates with changes in prolactin trafficking and in annexin VI recruitment to membranes. *Biochimica et biophysica acta*, 1464(1):83–94, Mar. 2000. ISSN 0006-3002. URL http://www.ncbi.nlm.nih.gov/pubmed/10704922.

M. Le Hir, B. Kaissling, and U. C. Dubach. Distal tubular segments of the rabbit kidney after adaptation to altered Na- and K-intake. II. Changes in Na-K-ATPase activity. *Cell and tissue research*, 224(3):493–504, Jan. 1982. ISSN 0302-766X. URL http://www.ncbi.nlm.nih.gov/pubmed/6288247.

Y. J. Lee and H. J. Han. Regulatory mechanisms of Na(+)/glucose cotransporters in renal proximal tubule cells. *Kidney international. Supplement*, (106):S27–35, Aug. 2007. ISSN 0098-6577. doi: 10.1038/sj.ki.5002383. URL http://www.ncbi.nlm.nih.gov/pubmed/17653207.

L. Li, R. M. Garikepati, S. Tsukerman, D. Kohan, J. B. Wade, S. Tiwari, and C. M. Ecelbarger. Reduced ENaC activity and blood pressure in mice with genetic knockout of the insulin receptor in the renal collecting duct. *American journal of physiology. Renal physiology*, 304(3): F279–88, Feb. 2013. ISSN 1522-1466. doi: 10.1152/ajprenal.00161.2012. URL http://www.pubmedcentral.nih.gov/articlerender.fcgi?artid=3566522&tool=pmcentrez&rendertype=abstract.

X. Liang, M. B. Butterworth, K. W. Peters, and R. A. Frizzell. AS160 modulates aldosterone-stimulated epithelial sodium channel forward trafficking. *Molecular biology of the cell*, 21(12):2024–33, June 2010. ISSN 1939-4586. doi: 10.1091/mbc.E10-01-0042. URL http://www.pubmedcentral.nih.gov/articlerender.fcgi?artid=2883946&tool=pmcentrez&rendertype=abstract.

N. Lier, N. Gresko, M. Di Chiara, D. Loffing-Cueni, and J. Loffing. Immunofluorescent localization of the Rab-GAP protein TBC1D4 (AS160) in mouse kidney. *Histochemistry and cell biology*, 138(1):101–12, July 2012. ISSN 1432-119X. doi: 10.1007/s00418-012-0944-1. URL http://www.ncbi.nlm.nih.gov/pubmed/22466139.

K. C. Linden, C. L. DeHaan, Y. Zhang, S. Glowacka, A. J. Cox, D. J. Kelly, and S. Rogers. Renal expression and localization of the facilitative glucose transporters GLUT1 and GLUT12 in animal models of hypertension and diabetic nephropathy. *American journal of physiology. Renal physiology*, 290(1):F205–13, Jan. 2006. ISSN 1931-857X. doi: 10.1152/ajprenal.00237.2004. URL http://www.ncbi.nlm.nih.gov/pubmed/16091581.

J. Loffing and B. Kaissling. Sodium and calcium transport pathways along the mammalian distal nephron: from rabbit to human. *American journal of physiology. Renal physiology*, 284(4): F628–43, Apr. 2003. ISSN 1931-857X. doi: 10.1152/ajprenal.00217.2002. URL http://ajprenal.physiology.org/content/284/4/F628.

J. Loffing, D. Loffing-Cueni, V. Valderrabano, L. Kläusli, S. C. Hebert, B. C. Rossier, J. G. Hoenderop, R. J. Bindels, and B. Kaissling. Distribution of transcellular calcium and sodium

transport pathways along mouse distal nephron. *American journal of physiology. Renal physiology*, 281(6):F1021–7, Dec. 2001. ISSN 1931-857X. URL http://www.ncbi.nlm.nih.gov/pubmed/11704552.

D. Lombardi, T. Soldati, M. A. Riederer, Y. Goda, M. Zerial, and S. R. Pfeffer. Rab9 functions in transport between late endosomes and the trans Golgi network. *The EMBO journal*, 12(2): 677–82, Feb. 1993. ISSN 0261-4189. URL http://www.pubmedcentral.nih.gov/articlerender.fcgi?artid=413253&tool=pmcentrez&rendertype=abstract.

T. Ma, B. Yang, A. Gillespie, E. J. Carlson, C. J. Epstein, and A. S. Verkman. Severely impaired urinary concentrating ability in transgenic mice lacking aquaporin-1 water channels. *The Journal of biological chemistry*, 273(8):4296–9, Feb. 1998. ISSN 0021-9258. URL http://www.ncbi.nlm.nih.gov/pubmed/9468475.

N. Mastroianni, A. Bettinelli, M. Bianchetti, G. Colussi, M. De Fusco, F. Sereni, A. Ballabio, and G. Casari. Novel molecular variants of the Na-Cl cotransporter gene are responsible for Gitelman syndrome. *American journal of human genetics*, 59(5):1019–26, Nov. 1996. ISSN 0002-9297. URL http://www.pubmedcentral.nih.gov/articlerender.fcgi?artid=1914834&tool=pmcentrez&rendertype=abstract.

M. Matsuda and R. A. DeFronzo. Insulin sensitivity indices obtained from oral glucose tolerance testing: comparison with the euglycemic insulin clamp. *Diabetes care*, 22(9):1462–70, Sept. 1999. ISSN 0149-5992. URL http://www.ncbi.nlm.nih.gov/pubmed/10480510.

H. Mayan, I. Vered, M. Mouallem, M. Tzadok-Witkon, R. Pauzner, and Z. Farfel. Pseudohypoaldosteronism type II: marked sensitivity to thiazides, hypercalciuria, normomagnesemia, and low bone mineral density. *The Journal of clinical endocrinology and metabolism*, 87(7):3248–54, July 2002. ISSN 0021-972X. doi: 10.1210/jcem.87.7.8449. URL http://www.ncbi.nlm.nih.gov/pubmed/12107233.

J. A. McCormick and D. H. Ellison. *Comprehensive Physiology*, volume 5. John Wiley & Sons, Inc., Hoboken, NJ, USA, Jan. 2011. ISBN 9780470650714. doi: 10.1002/cphy.c140002. URL http://www.ncbi.nlm.nih.gov/pubmed/25589264.

J. A. McCormick, K. Mutig, J. H. Nelson, T. Saritas, E. J. Hoorn, C.-L. Yang, S. Rogers, J. Curry, E. Delpire, S. Bachmann, and D. H. Ellison. A SPAK isoform switch modulates renal salt transport and blood pressure. *Cell metabolism*, 14(3):352–64, Sept. 2011. ISSN 1932-7420. doi: 10.1016/j.cmet.2011.07.009. URL http://www.pubmedcentral.nih.gov/articlerender.fcgi?artid=3172576&tool=pmcentrez&rendertype=abstract.

A. A. McDonough. Mechanisms of proximal tubule sodium transport regulation that link extracellular fluid volume and blood pressure. *American journal of physiology. Regulatory, integrative and comparative physiology*, 298(4):R851–61, Apr. 2010. ISSN 1522-1490. doi: 10.1152/ajpregu.00002.2010. URL http://www.pubmedcentral.nih.gov/articlerender.fcgi?artid=2853398&tool=pmcentrez&rendertype=abstract.

D. L. McGill. Characterization of the adipocyte ghost (Na+,K+) pump. Insights into the insulin regulation of the adipocyte (Na+,K+) pump. *The Journal of biological chemistry*, 266(24): 15817–23, Aug. 1991. ISSN 0021-9258. URL http://www.ncbi.nlm.nih.gov/pubmed/1651921.

D. L. McGill and G. Guidotti. Insulin stimulates both the alpha 1 and the alpha 2 isoforms of the rat adipocyte (Na+,K+) ATPase. Two mechanisms of stimulation. *The Journal of biological chemistry*, 266(24):15824–31, Aug. 1991. ISSN 0021-9258. URL http://www.ncbi.nlm.nih.gov/pubmed/1651922.

A. I. Mendes, P. Matos, S. Moniz, and P. Jordan. Protein kinase WNK1 promotes cell surface expression of glucose transporter GLUT1 by regulating a Tre-2/USP6-BUB2-Cdc16 domain family member 4 (TBC1D4)-Rab8A complex. *The Journal of biological chemistry*, 285(50): 39117–26, Dec. 2010. ISSN 1083-351X. doi: 10.1074/jbc.M110.159418. URL http://www.pubmedcentral.nih.gov/articlerender.fcgi?artid=2998075&tool=pmcentrez&rendertype=abstract.

A. Mercier-Zuber and K. M. O'Shaughnessy. Role of SPAK and OSR1 signalling in the regulation of NaCl cotransporters. *Current opinion in nephrology and hypertension*, 20(5): 534–40, Sept. 2011. ISSN 1473-6543. doi: 10.1097/MNH.0b013e3283484b06. URL http://www.ncbi.nlm.nih.gov/pubmed/21610494.

A. H. Meyer, I. Katona, M. Blatow, A. Rozov, and H. Monyer. In vivo labeling of parvalbumin-positive interneurons and analysis of electrical coupling in identified neurons. *The Journal of neuroscience : the official journal of the Society for Neuroscience*, 22(16):7055–64, Aug. 2002a. ISSN 1529-2401. doi: 20026742. URL http://www.ncbi.nlm.nih.gov/pubmed/12177202.

C. Meyer, J. M. Dostou, S. L. Welle, and J. E. Gerich. Role of human liver, kidney, and skeletal muscle in postprandial glucose homeostasis. *American journal of physiology. Endocrinology and metabolism*, 282(2):E419–27, Feb. 2002b. ISSN 0193-1849. doi: 10.1152/ajpendo.00032.2001. URL http://www.ncbi.nlm.nih.gov/pubmed/11788375.

D. Meyre, M. Farge, C. Lecoeur, C. Proenca, E. Durand, F. Allegaert, J. Tichet, M. Marre, B. Balkau, J. Weill, J. Delplanque, and P. Froguel. R125W coding variant in TBC1D1 confers risk for familial obesity and contributes to linkage on chromosome 4p14 in the French population. *Human molecular genetics*, 17(12):1798–802, June 2008. ISSN 1460-2083. doi: 10.1093/hmg/ddn070. URL http://www.ncbi.nlm.nih.gov/pubmed/18325908.

V. E. Mick, O. A. Itani, R. W. Loftus, R. F. Husted, T. J. Schmidt, and C. P. Thomas. The alpha-subunit of the epithelial sodium channel is an aldosterone-induced transcript in mammalian collecting ducts, and this transcriptional response is mediated via distinct cis-elements in the 5'-flanking region of the gene. *Molecular endocrinology (Baltimore, Md.)*, 15(4):575–88, Apr. 2001. ISSN 0888-8809. doi: 10.1210/mend.15.4.0620. URL http://www.ncbi.nlm.nih.gov/pubmed/11266509.

C. P. Mîinea, H. Sano, S. Kane, E. Sano, M. Fukuda, J. Peränen, W. S. Lane, and G. E. Lienhard. AS160, the Akt substrate regulating GLUT4 translocation, has a functional Rab GTPase-activating protein domain. *The Biochemical journal*, 391(Pt 1):87–93, Oct. 2005. ISSN 1470-8728. doi: 10.1042/BJ20050887. URL http://www.pubmedcentral.nih.gov/articlerender.fcgi?artid=1237142&tool=pmcentrez&rendertype=abstract.

R. L. Miller, P. Zhang, T. Chen, A. Rohrwasser, and R. D. Nelson. Automated method for the isolation of collecting ducts. *American journal of physiology. Renal physiology*, 291(1):

F236–45, July 2006. ISSN 1931-857X. doi: 10.1152/ajprenal.00273.2005. URL http://www.ncbi.nlm.nih.gov/pubmed/16467129.

A. Mitrakou. Kidney: Its impact on glucose homeostasis and hormonal regulation. *Diabetes Research and Clinical Practice*, 93 Suppl 1:S66–S72, 2011. URL http://www.ncbi.nlm.nih.gov/pubmed/21864754.

T. Monkawa, I. Kurihara, K. Kobayashi, M. Hayashi, and T. Saruta. Novel mutations in thiazide-sensitive Na-Cl cotransporter gene of patients with Gitelman's syndrome. *Journal of the American Society of Nephrology : JASN*, 11(1):65–70, Jan. 2000. ISSN 1046-6673. URL http://www.ncbi.nlm.nih.gov/pubmed/10616841.

R. G. Morris, E. J. Hoorn, and M. A. Knepper. Hypokalemia in a mouse model of Gitelman's syndrome. *American journal of physiology. Renal physiology*, 290(6):F1416–20, June 2006. ISSN 1931-857X. doi: 10.1152/ajprenal.00421.2005. URL http://www.ncbi.nlm.nih.gov/pubmed/16434571.

D. B. Mount. Membrane trafficking and the regulation of NKCC2. *American journal of physiology. Renal physiology*, 290(3):F606–7, Mar. 2006. ISSN 1931-857X. doi: 10.1152/ajprenal.00410.2005. URL http://ajprenal.physiology.org/content/290/3/F606.

H. Murata, P. W. Hruz, and M. Mueckler. Indinavir inhibits the glucose transporter isoform Glut4 at physiologic concentrations. *AIDS (London, England)*, 16(6):859–63, Apr. 2002. ISSN 0269-9370. URL http://www.ncbi.nlm.nih.gov/pubmed/11919487.

K. Mutig, T. Saritas, S. Uchida, T. Kahl, T. Borowski, A. Paliege, A. Böhlick, M. Bleich, Q. Shan, and S. Bachmann. Short-term stimulation of the thiazide-sensitive Na+-Cl- cotransporter by vasopressin involves phosphorylation and membrane translocation. *American journal of physiology. Renal physiology*, 298(3):F502–9, Mar. 2010. ISSN 1522-1466. doi: 10.1152/ajprenal.00476.2009. URL http://www.ncbi.nlm.nih.gov/pubmed/20007345.

Y. Ng, G. Ramm, J. A. Lopez, and D. E. James. Rapid activation of Akt2 is sufficient to stimulate GLUT4 translocation in 3T3-L1 adipocytes. *Cell metabolism*, 7(4):348–56, Apr. 2008. ISSN 1550-4131. doi: 10.1016/j.cmet.2008.02.008. URL http://www.ncbi.nlm.nih.gov/pubmed/18396141.

S. Ngo, J. B. Barry, J. C. Nisbet, J. B. Prins, and J. P. Whitehead. Reduced phosphorylation of AS160 contributes to glucocorticoid-mediated inhibition of glucose uptake in human and murine adipocytes. *Molecular and cellular endocrinology*, 302(1):33–40, Apr. 2009. ISSN 0303-7207. doi: 10.1016/j.mce.2008.10.020. URL http://www.ncbi.nlm.nih.gov/pubmed/19013499.

S. r. Nielsen, J. r. Frø kiaer, D. Marples, T.-H. Kwon, P. Agre, and M. A. Knepper. Aquaporins in the kidney: from molecules to medicine. *Physiological reviews*, 82(1):205–44, Jan. 2002. ISSN 0031-9333. doi: 10.1152/physrev.00024.2001. URL http://www.ncbi.nlm.nih.gov/pubmed/11773613.

D. Pacheco-Alvarez, P. S. Cristóbal, P. Meade, E. Moreno, N. Vazquez, E. Muñoz, A. Díaz, M. E. Juárez, I. Giménez, and G. Gamba. The Na+:Cl- cotransporter is activated and phosphorylated at the amino-terminal domain upon intracellular chloride depletion. *The*

Journal of biological chemistry, 281(39):28755–63, Sept. 2006. ISSN 0021-9258. doi: 10.1074/jbc.M603773200. URL http://www.ncbi.nlm.nih.gov/pubmed/16887815.

M. M. Pandit, K. A. Strait, T. Matsuda, and D. E. Kohan. Na delivery and ENaC mediate flow regulation of collecting duct endothelin-1 production. *American journal of physiology. Renal physiology*, 302(10):F1325–30, May 2012. ISSN 1522-1466. doi: 10.1152/ajprenal.00034.2012. URL http://www.pubmedcentral.nih.gov/articlerender.fcgi?artid=3362067&tool=pmcentrez&rendertype=abstract.

H. J. Park, J. N. Curry, and J. A. McCormick. Regulation of NKCC2 activity by inhibitory SPAK isoforms: KS-SPAK is a more potent inhibitor than SPAK2. *American journal of physiology. Renal physiology*, 305(12):F1687–96, Dec. 2013. ISSN 1522-1466. doi: 10.1152/ajprenal.00211.2013. URL http://www.ncbi.nlm.nih.gov/pubmed/24133122.

T. S. Pavlov, D. V. Ilatovskaya, V. Levchenko, L. Li, C. M. Ecelbarger, and A. Staruschenko. Regulation of ENaC in mice lacking renal insulin receptors in the collecting duct. *FASEB journal : official publication of the Federation of American Societies for Experimental Biology*, 27(7):2723–32, July 2013. ISSN 1530-6860. doi: 10.1096/fj.12-223792. URL http://www.ncbi.nlm.nih.gov/pubmed/23558339.

N. B. Pedersen, M. V. Hofmeister, L. L. Rosenbaek, J. Nielsen, and R. A. Fenton. Vasopressin induces phosphorylation of the thiazide-sensitive sodium chloride cotransporter in the distal convoluted tubule. *Kidney international*, 78(2):160–9, July 2010. ISSN 1523-1755. doi: 10.1038/ki.2010.130. URL http://www.ncbi.nlm.nih.gov/pubmed/20445498.

J. Peränen, P. Auvinen, H. Virta, R. Wepf, and K. Simons. Rab8 promotes polarized membrane transport through reorganization of actin and microtubules in fibroblasts. *The Journal of cell biology*, 135(1):153–67, Oct. 1996. ISSN 0021-9525. URL http://www.pubmedcentral.nih.gov/articlerender.fcgi?artid=2121014&tool=pmcentrez&rendertype=abstract.

J. B. Pereira-Leal and M. C. Seabra. The mammalian Rab family of small GTPases: definition of family and subfamily sequence motifs suggests a mechanism for functional specificity in the Ras superfamily. *Journal of molecular biology*, 301(4):1077–87, Aug. 2000. ISSN 0022-2836. doi: 10.1006/jmbi.2000.4010. URL http://www.ncbi.nlm.nih.gov/pubmed/10966806.

N. Picard, K. Trompf, C.-L. Yang, R. L. Miller, M. Carrel, D. Loffing-Cueni, R. A. Fenton, D. H. Ellison, and J. Loffing. Protein Phosphatase 1 Inhibitor-1 Deficiency Reduces Phosphorylation of Renal NaCl Cotransporter and Causes Arterial Hypotension. *Journal of the American Society of Nephrology : JASN*, Nov. 2014. ISSN 1533-3450.

T. Pisitkun, V. Jacob, S. M. Schleicher, C.-L. Chou, M.-J. Yu, and M. A. Knepper. Akt and ERK1/2 pathways are components of the vasopressin signaling network in rat native IMCD. *American journal of physiology. Renal physiology*, 295(4):F1030–43, Oct. 2008. ISSN 1931-857X. doi: 10.1152/ajprenal.90339.2008. URL http://www.pubmedcentral.nih.gov/articlerender.fcgi?artid=2574714&tool=pmcentrez&rendertype=abstract.

S. Pradervand, A. Zuber Mercier, G. Centeno, O. Bonny, and D. Firsov. A comprehensive analysis of gene expression profiles in distal parts of the mouse renal tubule. *Pflügers Archiv : European journal of physiology*, 460(6):925–52, Nov. 2010. ISSN 1432-2013. doi: 10.1007/s00424-010-0863-8. URL http://www.ncbi.nlm.nih.gov/pubmed/20686783.

S. M. Rahman, A. Dobrzyn, P. Dobrzyn, S.-H. Lee, M. Miyazaki, and J. M. Ntambi. Stearoyl-CoA desaturase 1 deficiency elevates insulin-signaling components and down-regulates protein-tyrosine phosphatase 1B in muscle. *Proceedings of the National Academy of Sciences of the United States of America*, 100(19):11110–5, Sept. 2003. ISSN 0027-8424. doi: 10.1073/pnas.1934571100. URL http://www.pubmedcentral.nih.gov/articlerender.fcgi?artid=196935&tool=pmcentrez&rendertype=abstract.

G. Ramm, M. Larance, M. Guilhaus, and D. E. James. A role for 14-3-3 in insulin-stimulated GLUT4 translocation through its interaction with the RabGAP AS160. *The Journal of biological chemistry*, 281(39):29174–80, Sept. 2006. ISSN 0021-9258. doi: 10.1074/jbc.M603274200. URL http://www.ncbi.nlm.nih.gov/pubmed/16880201.

V. K. Randhawa, S. Ishikura, I. Talior-Volodarsky, A. W. P. Cheng, N. Patel, J. H. Hartwig, and A. Klip. GLUT4 vesicle recruitment and fusion are differentially regulated by Rac, AS160, and Rab8A in muscle cells. *The Journal of biological chemistry*, 283(40):27208–19, Oct. 2008. ISSN 0021-9258. doi: 10.1074/jbc.M804282200. URL http://www.ncbi.nlm.nih.gov/pubmed/18650435.

S. Rea and D. E. James. Moving GLUT4: the biogenesis and trafficking of GLUT4 storage vesicles. *Diabetes*, 46(11):1667–77, Nov. 1997. ISSN 0012-1797. URL http://www.ncbi.nlm.nih.gov/pubmed/9356011.

R. F. Reilly, C. A. Shugrue, D. Lattanzi, and D. Biemesderfer. Immunolocalization of the Na+/Ca2+ exchanger in rabbit kidney. *The American journal of physiology*, 265(2 Pt 2): F327–32, Aug. 1993. ISSN 0002-9513. URL http://www.ncbi.nlm.nih.gov/pubmed/8368343.

W. L. Rice, Y. Zhang, Y. Chen, T. Matsuzaki, D. Brown, and H. A. J. Lu. Differential, phosphorylation dependent trafficking of AQP2 in LLC-PK1 cells. *PloS one*, 7(2):e32843, Jan. 2012. ISSN 1932-6203. doi: 10.1371/journal.pone.0032843. URL http://www.pubmedcentral.nih.gov/articlerender.fcgi?artid=3293519&tool=pmcentrez&rendertype=abstract.

C. Richardson, F. H. Rafiqi, H. k. K. R. Karlsson, N. Moleleki, A. Vandewalle, D. G. Campbell, N. A. Morrice, and D. R. Alessi. Activation of the thiazide-sensitive Na+-Cl- cotransporter by the WNK-regulated kinases SPAK and OSR1. *Journal of cell science*, 121(Pt 5):675–84, Mar. 2008. ISSN 0021-9533. doi: 10.1242/jcs.025312. URL http://www.ncbi.nlm.nih.gov/pubmed/18270262.

M. A. Riederer, T. Soldati, A. D. Shapiro, J. Lin, and S. R. Pfeffer. Lysosome biogenesis requires Rab9 function and receptor recycling from endosomes to the trans-Golgi network. *The Journal of cell biology*, 125(3):573–82, May 1994. ISSN 0021-9525. URL http://www.pubmedcentral.nih.gov/articlerender.fcgi?artid=2119986&tool=pmcentrez&rendertype=abstract.

T. Rieg, T. Tang, S. Uchida, H. K. Hammond, R. A. Fenton, and V. Vallon. Adenylyl cyclase 6 enhances NKCC2 expression and mediates vasopressin-induced phosphorylation of NKCC2 and NCC. *The American journal of pathology*, 182(1):96–106, Jan. 2013. ISSN 1525-2191. doi: 10.1016/j.ajpath.2012.09.014. URL http://www.pubmedcentral.nih.gov/articlerender.fcgi?artid=3532715&tool=pmcentrez&rendertype=abstract.

A. D. M. Riquier-Brison, P. K. K. Leong, K. Pihakaski-Maunsbach, and A. A. McDonough. Angiotensin II stimulates trafficking of NHE3, NaPi2, and associated proteins into the

proximal tubule microvilli. *American journal of physiology. Renal physiology*, 298(1):F177–86, Jan. 2010. ISSN 1522-1466. doi: 10.1152/ajprenal.00464.2009. URL http://www.pubmedcentral.nih.gov/articlerender.fcgi?artid=2806122&tool=pmcentrez&rendertype=abstract.

J. H. Robben, N. V. A. M. Knoers, and P. M. T. Deen. Cell biological aspects of the vasopressin type-2 receptor and aquaporin 2 water channel in nephrogenic diabetes insipidus. *American journal of physiology. Renal physiology*, 291(2):F257–70, Aug. 2006. ISSN 1931-857X. doi: 10.1152/ajprenal.00491.2005. URL http://www.ncbi.nlm.nih.gov/pubmed/16825342.

A. Rojek, E.-M. Füchtbauer, T.-H. Kwon, J. r. Frø kiaer, and S. r. Nielsen. Severe urinary concentrating defect in renal collecting duct-selective AQP2 conditional-knockout mice. *Proceedings of the National Academy of Sciences of the United States of America*, 103(15): 6037–42, Apr. 2006. ISSN 0027-8424. doi: 10.1073/pnas.0511324103. URL http://www.pubmedcentral.nih.gov/articlerender.fcgi?artid=1421336&tool=pmcentrez&rendertype=abstract.

C. Ronzaud, D. Loffing-Cueni, P. Hausel, A. Debonneville, S. R. Malsure, N. Fowler-Jaeger, N. A. Boase, R. Perrier, M. Maillard, B. Yang, J. B. Stokes, R. Koesters, S. Kumar, E. Hummler, J. Loffing, and O. Staub. Renal tubular NEDD4-2 deficiency causes NCC-mediated salt-dependent hypertension. *The Journal of clinical investigation*, 123(2):657–65, Feb. 2013. ISSN 1558-8238. doi: 10.1172/JCI61110. URL http://www.pubmedcentral.nih.gov/articlerender.fcgi?artid=3561795&tool=pmcentrez&rendertype=abstract.

B. D. Ross, J. Espinal, and P. Silva. Glucose metabolism in renal tubular function. *Kidney international*, 29(1):54–67, Jan. 1986. ISSN 0085-2538.

B. C. Rossier, O. Staub, and E. Hummler. Genetic dissection of sodium and potassium transport along the aldosterone-sensitive distal nephron: importance in the control of blood pressure and hypertension. *FEBS letters*, 587(13):1929–41, June 2013. ISSN 1873-3468. doi: 10.1016/j.febslet.2013.05.013. URL http://www.ncbi.nlm.nih.gov/pubmed/23684652.

D. J. Rozansky, T. Cornwall, A. R. Subramanya, S. Rogers, Y.-F. Yang, L. L. David, X. Zhu, C.-L. Yang, and D. H. Ellison. Aldosterone mediates activation of the thiazide-sensitive Na-Cl cotransporter through an SGK1 and WNK4 signaling pathway. *The Journal of clinical investigation*, 119(9):2601–12, Sept. 2009. ISSN 1558-8238. doi: 10.1172/JCI38323. URL http://www.pubmedcentral.nih.gov/articlerender.fcgi?artid=2735908&tool=pmcentrez&rendertype=abstract.

D. Ruppli. *Development and characterization of a cell model to monitor the activity of the thiazide-sensitive NaCl-cotransporter under various conditions.* Master thesis, 2012.

N. Sáinz, A. Rodríguez, V. Catalán, S. Becerril, B. Ramírez, A. Lancha, E. Burgos-Ramos, J. Gómez-Ambrosi, and G. Frühbeck. Leptin reduces the expression and increases the phosphorylation of the negative regulators of GLUT4 traffic TBC1D1 and TBC1D4 in muscle of ob/ob mice. *PloS one*, 7(1):e29389, Jan. 2012. ISSN 1932-6203. doi: 10.1371/journal.pone.0029389. URL http://www.pubmedcentral.nih.gov/articlerender.fcgi?artid=3253781&tool=pmcentrez&rendertype=abstract.

T. Saito, S. E. Ishikawa, S. Sasaki, T. Nakamura, K. Rokkaku, A. Kawakami, K. Honda, and F. Marumo. Urinary excretion of aquaporin-2 in the diagnosis of central diabetes insipidus. *The Journal of clinical endocrinology and metabolism*, 82(6):1823–7, June 1997. ISSN 0021-972X. doi: 10.1210/jcem.82.6.3984. URL http://www.ncbi.nlm.nih.gov/pubmed/9177390.

T. Saito, S. Ishikawa, T. Ito, H. Oda, F. Ando, M. Higashiyama, S. Nagasaka, and M. Hieda. Urinary excretion of aquaporin-2 water channel differentiates psychogenic polydipsia from central diabetes insipidus. *The Journal of clinical endocrinology and metabolism*, 84(6):2235–7, June 1999. ISSN 0021-972X. doi: 10.1210/jcem.84.6.5715. URL http://www.ncbi.nlm.nih.gov/pubmed/10372737.

P. San-Cristobal, D. Pacheco-Alvarez, C. Richardson, A. M. Ring, N. Vazquez, F. H. Rafiqi, D. Chari, K. T. Kahle, Q. Leng, N. A. Bobadilla, S. C. Hebert, D. R. Alessi, R. P. Lifton, and G. Gamba. Angiotensin II signaling increases activity of the renal Na-Cl cotransporter through a WNK4-SPAK-dependent pathway. *Proceedings of the National Academy of Sciences of the United States of America*, 106(11):4384–9, Mar. 2009. ISSN 1091-6490. doi: 10.1073/pnas.0813238106. URL http://www.pubmedcentral.nih.gov/articlerender.fcgi?artid=2647339&tool=pmcentrez&rendertype=abstract.

H. Sano, S. Kane, E. Sano, C. P. Mîinea, J. M. Asara, W. S. Lane, C. W. Garner, and G. E. Lienhard. Insulin-stimulated phosphorylation of a Rab GTPase-activating protein regulates GLUT4 translocation. *The Journal of biological chemistry*, 278(17):14599–602, Apr. 2003. ISSN 0021-9258. doi: 10.1074/jbc.C300063200. URL http://www.ncbi.nlm.nih.gov/pubmed/12637568.

H. Sano, L. Eguez, M. N. Teruel, M. Fukuda, T. D. Chuang, J. A. Chavez, G. E. Lienhard, and T. E. McGraw. Rab10, a target of the AS160 Rab GAP, is required for insulin-stimulated translocation of GLUT4 to the adipocyte plasma membrane. *Cell metabolism*, 5(4):293–303, Apr. 2007. ISSN 1550-4131. doi: 10.1016/j.cmet.2007.03.001. URL http://www.ncbi.nlm.nih.gov/pubmed/17403373.

H. Sano, W. G. Roach, G. R. Peck, M. Fukuda, and G. E. Lienhard. Rab10 in insulin-stimulated GLUT4 translocation. *The Biochemical journal*, 411(1):89–95, Apr. 2008. ISSN 1470-8728. doi: 10.1042/BJ20071318. URL http://www.ncbi.nlm.nih.gov/pubmed/18076383.

H. Sano, G. R. Peck, A. N. Kettenbach, S. A. Gerber, and G. E. Lienhard. Insulin-stimulated GLUT4 protein translocation in adipocytes requires the Rab10 guanine nucleotide exchange factor Dennd4C. *The Journal of biological chemistry*, 286(19):16541–5, May 2011. ISSN 1083-351X. doi: 10.1074/jbc.C111.228908. URL http://www.pubmedcentral.nih.gov/articlerender.fcgi?artid=3089496&tool=pmcentrez&rendertype=abstract.

T. Saritas, A. Borschewski, J. A. McCormick, A. Paliege, C. Dathe, S. Uchida, A. Terker, N. Himmerkus, M. Bleich, S. Demaretz, K. Laghmani, E. Delpire, D. H. Ellison, S. Bachmann, and K. Mutig. SPAK differentially mediates vasopressin effects on sodium cotransporters. *Journal of the American Society of Nephrology : JASN*, 24(3):407–18, Feb. 2013. ISSN 1533-3450. doi: 10.1681/ASN.2012040404. URL http://www.pubmedcentral.nih.gov/articlerender.fcgi?artid=3582200&tool=pmcentrez&rendertype=abstract.

S. Schuck, M. J. Gerl, A. Ang, A. Manninen, P. Keller, I. Mellman, and K. Simons. Rab10 is involved in basolateral transport in polarized Madin-Darby canine kidney cells. *Traffic (Copenhagen, Denmark)*, 8(1):47–60, Jan. 2007. ISSN 1398-9219. doi: 10.1111/j.1600-0854.2006.00506.x. URL http://www.ncbi.nlm.nih.gov/pubmed/17132146.

S. M. Schultze, B. A. Hemmings, M. Niessen, and O. Tschopp. PI3K/AKT, MAPK and AMPK signalling: protein kinases in glucose homeostasis. *Expert reviews in molecular medicine*, 14:e1, Jan. 2012. ISSN 1462-3994. doi: 10.1017/S1462399411002109. URL http://www.ncbi.nlm.nih.gov/pubmed/22233681.

S. L. Schwartz, C. Cao, O. Pylypenko, A. Rak, and A. Wandinger-Ness. Rab GTPases at a glance. *Journal of cell science*, 120(Pt 22):3905–10, Nov. 2007. ISSN 0021-9533. doi: 10.1242/jcs.015909. URL http://jcs.biologists.org/content/120/22/3905.long.

B. Seaton and A. Ali. Simplified manual high performance clinical chemistry methods for developing countries. *Medical laboratory sciences*, 41(4):327–36, Oct. 1984. ISSN 0308-3616. URL http://www.ncbi.nlm.nih.gov/pubmed/6513735.

E. Sohara, T. Rai, S.-S. Yang, A. Ohta, S. Naito, M. Chiga, N. Nomura, S.-H. Lin, A. Vandewalle, E. Ohta, S. Sasaki, and S. Uchida. Acute insulin stimulation induces phosphorylation of the Na-Cl cotransporter in cultured distal mpkDCT cells and mouse kidney. *PloS one*, 6(8):e24277, Jan. 2011. ISSN 1932-6203. doi: 10.1371/journal.pone.0024277. URL http://www.pubmedcentral.nih.gov/articlerender.fcgi?artid=3164195&tool=pmcentrez&rendertype=abstract.

J. Song, X. Hu, S. Riazi, S. Tiwari, J. B. Wade, and C. A. Ecelbarger. Regulation of blood pressure, the epithelial sodium channel (ENaC), and other key renal sodium transporters by chronic insulin infusion in rats. *American journal of physiology. Renal physiology*, 290(5): F1055–64, May 2006. ISSN 1931-857X. doi: 10.1152/ajprenal.00108.2005. URL http://www.ncbi.nlm.nih.gov/pubmed/16303859.

M. V. Sorensen, S. Grossmann, M. Roesinger, N. Gresko, A. P. Todkar, G. Barmettler, U. Ziegler, A. Odermatt, D. Loffing-Cueni, and J. Loffing. Rapid dephosphorylation of the renal sodium chloride cotransporter in response to oral potassium intake in mice. *Kidney international*, 83(5):811–24, Feb. 2013. ISSN 1523-1755. doi: 10.1038/ki.2013.14. URL http://www.ncbi.nlm.nih.gov/pubmed/23447069.

O. Staub, S. Dho, P. Henry, J. Correa, T. Ishikawa, J. McGlade, and D. Rotin. WW domains of Nedd4 bind to the proline-rich PY motifs in the epithelial Na+ channel deleted in Liddle's syndrome. *The EMBO journal*, 15(10):2371–80, May 1996. ISSN 0261-4189. URL http://www.pubmedcentral.nih.gov/articlerender.fcgi?artid=450167&tool=pmcentrez&rendertype=abstract.

J. Stegbauer, S. B. Gurley, M. A. Sparks, M. Woznowski, D. E. Kohan, M. Yan, R. W. Lehrich, and T. M. Coffman. AT1 receptors in the collecting duct directly modulate the concentration of urine. *Journal of the American Society of Nephrology : JASN*, 22(12):2237–46, Dec. 2011. ISSN 1533-3450. doi: 10.1681/ASN.2010101095. URL http://www.pubmedcentral.nih.gov/articlerender.fcgi?artid=3250205&tool=pmcentrez&rendertype=abstract.

H. Stenmark. Rab GTPases as coordinators of vesicle traffic. *Nature reviews. Molecular cell biology*, 10(8):513–25, Aug. 2009. ISSN 1471-0080. doi: 10.1038/nrm2728. URL http://www.ncbi.nlm.nih.gov/pubmed/19603039.

S. Stone, V. Abkevich, D. L. Russell, R. Riley, K. Timms, T. Tran, D. Trem, D. Frank, S. Jammulapati, C. D. Neff, D. Iliev, R. Gress, G. He, G. C. Frech, T. D. Adams, M. H. Skolnick, J. S. Lanchbury, A. Gutin, S. C. Hunt, and D. Shattuck. TBC1D1 is a candidate for a severe obesity gene and evidence for a gene/gene interaction in obesity predisposition. *Human molecular genetics*, 15(18):2709–20, Sept. 2006. ISSN 0964-6906. doi: 10.1093/hmg/ddl204. URL http://www.ncbi.nlm.nih.gov/pubmed/16893906.

A. R. Subramanya, C.-L. Yang, X. Zhu, and D. H. Ellison. Dominant-negative regulation of WNK1 by its kidney-specific kinase-defective isoform. *American journal of physiology. Renal physiology*, 290(3):F619–24, Mar. 2006. ISSN 1931-857X. doi: 10.1152/ajprenal.00280.2005. URL http://www.ncbi.nlm.nih.gov/pubmed/16204408.

V. Summa, D. Mordasini, F. Roger, M. Bens, P. Y. Martin, A. Vandewalle, F. Verrey, and E. Féraille. Short term effect of aldosterone on Na,K-ATPase cell surface expression in kidney collecting duct cells. *The Journal of biological chemistry*, 276(50):47087–93, Dec. 2001. ISSN 0021-9258. doi: 10.1074/jbc.M107165200. URL http://www.ncbi.nlm.nih.gov/pubmed/11598118.

D. Sun, N. Nguyen, T. R. DeGrado, M. Schwaiger, and F. C. Brosius. Ischemia induces translocation of the insulin-responsive glucose transporter GLUT4 to the plasma membrane of cardiac myocytes. *Circulation*, 89(2):793–8, Feb. 1994. ISSN 0009-7322. URL http://www.ncbi.nlm.nih.gov/pubmed/8313568.

K. Susa, E. Sohara, K. Isobe, M. Chiga, T. Rai, S. Sasaki, and S. Uchida. WNK-OSR1/SPAK-NCC signal cascade has circadian rhythm dependent on aldosterone. *Biochemical and biophysical research communications*, 427(4):743–7, Nov. 2012. ISSN 1090-2104. doi: 10.1016/j.bbrc.2012.09.130. URL http://www.ncbi.nlm.nih.gov/pubmed/23044422.

F. Szekeres, A. Chadt, R. Z. Tom, A. S. Deshmukh, A. V. Chibalin, M. Björnholm, H. Al-Hasani, and J. R. Zierath. The Rab-GTPase-activating protein TBC1D1 regulates skeletal muscle glucose metabolism. *American journal of physiology. Endocrinology and metabolism*, 303(4): E524–33, Aug. 2012. ISSN 1522-1555. doi: 10.1152/ajpendo.00605.2011. URL http://www.ncbi.nlm.nih.gov/pubmed/22693207.

F. S. Thong, P. J. Bilan, and A. Klip. The Rab GTPase-Activating Protein AS160 Integrates Akt, Protein Kinase C, and AMP-Activated Protein Kinase Signals Regulating GLUT4 Traffic. *Diabetes*, 56(2):414–423, Feb. 2007. ISSN 0012-1797. doi: 10.2337/db06-0900. URL http://diabetes.diabetesjournals.org/content/56/2/414.long.

B. Thorens. Facilitated glucose transporters in epithelial cells. *Annual review of physiology*, 55: 591–608, Jan. 1993. ISSN 0066-4278. doi: 10.1146/annurev.ph.55.030193.003111. URL http://www.ncbi.nlm.nih.gov/pubmed/8466187.

S. Tiwari, L. Nordquist, V. K. M. Halagappa, and C. A. Ecelbarger. Trafficking of ENaC subunits in response to acute insulin in mouse kidney. *American journal of physiology. Renal*

physiology, 293(1):F178–85, July 2007. ISSN 1931-857X. doi: 10.1152/ajprenal.00447.2006. URL http://www.ncbi.nlm.nih.gov/pubmed/17389677.

J. T. Treebak, E. B. Taylor, C. A. Witczak, D. An, T. Toyoda, H.-J. Koh, J. Xie, E. P. Feener, J. r. F. P. Wojtaszewski, M. F. Hirshman, and L. J. Goodyear. Identification of a novel phosphorylation site on TBC1D4 regulated by AMP-activated protein kinase in skeletal muscle. *American journal of physiology. Cell physiology*, 298(2):C377–85, Mar. 2010. ISSN 1522-1563. doi: 10.1152/ajpcell.00297.2009. URL http://www.pubmedcentral.nih.gov/articlerender.fcgi?artid=2822490&tool=pmcentrez&rendertype=abstract.

K. Trompf. *Regulation of kidney DCT cell function*. PhD thesis, Universtity of Zurich, Switzerland, 2013.

T. Tsuboi and M. Fukuda. The C2B domain of rabphilin directly interacts with SNAP-25 and regulates the docking step of dense core vesicle exocytosis in PC12 cells. *The Journal of biological chemistry*, 280(47):39253–9, Nov. 2005. ISSN 0021-9258. doi: 10.1074/jbc.M507173200. URL http://www.ncbi.nlm.nih.gov/pubmed/16203731.

S. Uchida and H. Endou. Substrate specificity to maintain cellular ATP along the mouse nephron. *The American journal of physiology*, 255(5 Pt 2):F977–83, Nov. 1988. ISSN 0002-9513. URL http://www.ncbi.nlm.nih.gov/pubmed/2847554.

V. Vallon, J. Schroth, F. Lang, D. Kuhl, and S. Uchida. Expression and phosphorylation of the Na+-Cl- cotransporter NCC in vivo is regulated by dietary salt, potassium, and SGK1. *American journal of physiology. Renal physiology*, 297(3):F704–12, Sept. 2009. ISSN 1522-1466. doi: 10.1152/ajprenal.00030.2009. URL http://www.pubmedcentral.nih.gov/articlerender.fcgi?artid=2739704&tool=pmcentrez&rendertype=abstract.

R. Villa-Bellosta, S. Ravera, V. Sorribas, G. Stange, M. Levi, H. Murer, J. Biber, and I. C. Forster. The Na+-Pi cotransporter PiT-2 (SLC20A2) is expressed in the apical membrane of rat renal proximal tubules and regulated by dietary Pi. *American journal of physiology. Renal physiology*, 296(4):F691–9, Apr. 2009. ISSN 1931-857X. doi: 10.1152/ajprenal.90623.2008. URL http://www.pubmedcentral.nih.gov/articlerender.fcgi?artid=2670642&tool=pmcentrez&rendertype=abstract.

A. C. Vitari, M. Deak, N. A. Morrice, and D. R. Alessi. The WNK1 and WNK4 protein kinases that are mutated in Gordon's hypertension syndrome phosphorylate and activate SPAK and OSR1 protein kinases. *The Biochemical journal*, 391(Pt 1):17–24, Oct. 2005. ISSN 1470-8728. doi: 10.1042/BJ20051180. URL http://www.pubmedcentral.nih.gov/articlerender.fcgi?artid=1237134&tool=pmcentrez&rendertype=abstract.

T. Voets, B. Nilius, S. Hoefs, A. W. C. M. van der Kemp, G. Droogmans, R. J. M. Bindels, and J. G. J. Hoenderop. TRPM6 forms the Mg2+ influx channel involved in intestinal and renal Mg2+ absorption. *The Journal of biological chemistry*, 279(1):19–25, Jan. 2004. ISSN 0021-9258. doi: 10.1074/jbc.M311201200. URL http://www.ncbi.nlm.nih.gov/pubmed/14576148.

C. A. Wagner, D. Loffing-Cueni, Q. Yan, N. Schulz, P. Fakitsas, M. Carrel, T. Wang, F. Verrey, J. P. Geibel, G. Giebisch, S. C. Hebert, and J. Loffing. Mouse model of type II Bartter's syndrome. II. Altered expression of renal sodium- and water-transporting proteins. *American*

journal of physiology. Renal physiology, 294(6):F1373–80, June 2008. ISSN 1931-857X. doi: 10.1152/ajprenal.00613.2007. URL http://www.ncbi.nlm.nih.gov/pubmed/18322017.

H. Y. Wang, S. Ducommun, C. Quan, B. Xie, M. Li, D. H. Wasserman, K. Sakamoto, C. Mackintosh, and S. Chen. AS160 deficiency causes whole-body insulin resistance via composite effects in multiple tissues. *The Biochemical journal*, 449(2):479–89, Jan. 2013. ISSN 1470-8728. doi: 10.1042/BJ20120702. URL http://www.biochemj.org/bj/449/0479/bj4490479.htm.

W. Wang, C. Li, L. N. Nejsum, H. Li, S. W. Kim, T.-H. Kwon, T. E. N. Jonassen, M. A. Knepper, K. Thomsen, J. r. Frø kiaer, and S. r. Nielsen. Biphasic effects of ANP infusion in conscious, euvolumic rats: roles of AQP2 and ENaC trafficking. *American journal of physiology. Renal physiology*, 290(2):F530–41, Feb. 2006. ISSN 1931-857X. doi: 10.1152/ajprenal.00070.2005. URL http://www.ncbi.nlm.nih.gov/pubmed/16174867.

W. Wang, J. Martindale, and J. M. Metzger. Parvalbumin: Targeting calcium handling in cardiac diastolic dysfunction. *General physiology and biophysics*, 28 Spec No:F3–6, Jan. 2009. ISSN 0231-5882. URL http://www.ncbi.nlm.nih.gov/pubmed/20093724.

Z. Q. Wang, H. M. Siragy, R. A. Felder, and R. M. Carey. Preferential release of renal dopamine into the tubule lumen: effect of chronic sodium loading. *Clinical and experimental hypertension (New York, N.Y.)*, 19(1-2):107–16, 1993. ISSN 1064-1963. URL http://www.ncbi.nlm.nih.gov/pubmed/9028639.

D. Wiemuth, J. S. Lott, K. Ly, Y. Ke, P. Teesdale-Spittle, P. M. Snyder, and F. J. McDonald. Interaction of serum- and glucocorticoid regulated kinase 1 (SGK1) with the WW-domains of Nedd4-2 is required for epithelial sodium channel regulation. *PloS one*, 5(8):e12163, Jan. 2010. ISSN 1932-6203. doi: 10.1371/journal.pone.0012163. URL http://www.pubmedcentral.nih.gov/articlerender.fcgi?artid=2921341&tool=pmcentrez&rendertype=abstract.

F. H. Wilson, S. Disse-Nicodème, K. A. Choate, K. Ishikawa, C. Nelson-Williams, I. Desitter, M. Gunel, D. V. Milford, G. W. Lipkin, J. M. Achard, M. P. Feely, B. Dussol, Y. Berland, R. J. Unwin, H. Mayan, D. B. Simon, Z. Farfel, X. Jeunemaitre, and R. P. Lifton. Human hypertension caused by mutations in WNK kinases. *Science (New York, N.Y.)*, 293(5532): 1107–12, Aug. 2001. ISSN 0036-8075. doi: 10.1126/science.1062844. URL http://www.ncbi.nlm.nih.gov/pubmed/11498583.

X. Wu, F. Wang, K. Rao, J. R. Sellers, and J. A. Hammer. Rab27a is an essential component of melanosome receptor for myosin Va. *Molecular biology of the cell*, 13(5):1735–49, May 2002. ISSN 1059-1524. doi: 10.1091/mbc.01-12-0595. URL http://www.pubmedcentral.nih.gov/articlerender.fcgi?artid=111140&tool=pmcentrez&rendertype=abstract.

B. E. Xu, B. H. Lee, X. Min, L. Lenertz, C. J. Heise, S. Stippec, E. J. Goldsmith, and M. H. Cobb. WNK1: analysis of protein kinase structure, downstream targets, and potential roles in hypertension. *Cell research*, 15(1):6–10, Jan. 2005. ISSN 1001-0602. doi: 10.1038/sj.cr.7290256. URL http://www.ncbi.nlm.nih.gov/pubmed/15686619.

B. Yang, D. Zhao, L. Qian, and A. S. Verkman. Mouse model of inducible nephrogenic diabetes insipidus produced by floxed aquaporin-2 gene deletion. *American journal of physiology. Renal*

physiology, 291(2):F465–72, Aug. 2006. ISSN 1931-857X. doi: 10.1152/ajprenal.00494.2005. URL http://www.ncbi.nlm.nih.gov/pubmed/16434568.

C.-L. Yang, X. Zhu, Z. Wang, A. R. Subramanya, and D. H. Ellison. Mechanisms of WNK1 and WNK4 interaction in the regulation of thiazide-sensitive NaCl cotransport. *The Journal of clinical investigation*, 115(5):1379–87, May 2005. ISSN 0021-9738. doi: 10.1172/JCI22452. URL http://www.pubmedcentral.nih.gov/articlerender.fcgi?artid=1074678&tool=pmcentrez&rendertype=abstract.

S.-S. Yang, T. Morimoto, T. Rai, M. Chiga, E. Sohara, M. Ohno, K. Uchida, S.-H. Lin, T. Moriguchi, H. Shibuya, Y. Kondo, S. Sasaki, and S. Uchida. Molecular pathogenesis of pseudohypoaldosteronism type II: generation and analysis of a Wnk4(D561A/+) knockin mouse model. *Cell metabolism*, 5(5):331–44, May 2007. ISSN 1550-4131. doi: 10.1016/j.cmet.2007.03.009. URL http://www.ncbi.nlm.nih.gov/pubmed/17488636.

S.-I. Yoshimura, J. Egerer, E. Fuchs, A. K. Haas, and F. A. Barr. Functional dissection of Rab GTPases involved in primary cilium formation. *The Journal of cell biology*, 178(3):363–9, July 2007. ISSN 0021-9525. doi: 10.1083/jcb.200703047. URL http://www.pubmedcentral.nih.gov/articlerender.fcgi?artid=2064854&tool=pmcentrez&rendertype=abstract.

S.-i. Yoshimura, A. Gerondopoulos, A. Linford, D. J. Rigden, and F. A. Barr. Family-wide characterization of the DENN domain Rab GDP-GTP exchange factors. *The Journal of cell biology*, 191(2):367–81, Oct. 2010. ISSN 1540-8140. doi: 10.1083/jcb.201008051. URL http://www.pubmedcentral.nih.gov/articlerender.fcgi?artid=2958468&tool=pmcentrez&rendertype=abstract.

A. Zeigerer, M. K. McBrayer, and T. E. McGraw. Insulin stimulation of GLUT4 exocytosis, but not its inhibition of endocytosis, is dependent on RabGAP AS160. *Molecular biology of the cell*, 15(10):4406–15, Oct. 2004. ISSN 1059-1524. doi: 10.1091/mbc.E04-04-0333. URL http://www.pubmedcentral.nih.gov/articlerender.fcgi?artid=519136&tool=pmcentrez&rendertype=abstract.

Y. Zhou, H. Huang, H.-H. Chang, J. Du, J. F. Wu, C.-Y. Wang, and M.-H. Wang. Induction of renal 20-hydroxyeicosatetraenoic acid by clofibrate attenuates high-fat diet-induced hypertension in rats. *The Journal of pharmacology and experimental therapeutics*, 317(1):11–8, Apr. 2006. ISSN 0022-3565. doi: 10.1124/jpet.105.095356. URL http://www.ncbi.nlm.nih.gov/pubmed/16339392.

A. M. Zuber, D. Singer, J. M. Penninger, B. C. Rossier, and D. Firsov. Increased renal responsiveness to vasopressin and enhanced V2 receptor signaling in RGS2-/- mice. *Journal of the American Society of Nephrology : JASN*, 18(6):1672–8, June 2007. ISSN 1046-6673. doi: 10.1681/ASN.2007010032. URL http://www.ncbi.nlm.nih.gov/pubmed/17475820.

Marianna Di Chiara

Personal details

Birth	**2nd of July 1985**, *Calw, Germany*.
Address	**Murhaldenweg 14**, *CH-8057 Zurich*.
Phone (mobile)	**+41 762732053**.
Phone (private)	**+41 445547970**.
Email	**marianna.dichiara@anatom.uzh.ch**.

Summary

With my bachelor studies in Biological Sciences (Konstanz, Germany) and my master studies in Medical Biology (Lausanne, Switzerland), I acquired knowledge in molecular- and microbiology, biochemistry, animal and human physiology, anatomy, pathology and pharmacology. During my PhD at the Institute of Anatomy at the University of Zurich with Prof. Loffing and within the Life Science Graduate School Zurich program of Integrative Molecular Medicine, I got the opportunity to deepen my laboratory skills and scientific knowledge. To my laboratory experiences count many molecular analyzing techniques like cell culture, cloning, cell sorting (FACS, COPAS), sequencing, gene/protein extraction, qRT-PCR, ELISA, blood extraction, blood gas analysis, qRT-PCR, microarray, immunoblotting, IHC and ICC, microscopy, but also troubleshooting, animal/mice handling (e.g. injections, metabolic experiments), scientific writing, and supervising and teaching students.

Education

University

2010-2014 **University of Zurich**, *PhD Studies, Integrative Molecular Medicine*, Zurich, Switzerland.

2008-2010 **University of Lausanne**, *Master Studies, Medical Biology*, Lausanne, Switzerland.

2005-2008 **University of Konstanz**, *Bachelor Studies, Biological Sciences*, Konstanz, Germany.

School

1996-2005 **Gymnasium**, *Hermann Hesse-Gymnasium*, Calw, Germany.

Laboratory experience

04/2010-06/2014 **PhD thesis**, *The Role of the Rab GTPase-Activating Protein TBC1D4 (AS160) in Mouse Kidney*, University of Zurich, Institute of Anatomy.
Prof. Johannes Loffing

02/2009-02/2010 **Master thesis**, *Interplay of PXR and PPAR-α Activity in Response to Xenobiotics*, University of Lausanne, Integrative Center of Genomics.
Prof. Beatrice Desvergne

10/2008-12/2008 **Premaster thesis**, *Effects of Aldosterone on Mineralocorticoid Receptor Modification*, University of Lausanne, Department of Pharmacology and Toxicology.
Prof. Olivier Staub

01/2008-06/2008 **Bachelor thesis**, *Charakterisierung von chimären PARP-1 Proteinen im induzierten Zelltod*, University of Konstanz, Molecular Toxicology.
Prof. Alexander Bürkle

Working and teaching experience

12/2014-09/2015 **Swiss Paediatric Oncology Group SPOG, Berne, Switzerland**, *Co-worker Regulatory Affairs*.

04/2011-12/2013 **University of Zurich, Switzerland**, *Molecular Anatomy, Prof. Johannes Loffing*, Supervison MD students Histology I-III and exam-assistance.

02/2011-12/2011 **University of Zurich, Switzerland**, *Molecular Anatomy, Prof. Johannes Loffing*, Laboratory supervison of a master student in biochemistry.

08/2008-09/2008 **Universitätsklinikum Freiburg, Germany**, *Neurosurgery, PD Dr. Marcia Marchein*, Internship: Angiogenesis of brain tumors.

08/2006-03/2007 **University of Konstanz, Germany**, *Evolutionary Biology, Prof. Axel Meyer*, Student assistant, Zebra fish research.

Publications

July 2012 **Natasha Lier, Nikolay Gresko, Marianna Di Chiara, Dominique Loffing-Cueni, and Johannes Loffing**, *Immunofluorescent localization of the Rab-GAP protein TBC1D4 (AS160) in mouse kidney*, Histochemistry and cell biology, vol. 138, no. 1, pp. 1012.

October 2012 **Abhijeet Todkar, Marianna Di Chiara, Dominique Loffing-Cueni, Carla Bettoni, Markus Mohaupt, Johannes Loffing, and Carsten A. Wagner**, *Aldosterone deficiency adversely affects pregnancy outcome in mice*, Pfluegers Archiv, European Journal of Physiology, vol. 464, no. 4, pp. 33143.

in submission **Marianna Di Chiara, Bob Glaudemans, Dominique Loffing-Cueni, Alex Odermatt, Olivier Devuyst, Nourdine Faresse, and Johannes Loffing**, *The RabGAP TBC1D4 is dispensable for the control of sodium and water homeostasis but regulates GLUT4 in mouse kidney*, American Journal of Physiology, Renal Physiology, n.a.

Murhaldenweg 14 – CH-8057 Zurich
+41 762732053 • ☎ +41 445547970
• ✉ marianna.dichiara@anatom.uzh.ch

Conferences (a selection)

June 2011 **ImMed PhD Retreat Jungfraujoch/Kleine Scheidegg, Switzerland**, *Di Chiara M., Loffing-Cueni D., Lier N., Gresko N., Loffing J.* , The role of the Rab GTPase-activating-proteins TBC1D4 (AS160) and TBC1D1 for sodium and glucose homeostasis in vivo, poster presentation.

August 2011 **7th Symposium of the ZIHP, Zurich, Switzerland**, *Di Chiara M., Loffing-Cueni D., Lier N., Gresko N., Loffing J.*, The role of the Rab GTPase-activating-proteins TBC1D4 (AS160) and TBC1D1 for sodium and glucose homeostasis in vivo, poster presentation.

August 2013 **9th Symposium of the ZIHP Zurich, Switzerland**, *Glaudemans B., Loffing-Cueni D., Odermatt A., Devuyst O., Faresse N., Loffing J.*, The Rab-GAP protein TBC1D4 (AS160) regulates GLUT4 but not ENaC, NaKATPase and AQP2 in mouse kidney, presentation.

November 2013 **ASN-Annual Meeting, Atlanta (Georgia), USA**, *Di Chiara M., Glaudemans B., Loffing-Cueni D., Odermatt A., Devuyst O., Faresse N., Loffing J.*, The Rab-GAP protein TBC1D4 (AS160) regulates GLUT4 but not ENaC, NaKATPase and AQP2 in mouse kidney, poster presentation.

Skills

Laboratory **animal handling, cell culture, fluorescence-based cell activity and immunological assays, blood gas analysis, microscopy, qRT-PCR, sequencing, microarray, Western blotting, etc**.

IT **LaTeX, MSOffice (incl. Outlook), GraphPrism, SwissProt, BLAST, etc**.

Organisation **Poster and presentation jury, moderation, organisation of 9th ZIHP Symposium 2013, Zurich, Switzerland**.

Languages

German **mother tongue**

Italian **mother tongue**

English **professional**

French **professional**

Spanish **advanced**

Danish **intermediate**

Hobbies

music **playing the flute in a music band for over 15 years**.

sport **Volleyball, Zumba, hiking**.

others **reading, learning new languages, etc**.

Zurich, July 13, 2015

Murhaldenweg 14 – CH-8057 Zurich
+41 762732053 • ☎ *+41 445547970*
• ✉ *marianna.dichiara@anatom.uzh.ch*